AD-A047 316 GTE SYLVANIA INC MOUNTAIN VIEW CALIF ELECTRONIC SYST--ETC F/G 17/1
ELECTRET TAPE DETECTION SYSTEM.(U)
SEP 77 G K MILLER

UNCLASSIFIED

F30602-76-C-0375

RADC-TR-77-298

NL

1 OF 2
AD A047316

AD A

ELECTRET TAPE DETECTION SYSTEM

GTE Sylvania Inc.

Approved for public release; distribution unlimited.

DDC

This report has been reviewed by the RADC Information Office (OI) and is releasable to the National Technical Information Service (NTIS). At NTIS it will be releasable to the general public including foreign nations.

This report has been reviewed and is approved for publication.

APPROVED: William F. Gavin Jr.

WILLIAM F. GAVIN JR.
Project Engineer

APPROVED: Owen R. Lawtr

OWEN R. LAWTER, Colonel, USAF
Chief, Surveillance Division

FOR THE COMMANDER: John P. Huss

JOHN P. HUSS
Acting Chief, Plans Office

If your address has changed or if you wish to be removed from the RADC mailing list, or if the addressee is no longer employed by your organization, please notify RADC (OCDS) Griffiss AFB NY 13441. This will assist us in maintaining a current mailing list.

Do not return this copy. Retain or destroy.

UNCLASSIFIED

SECURITY CLASSIFICATION OF THIS PAGE (When Data Entered)

(19) REPORT DOCUMENTATION PAGE		READ INSTRUCTIONS BEFORE COMPLETING FORM
1. REPORT NUMBER (18) RADC-TR-77-298	2. GOVT ACCESSION NO.	3. RECIPIENT'S CATALOG NUMBER
4. TITLE (and Subtitle) (6) ELECTRET TAPE DETECTION SYSTEM		5. TYPE OF REPORT & PERIOD COVERED (9) Final Technical Report, Jun 76 — July 77
		6. PERFORMING ORG. REPORT NUMBER NA
7. AUTHOR(s) Dr. G. Kirby Miller (10)		8. CONTRACT OR GRANT NUMBER(s) (15) F30602-76-C-0375
9. PERFORMING ORGANIZATION NAME AND ADDRESS GTE Sylvania Inc. Electronics Systems Group/Western Division P O Box 188, Mountain View CA 94042		10. PROGRAM ELEMENT, PROJECT, TASK AREA & WORK UNIT NUMBERS (16) 62702F 6515132F (17) 13
11. CONTROLLING OFFICE NAME AND ADDRESS Rome Air Development Center (OCDS) Griffiss AFB NY 13441		12. REPORT DATE (11) Sept 1977
		13. NUMBER OF PAGES 102
14. MONITORING AGENCY NAME & ADDRESS (if different from Controlling Office) Same (12) 105p.		15. SECURITY CLASS. (of this report) UNCLASSIFIED
		15a. DECLASSIFICATION/DOWNGRADING SCHEDULE NA

16. DISTRIBUTION STATEMENT (of this Report)

Approved for public release; distribution unlimited.

17. DISTRIBUTION STATEMENT (of the abstract entered in Block 20, if different from Report)

Same

18. SUPPLEMENTARY NOTES

RADC Project Engineer: William F. Gavin, Jr. (OCDS)

19. KEY WORDS (Continue on reverse side if necessary and identify by block number)

Transducers
Ultrasonics
Surveillance
Detection
Sensors

20. ABSTRACT (Continue on reverse side if necessary and identify by block number)

This report covers the second phase of a program to investigate and develop a new line transducer concept based on an active ultrasonic electret tape transducer. It updates the computer model developed to assess the various transducer parameters. It describes an improved method that was developed for reliably charging electrets both uniformed and to a desired charge level. It also presents results obtained from laboratory tests of various electret tape transducer samples.

DD FORM 1 JAN 73 1473 EDITION OF 1 NOV 65 IS OBSOLETE

UNCLASSIFIED

SECURITY CLASSIFICATION OF THIS PAGE (When Data Entered)

406 571

SUMMARY

This report covers the second phase of a program to investigate and develop a new line intrusion detection concept based on an active ultrasonic electret tape transducer. The idea is to electrically drive a long multi-layered tape transducer having an electret layer and elastically coupled (moving) layers at an ultrasonic frequency so that it radiates a narrow beam of ultrasound all along its length. An object moving into the ensonified region reflects some of the energy back to the tape transducer. The reflected signal is picked up by the tape transducer acting as a microphone and is separated from the driving signal by a special hybrid electronic package that utilizes the Doppler shift in the reflected signal. A processor then operates on the received signal to generate the appropriate alarm.

In the first phase, this concept was shown to be feasible, at least on a small scale, using separate radiating and receiving transducers that are short and rigid. The objective of this effort is to determine feasibility on a more realistic scale by developing an improved long tape transducer that is flexible and manufacturable, by developing the signal extracting electronics, and by integrating the tape and electronics into a demonstrable system.

The approach includes both analytical and experimental tasks. The major accomplishments and conclusions are listed below.

1. The use of a computer model believed to simulate all the important aspects of the electrical drive, acoustic radiation, target reflection, and receiving transduction processes in the single transducer detection concept, has resulted in an optimum transducer design whose parameters depend only on the Q of the driving elements. The optimum design parameters turn out to be reasonable and obtainable (see Section 2.2.4).

2. A simple method for reliably charging electrets uniformly and to a desired level has been developed and adapted for use on a continuous tape basis (see Section 3.1).

3. Potential tape manufacturers feel that the vactret tape design would not be difficult for them to make and that the dimensions and materials all fall well within the commercial state-of-the-art (see Section 3.3.2).

4. The ultrasonic doppler detection concept, based on electret tape transducers, has been demonstrated to be viable in two different ways. For the first time ever, a single transducer electret tape was successfully used as a radiator and receiver simultaneously to achieve a short range detection capability. So far the longest sample used in this way is 3 m in length. The concept was also successfully demonstrated for a 9 m length using two side-by-side single transducer tapes (thus simulating a dual transducer tape), (see Section 4.3).

5. It appears that unless significant improvements in the transducer or in the driving and processing circuitry are made, single transducer tapes may only be practical for relatively short lengths (somewhere between 3 and 30 m) (see Section 4.3).

6. Dual transducer tapes (two transducers on the same tape substrate), however, are expected to be practical for considerably greater lengths. In addition to several other distinct advantages (see Section 5.2), they are expected to retain nearly all of the desirable attributes (see Section 1.1.1) of the single tape transducer.

TABLE OF CONTENTS

TABLE OF CONTENTS -- Continued

EVALUATION

The objective of this effort was to determine the feasibility of a new line transducer based on an active ultrasonic electret tape concept. It consists of a long multi-layered tape transducer having an electret layer which is driven at an ultrasonic frequency causing a moving layer to radiate this frequency all along its length. An object moving into this region reflects some energy back to the transducer which is detected and an alarm is generated. During the first phase (published under RADC TR-76-22), methods of charging the electret, bonding, and laminating the various layers, and suitable testing techniques were developed for small tape samples.

In this phase, the major problems that were addressed included: refining the computer model of the sensor, developing a reliable method of uniformly charging electrets, extending this technology to long samples, addressing the manufacturability of the tape transducer, and determining the constraints of a practical sensor. The ability to fabricate longer tape (up to 30 feet in the laboratory) has permitted the assessment of several possible configurations of the transducer. This resulted in the identification of the most promising configuration as a dual system whereby two independent transducers are fabricated on one substrate. This will permit concentration on this configuration for all future work.

The next phase will concentrate on the above dual system and will result in the delivery of such a system to RADC for field evaluation. The work documented in this report was accomplished in accordance with RADC Technical Planning Objective-Other-BISS.

WILLIAM F. GAVIN, JR.
Center Program Manager

Section 1

INTRODUCTION

This report records the details of an investigation funded by RADC Contract No. F30602-76-C-0375 performed August 1976 - June 1977 by the Security Systems Department of GTE Sylvania's Mountain View, California facility. This study is a continuation of an earlier preliminary investigation in which the concept was shown to be feasible a least on a small scale using separate radiating and receiving transducers. The objective of the current effort is to determine feasibility on a more realistic scale and to develop a laboratory model suitable for demonstrating the single transducer system concept in a more realistic way.

1.1 ELECTRET TAPE INTRUSION DETECTION CONCEPT

Sylvania's Security System Department (SSD), having been active in the security system area for over fifteen years, has been aware of the need for reliable perimeter intrusion detection systems for both government and commercial applications. In particular, there has been no such system that is rapidly deployable. To meet this need, the electret tape concept was developed.

The ACtive Ultrasonic Tape Intrusion Detection or ACUTID system is based on an active ultrasonic doppler detection scheme using a long, thin multi-layered tape (containing an electret layer) as the radiating and receiving transducer. This transducer is essentially an elongated electret microphone with configuration, materials and dimensions engineered to make it a good radiator as well. The highly directional ultrasonic CW beam radiated by the tape uniformly all along its length illuminates any object crossing it. This action causes a reflected doppler-shifted ultrasonic signal that is received by the tape and separated from the driving signal by special hybrid electronic circuitry. A special processor then operates on the received signal and generates the appropriate alarm.

1.1.1 Potential Advantages

Such an intrusion detector has a number of distinct advantages when compared with existing perimeter protection systems.

1. Since it does not require burial or special supports (such as a fence), it can be quickly rolled into place around a nearly arbitrary perimeter to be protected.
2. It can be manufactured with an adhesive on the non-radiating side so that it can be installed very quickly on reasonably smooth walls or ceilings.
3. Because of its mechanical flexibility, it can be fastened to irregular surfaces and go around corners.
4. Being active, it can be used even in very noisy environments where passive devices would be inoperable.
5. The very low volume of material per unit length coupled with current techniques for automatically making uniform laminated tapes in great lengths allow the likely cost for the transducer to be so low that expendable transducer systems may be practical.
6. Unlike most other perimeter protection systems, the ultrasonic electret tape system would not have stringent alignment or installation requirements.
7. Being acoustic, its operation does not provide an electromagnetic signal that could be used for terminal guidance of a hostile missile. Nor will it produce radiation that could interfere with the operation of SIGINT or ELINT collection equipment.

1.2 SCOPE AND ORGANIZATION OF INVESTIGATION

To meet the objectives of the study, the following tasks are identified:

1. Develop an improved long tape transducer by
   a. Optimizing it's materials and dimensions
   b. Increasing and controlling its charge density
   c. Improving its spatial uniformity

1.2 (Continued)

2. Develop the matching hybrid electronics.
3. Determine manufacturability and develop lab fabrication techniques.
4. Assemble and develop a demonstrable system that integrates the transducers and the hybrid electronics.

In the earlier program, the effort was concerned almost entirely with the transducer portion of the system. In this program, the primary effort is still centered on the tape transducer; however, the hybrid electronics package necessary for using the tape simultaneously as both receiver and transmitter is also developed, and considerable effort was expended in getting them to work together. The computer model was improved and used extensively in assessing both transducer and hybrid electronics developments. The major experimental tasks involved improving the charging techniques, examining various methods for fabricating the transducer with uniform layer spacings, and searching for more suitable materials.

In this report, the above activities are described under the sections 2. Analysis, 3. Fabrication Considerations and 4. Performance. These are followed by a conclusion and recommendations section.

Section 2

ANALYSIS

In the previous effort[1] a detailed electromechanical analysis of the tape transducer was derived and implemented on the digital computer. In the current effort the model was extended and improved in a number of ways. The three main developments are: the effects of inactive capacitance are included, the second harmonic distortion products are evaluated, and provision for including an externally supplied bias voltage is made. In addition, calculation of interlayer voltages were made so that possible breakdown conditions would be detected. As will be shown in this section, the use of the improved model led to the determination of optimum transducer designs that are believed to be one of the more important outcomes of this program.

2.1 THE COMPUTER MODEL

The derivation of the equations incorporating the extensions to the model are contained in Appendix A. Figure 2-1 shows the basic system simulated by the model. A power amplifier drives the tape with a sine wave voltage that may be superimposed on a DC bias voltage if desired. The source impedance, Z_s, includes the output impedance of the power amplifier in series with an inductor whose value is chosen so that $X_s = -X_i$ where X_i is the reactance of the total inactive capacitance, C_i in parallel with the input impedance of the active portion of the tape transducer.

Under appropriate electrical and geometrical conditions the action of the electrostatic forces between the charges driven onto the conductor of the moving layer (the current, i) and those stored on the electret layer σ_e, causes the moving layer to vibrate at the driving frequency, thus radiating a pressure wave away from the outer surface of the tape. If the radiated pressure wave strikes an object, a portion of the energy is reflected back to the tape. This reflected pressure wave causes the moving layer to be displaced slightly at the driving

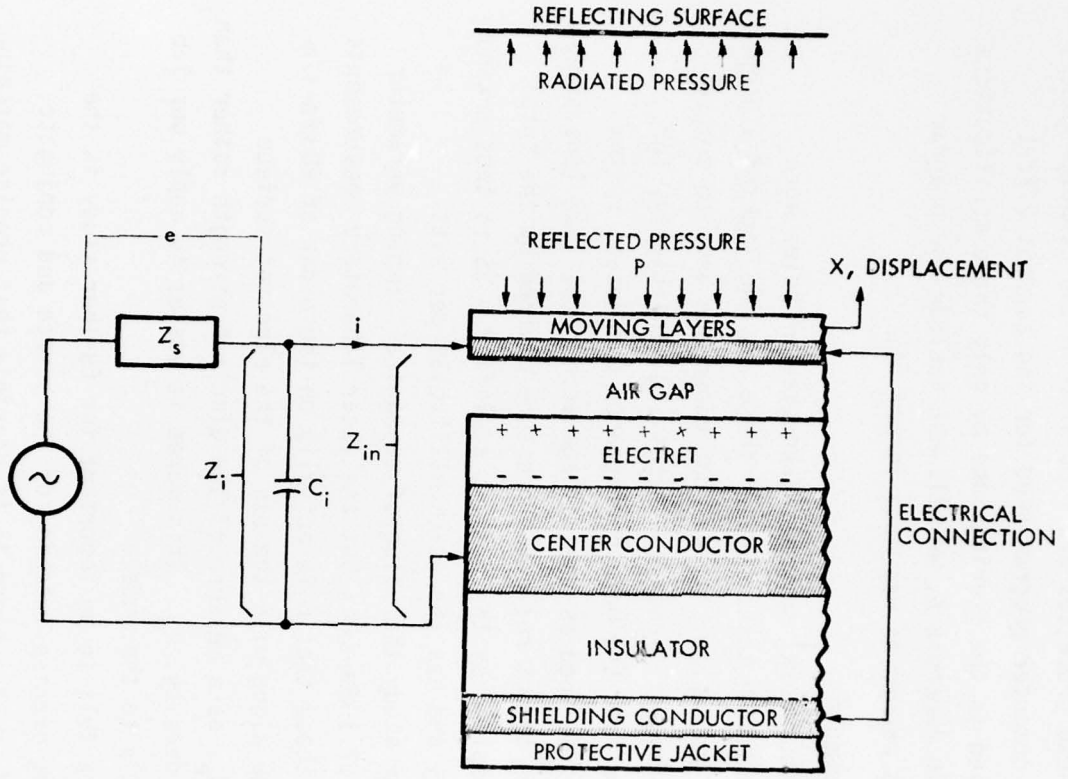

Figure 2-1. Basic System Modeled by Computer

2.1 -- Continued

frequency rate modified by any doppler shift caused by motion of the reflector. The transducer then develops a charge flow proportional to the displacement that can be observed as a voltage across the series inductor. All of these processes are simulated in the computer model.

Because the computer program used for the current effort differs from that used in the previous one by only those modifications discussed here and in Appendix A, we will not include the program code as part of this report as was done in Ref. 1.

2.1.1 Some Improvements

In the previous work[1] several weaknesses or holes were recognized in the modeling task. One of these was the lack of a proper overall performance parameter. It was not known how best to compromise between radiation efficiency and receiving sensitivity, for example. For this effort the main performance parameter, system sensitivity (SS), is defined as the voltage across the load (the series inductor) due to the target reflected pressure divided by the total electrical power supplied by the driving amplifier. SS is thus a kind of system efficiency and has the units millivolts per watt.

In the prior study the value of mechanical damping parameter D was on the order of 1 kPa-s/m, but the later laboratory measurements indicated the likelihood that D is actually on the order of 20 kPa-s/m. This change was made along with the use of the electret surface potential voltage V_e, as a measure of the electret strength rather than the surface charge density, σ_e. This makes it easier to apply our lab measurements directly to the model.

Another area felt to be important for further study is the effect of not having precise matching of the source and conjugate input reactances ($X_s = -X_i$) since it is possible that precise matching will be impractical.

2.2 MODELING PROCEDURES AND RESULTS

2.2.1 Standard Six -- Conjugate Impedance Matching

A new standard set of model parameters was used to study the effect of not matching the input impedance with the conjugate of the source impedance. It is the same as Std. 3 used in Ref. 1 except that:

Air Gap	a_o = 50 μm
Electret Thickness	d = 50 μm
Mechanical Damping	D = 20 kPa-s/m
Length	ℓ = 3 m
Electret Voltage	V_e = -300 V

The moving layer (as in Std. 3) is an aluminum-mylar laminate, 9 μm and 16.4 μm in thicknesses, respectively. This makes a moving mass density of 45 g/m^2.

Figure 2-2 shows what happens to SS (system sensitivity) as a function of frequency when the source impedance satisfies three different conditions. The best performance (highest curve) results from letting $Z_s = Z_{in}^*$. However, this requires that R_s (the source output resistance plus the DC resistance of the inductor) be a fraction of an ohm, e.g., 0.21 Ω at 40 kHz. The middle curve shows what happens when $X_s = -X_{in}$ ($X_s = \omega L$) but R_s = 1 Ω, a much more reasonable value for the inductor required (7.5 mH at 40 kHz) to satisfy $X_s = -X_{in}$. The SS is now considerably reduced (by about two-thirds at 40 kHz). The bottom curve shows what happens to SS when both R_s and L are fixed (1 Ω and 10 mH, respectively). Now the SS is degraded further at frequencies for which L is too small to match $-X_{in}$, but slightly enhanced for frequencies at which L is too large to match $-X_{in}$.

The effects of electret thickness and air gap were also studied in this set of runs (which were made before the inactive capacitance was included). The conclusions are:

1. Use the lowest frequency possible.
2. Match $X_s = -X_{in}$ exactly by proper choice of L.
3. Use the lowest achievable R_s.
4. Use the largest dielectric thickness and air gap compatible with $R_s \leq 1\,\Omega$ ($d \sim 50\,\mu m$, $a_o \sim 67\,\mu m$).

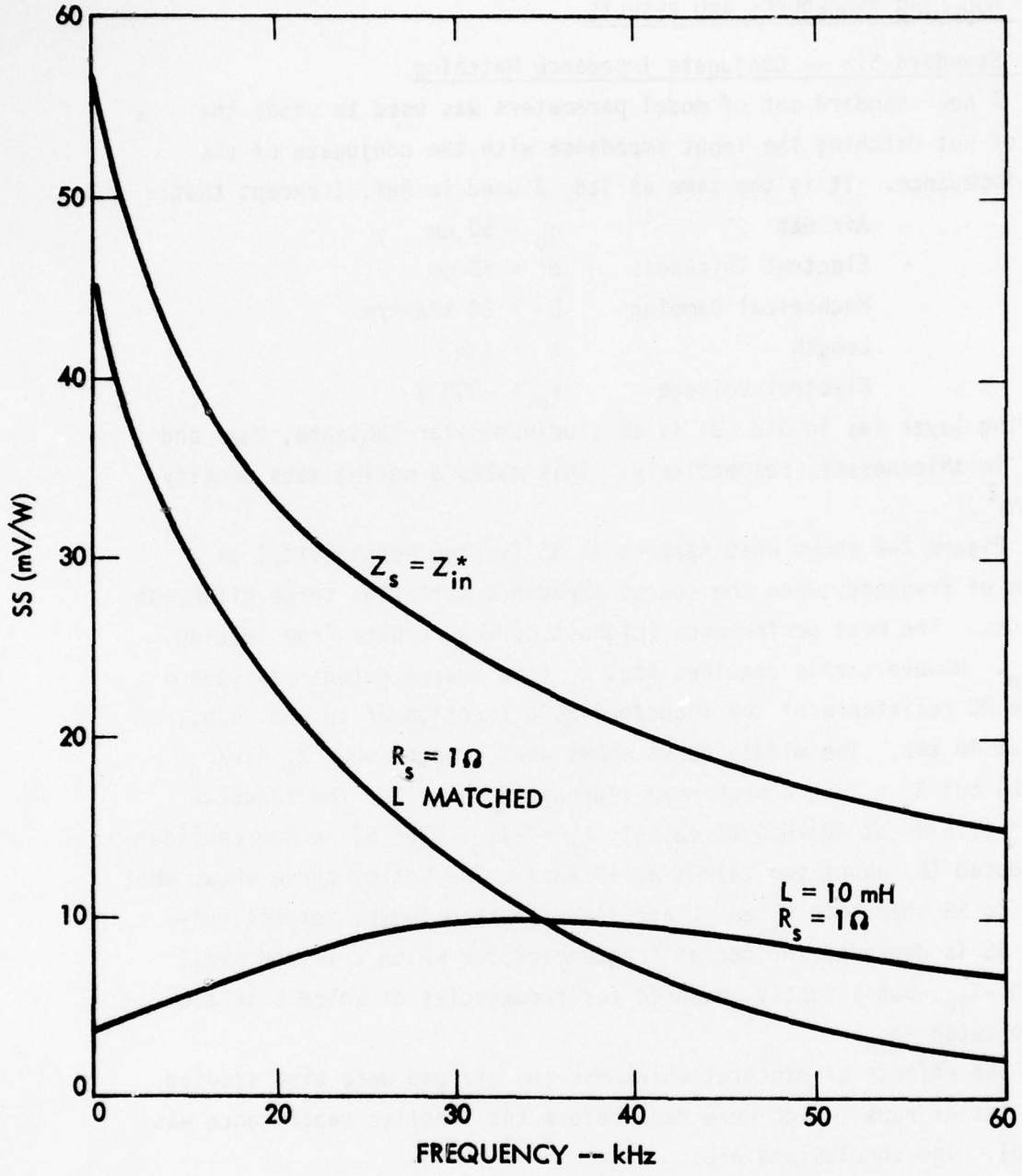

Figure 2-2. Effect of Source Impedance on System Sensitivity

2.2.1 -- Continued

The last conclusion is based on the facts that R_{in} decreases with increases in both d (electret thickness) and a_o (air gap), that probably $R_s < 1\,\Omega$ is impractical, and that $R_s \leq R_{in}$ is desirable.

2.2.2 Inactive Capacitance

After the analytical derivations (Appendix A) showed that the inactive capacitance could have significant effects on performance, the model was modified to incorporate the analysis. Also included were the second harmonic distortion calculation and the provision for supplying a DC bias. These were felt important in view of the rather high voltages that the analysis showed can occur across the tape even for moderate driving voltages. Since single-sided devices such as the modeled tape are known to be very non-linear (especially when the effective bias voltage is approached by the signal voltage), we wanted to know under what conditions and to what degree electrical power would be wasted in generating second harmonic signals.

The modified program was then run on Std. 6 again with the new inactive capacitance parameters, $y = 2\,mm$ and $\varepsilon_i = 2.26$ representing a 2 mm thick insulating layer of polyethylene between the center conductor and shielding conductor. The inactive capacitance also includes 10 pF minimum connection capacitance and the capacitance of the stationary edges of the moving layer. The program was also modified to set R_s to the larger of R_i or $1\,\Omega$ since it is felt unlikely that $R_s < 1\,\Omega$ is practical. For this set of runs, the effects of varying a_o, d, V_e (electret voltage) and M (moving mass/unit area) were studied.

The design conclusions of this set of runs follow:

1. Use $L = -X_i/\omega$ where X_i is the total input reactance (including C_i)
2. Use lowest frequency (20 kHz)
3. Use $d \leq 12.5\,\mu m$
4. Use $a_o = 67\,\mu m$
5. Use $M \simeq 150\,g/m^2$
6. Use $V_e \simeq 600\,V$
7. Minimize the mechanical damping.

2.2.2 -- Continued

Figures 2-3 through 2-9 support these conclusions. By far the greatest effect on SS is shown in Figure 2-3 where L = 4 mH and R_s = 1 Ω. The condition $L = -X_i/\omega$ is satisfied at 25 kHz where the sharp peak in performance occurs. Clearly matching inductance is of great importance, but the figure also indicates the possibility of making the adjustment by shifting the operating frequency. This is much easier than shifting the value of inductance in a high Q coil.

The rest of the figures support the rest of the conclusions in an obvious way. There are several other interesting results from this run that should be mentioned.

1. Radiation efficiencies on the order of a fraction of a percent should be achievable if $R_s \leq 1\,\Omega$ is realizable.
2. The open load sensitivity is consistently a few dB below the open circuit sensitivity. The difference is that the effect of inactive capacitance is included in the former.
3. For R_s = 1 Ω and a 1 V driving voltage, the signal voltage appearing across the tape conductors is 630 V at 20 kHz.
4. Since the series resistance $R_s + R_i$ is the only limit to the current when $X_s = -X_i$, a small fraction of an ampere is drawn from the driving amplifier per meter of tape (for 1 V drive).
5. The second harmonic distortion for Std. 6 at 20 kHz is 50%. This is surprisingly low considering the signal voltage across the tape is more than double the electret bias voltage. Figure 2-10 shows that as the electret voltage V_e, increases beyond 300 V, the 2nd harmonic distortion decreases rapidly. For V_e = 1 kV the distortion is only 5%.

2.2.3 Finding Optimum Parameter Sets

2.2.3.1 Breakdown Constraint

In Appendix B is derived a curve (repeated here in Figure 2-11) that shows the relation between the thickness, d, of the electret and

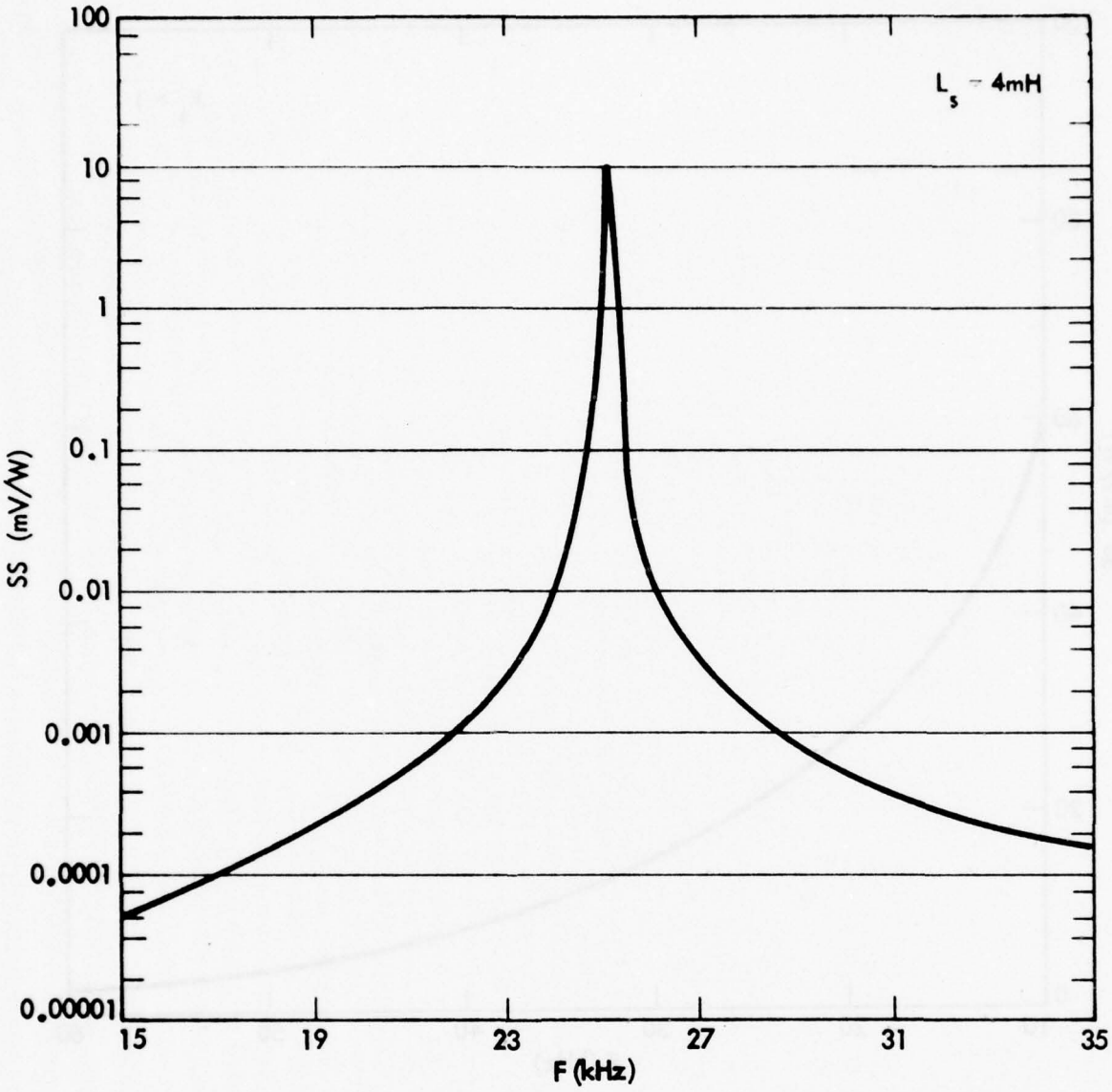

Figure 2-3. Effect of Fixed Inductance on System Sensitivity

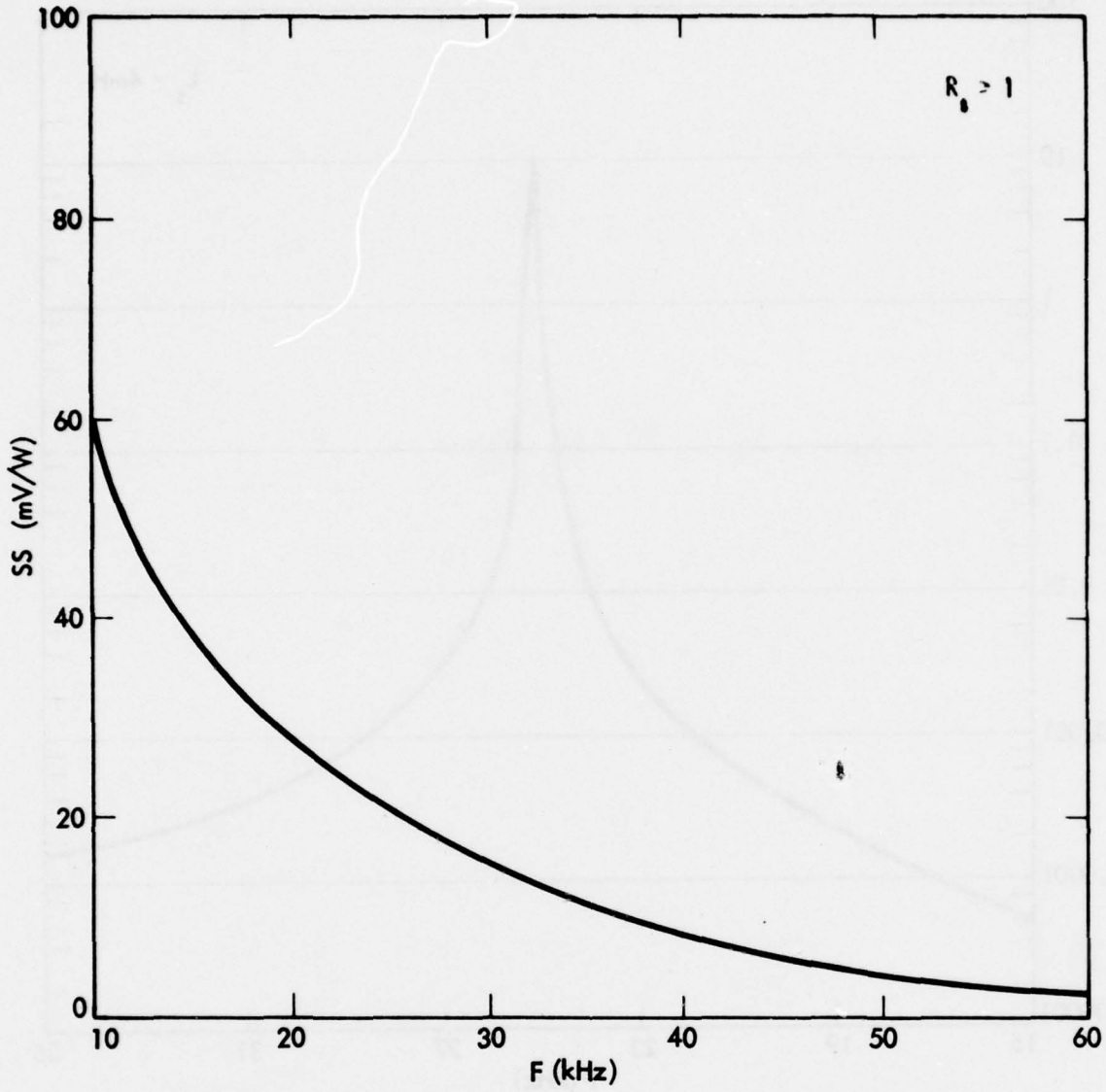

Figure 2-4. Effect of Frequency on System Sensitivity

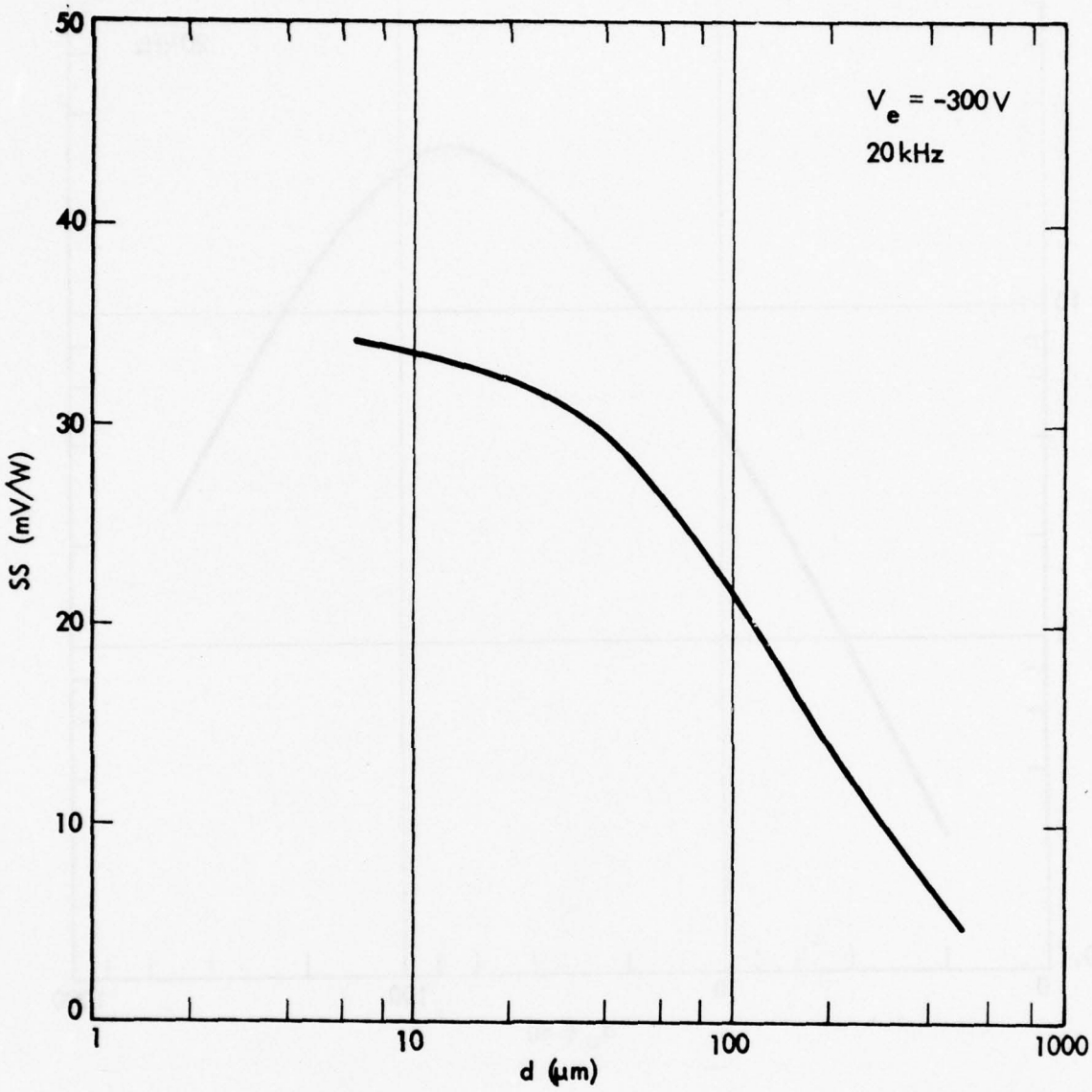

Figure 2-5. Effect of Electret Thickness on System Sensitivity

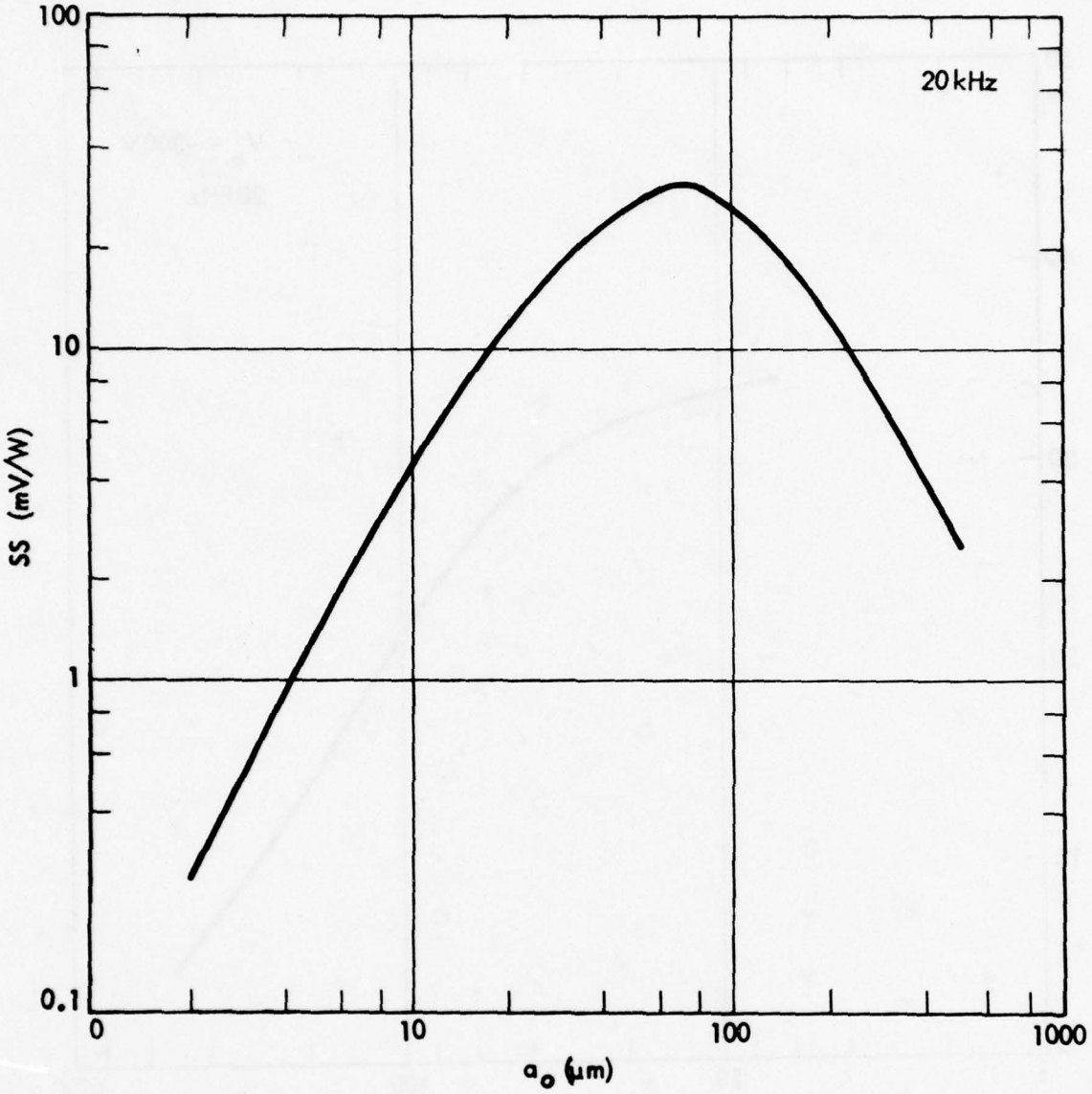

Figure 2-6. Effect of Air Gap on System Sensitivity

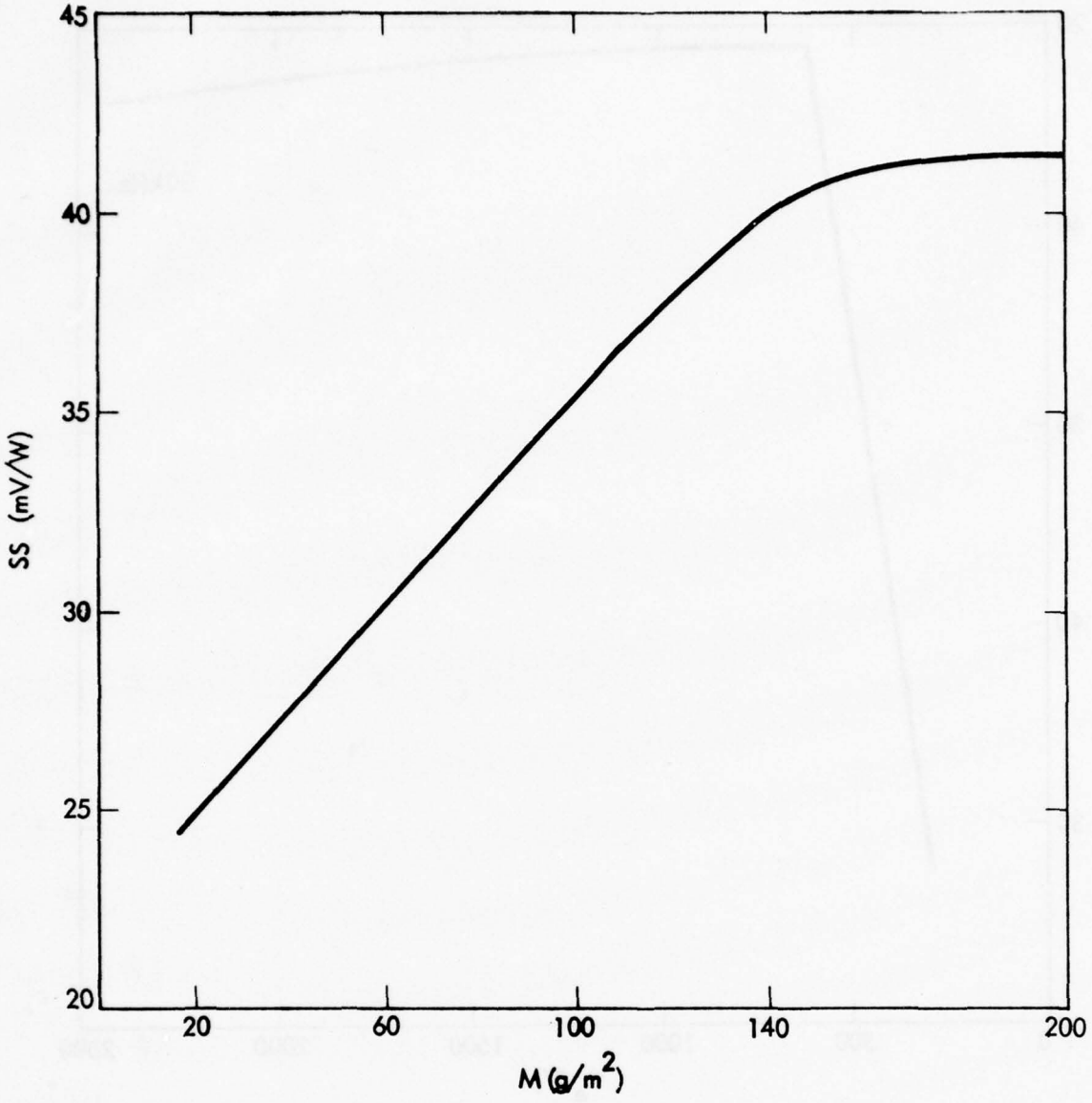

Figure 2-7. Effect of Moving Mass on System Sensitivity

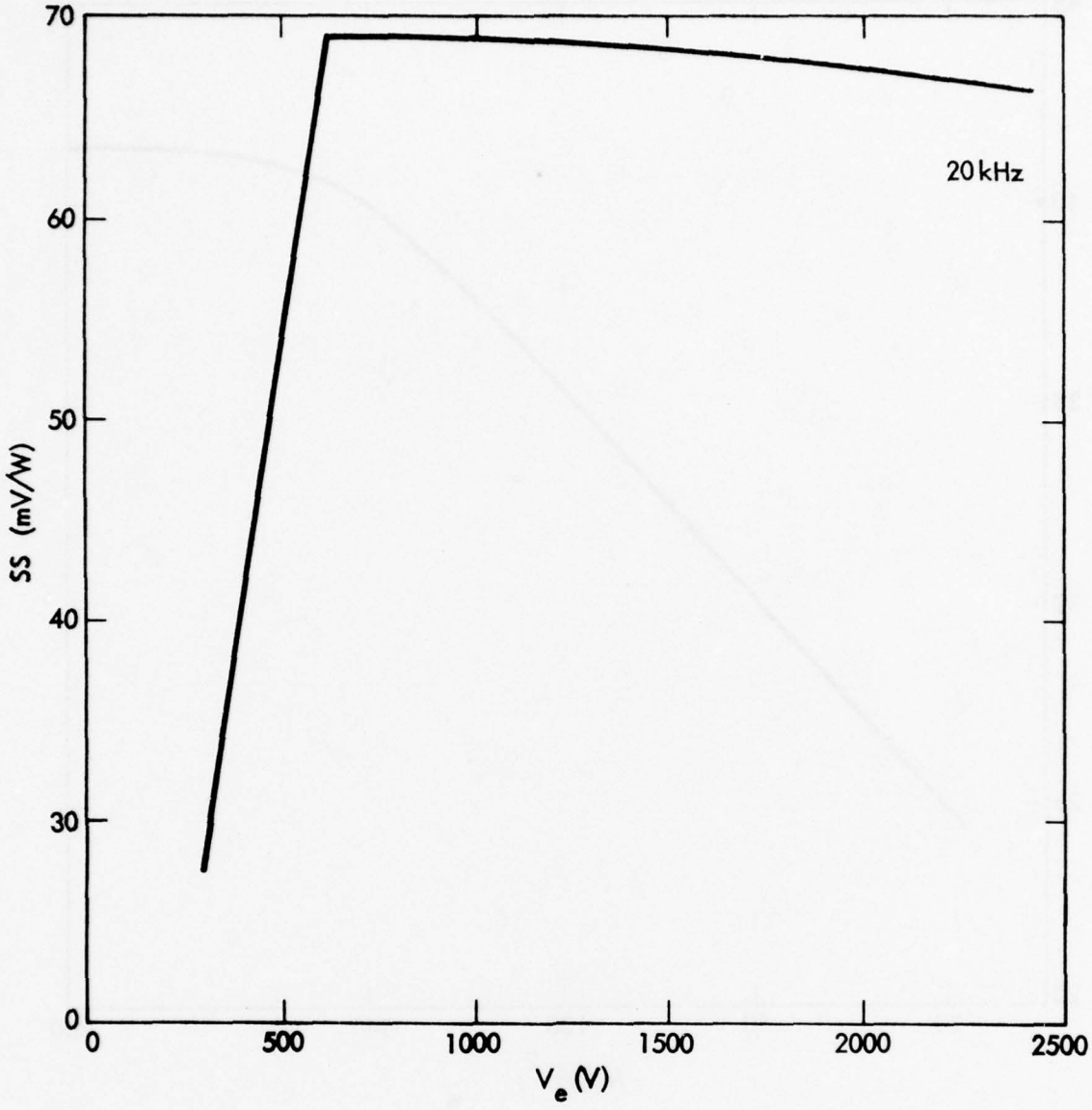

Figure 2-8. Effect of Electret Strength on System Sensitivity

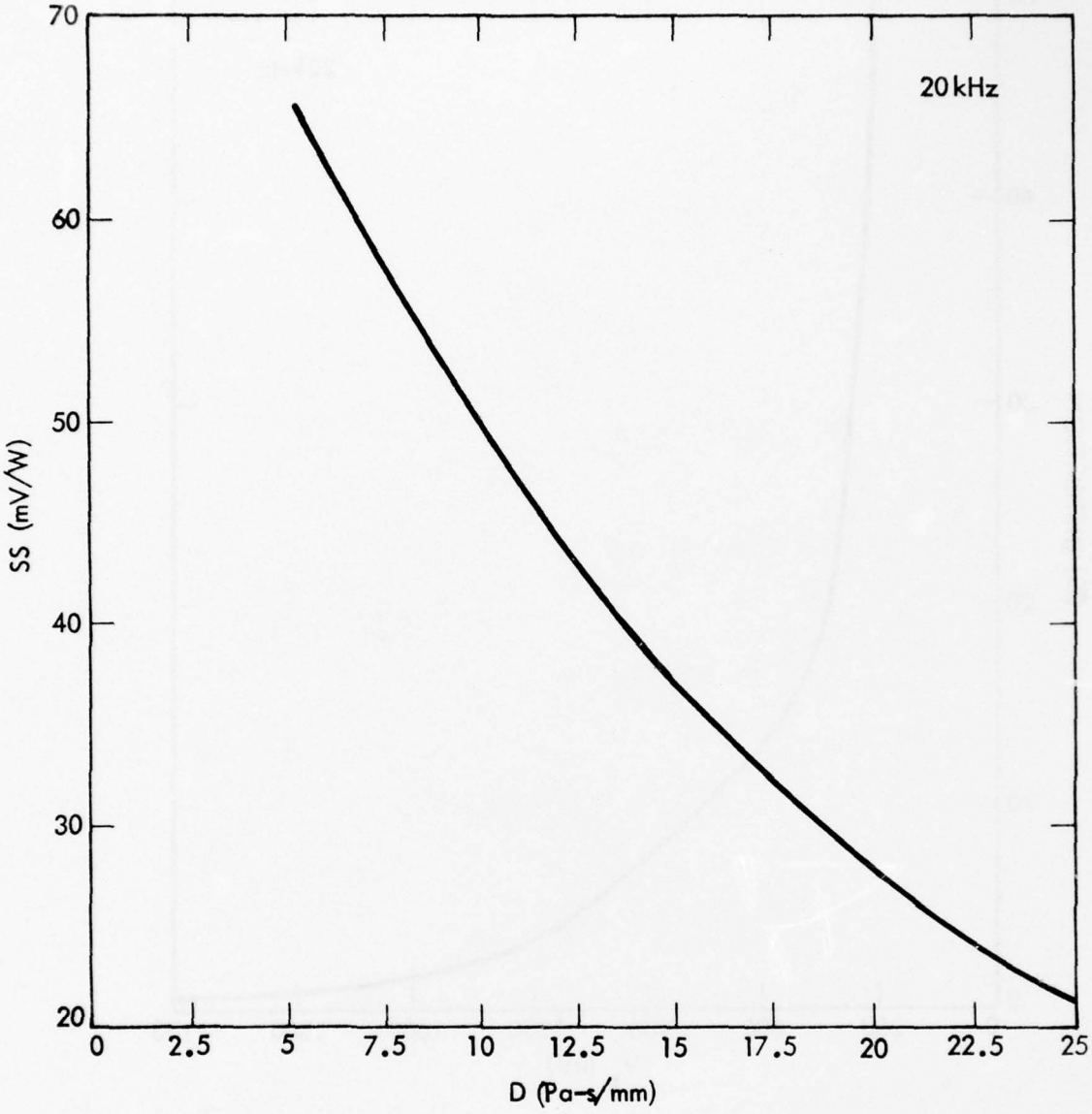

Figure 2-9. Effect of Mechanical Damping on System Sensitivity

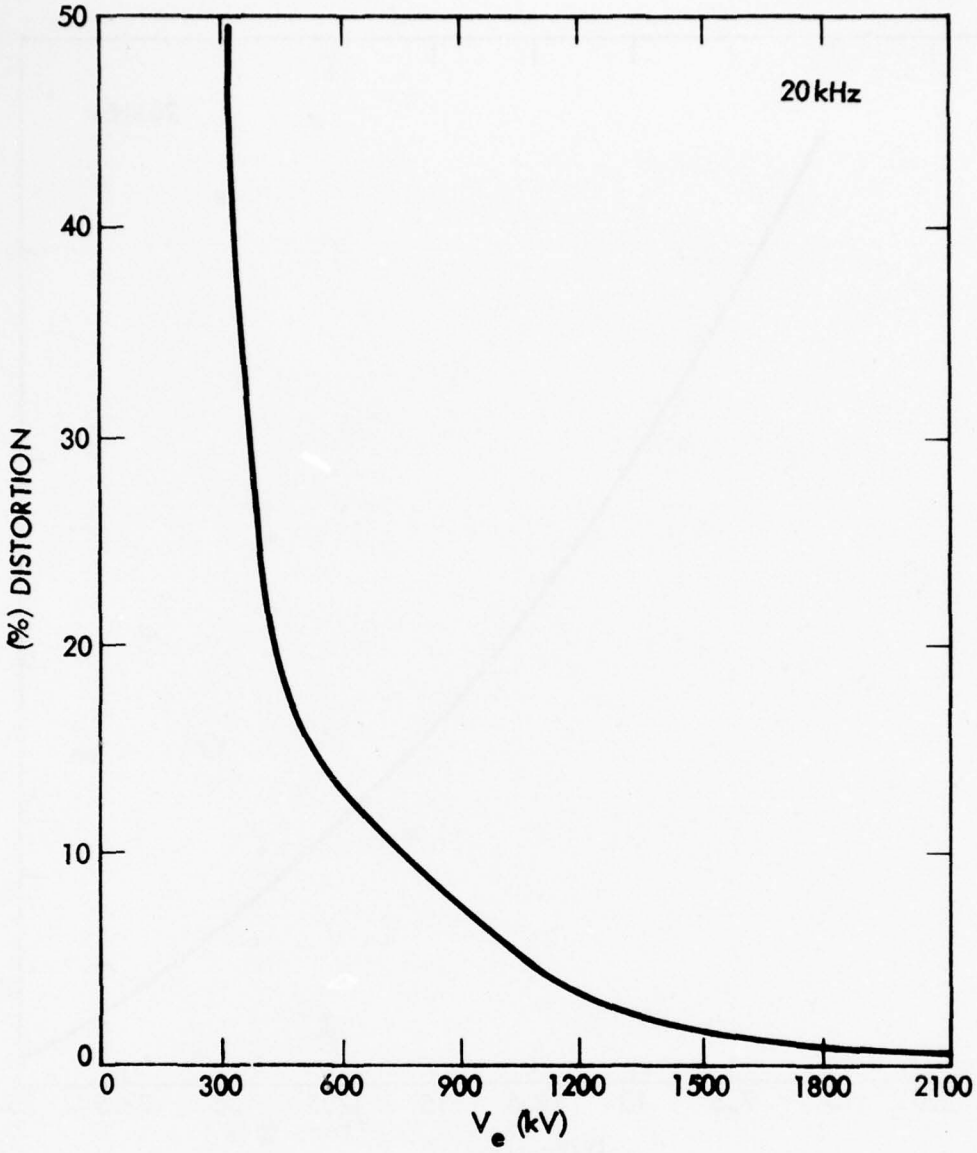

Figure 2-10. Effect of Electret Voltage on Distortion

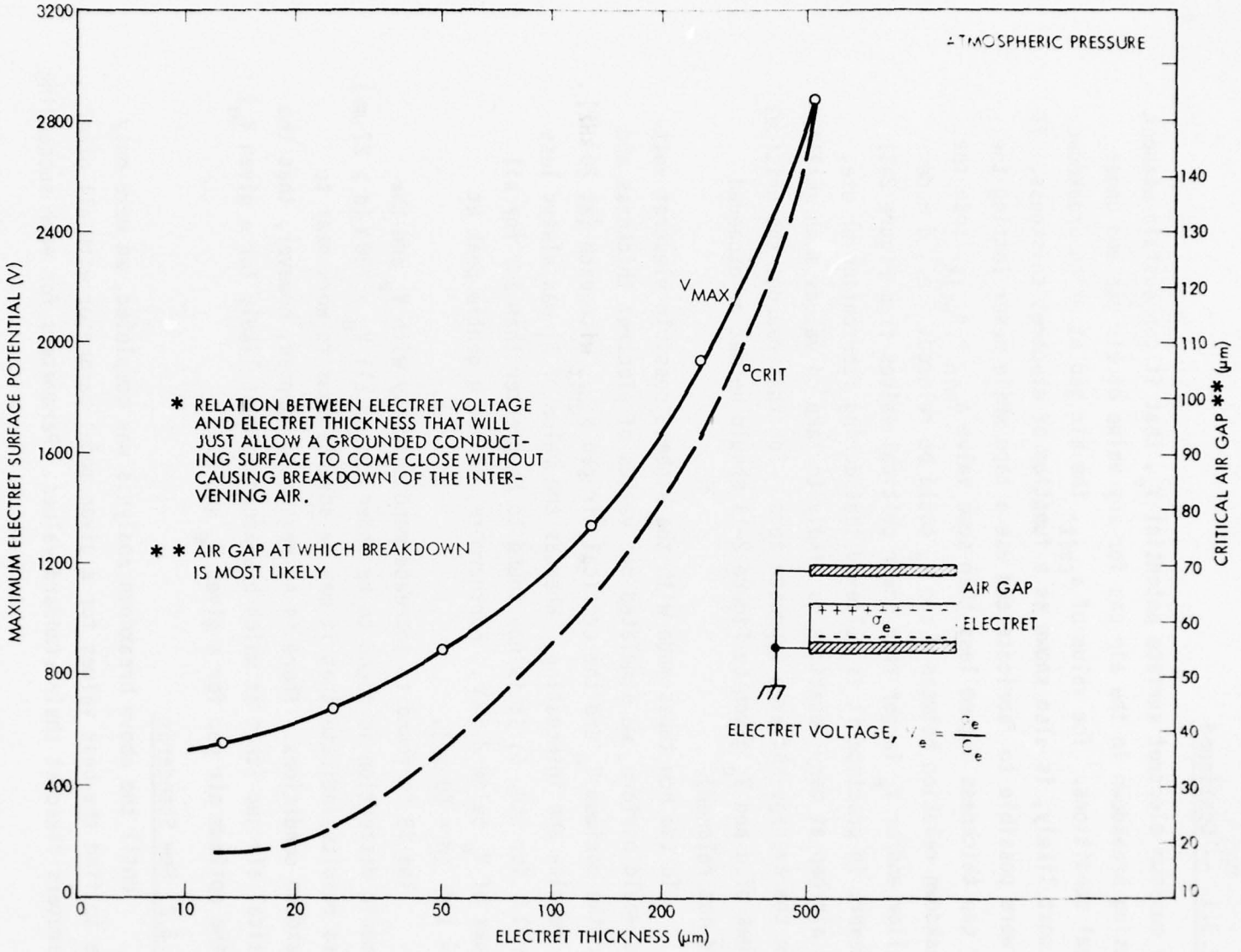

Figure 2-11. Maximum Breakdown - Free Electret Voltage vs. Electret Thickness

2.2.3.1 -- Continued

the maximum electret surface potential V_e, that it can sustain without causing breakdown in the air gap for any value of air gap and under ideal conditions. The value of a_{crit}, the air gap at which breakdown is most likely, is also shown as a function of electret thickness. If it were possible to fabricate and use a tape while never letting the air gap thickness become less than some value $a_{min} > a_{crit}$, then the breakdown relation between d and V_e could be relaxed; i.e., d made smaller and/or V_e larger than their critical values from Figure 2-11. However, in practice it is believed that during fabrication or use, the air gap at many locations is likely to take on values much smaller than the average and even approach zero. For this reason, the critical values of d and V_e given by Figure 2-11 should be met or exceeded (and not relaxed).

To see how tapes made with the highest possible electret voltages would perform, we simulated ten values of electret thickness and used the maximum V_e and the critical air gap a_{crit} with each (at 20 kHz). The results are interesting. Whereas the value of R_i was always less than 1 Ω for Std. 6, it is now found to be greater than 1 Ω for all values of V_e below 2.5 kV. Furthermore, it has a gentle peak at $V_e \doteq 1$ kV ($d = 60\ \mu m$).

The SS is found to increase monotonically with V_e and the harmonic distortion is found to be under 1% for all $V_e \geq 700$ V ($d \geq 27\ \mu m$). These results indicate that it may be advantageous to work near to breakdown conditions. There is no reason to suppose, however, that the critical air gap (that at which breakdown is most likely for a given V_e) is the optimum air gap for a given V_e and d.

2.2.3.2 New Standards

Until the above breakdown analysis was completed, we were only able to find the best values for a given model parameter with all other parameters fixed at their standard values. Parameters for each succeeding

2.2.3.2 -- Continued

standard are then modified at least in the direction (if not to the degree) indicated by results using the last standard. This amounts to a relaxation procedure that is very slow in converging to an optimum parameter set especially since the effects of the various parameters on SS are often strongly interdependent. Now we can pick pairs of d and V_e using Figure 2-11 and use the model to see what a_o gives the best results for each case.

In the previous runs using Std. 6, it was found desirable to use a larger V_e and a larger moving mass. Accordingly, Standards 7, 8, and 9 were chosen to have three different electret thicknesses, each charged to the maximum voltage V_e, and with the moving mass increased to bring down f_r the frequency of mechanical resonance to the 20 kHz region for an air gap of 70 μm. Table 2-1 gives the values of the main design parameters in Standards 6 to 10.

TABLE 2-1. SOME PARAMETER VALUES FOR STANDARDS 6 - 10.

	Std. 6	Std. 7	Std. 8	Std. 10	Std. 9
V_e(V)	-300	-530	-1080	-1500	-1960
d (μm)	50	12.5	76.2	155	254
a_o (μm)	50	70	70	70	70
M (kg/m^2)	41	123	123	123	123
f_r (kHz)	41.6	20.5	20.5	20.5	20.5

2.2.3.3 Results Using Standards 7, 8, and 9 $R_s \geq 1\,\Omega$

It was found that SS for these standards is considerably higher than for Std. 6. Further it was found that by varying the air gap, a best value could be found for each standard. These results are summarized in Table 2-2. The corresponding value of SS for Std. 6 was 28.

2.2.3.3 -- Continued

TABLE 2-2. PERFORMANCE FOR STANDARDS 7, 8, and 9 (20 kHz , $R_s \geq 1$)

	SS (mV/W)		a_o(μm)	
	Using			
Standard	Normal a_o	Optimum a_o	Normal	Optimum
7	71	78	70	83
8	96	133	70	120
9	160	195	70	140

It appears that we have found a tremendous improvement in system performance (20 to 195 mV/W). However, there is a slight snag. If we define the Q of the series indicator as $Q \equiv \omega L/R_s$ then the Q's implied by the above cases using optimum a_o are 1045, 1568, and 2540 respectively, for Stds. 7 to 9. Such Q's are probably too high for realizability.

2.2.3.4 Results Using Q Limits on the Inductor for Stds. 7 to 9

Since a Q of 500 appears to be close to the practical upper limit, Stds. 7 to 9 were re-examined using the criterion that $Q \leq 500$ (rather than $R_s \geq 1\,\Omega$). In other words $R_s = R_i$ unless $R_i < -X_i/Q$, in which case $R_s = -X_i/Q$ where Q = 500. The results are shown in Table 2-3. This time (with Q controlling the value of R_s) the SS is not improved so dramatically by the use of the best value of air gap (although performance is still considerably better than that for Std. 6). If a Q of 500 in the series inductor is achievable, these results indicate the desirability of working at as high an electret strength as possible (at least up to about V_e = 2 kV).

TABLE 2-3. PERFORMANCE FOR STANDARDS 7 to 9 (20 kHz , Q ≤ 500)

	SS (mV/W)		a_o (μm)	
	Using			
Standard	Normal a_o	Optimum a_o	Normal	Optimum
7	63	66	70	65
8	96	103	70	8[illegible]
9	120	128	70	57

However, by this time some laboratory measurements showed that lower Q's are much easier to achieve (they are also more economical). So we repeated the entire investigation of Stds. 7 to 9 (and added Std. 10) using Q's of 80 and 200. The results are plotted in Figures 2-12, 2-13 and 2-14, one for each value of Q. Each curve shows all the performance parameters along with the main design parameters for the conditions 20 kHz , a 1 V source voltage, a 3 m tape length and the optimum air gap for each V_e. From roughly top to bottom (Figure 2-12) the parameters are: V_a(V) the DC voltage across the air gap, I(mA) the current out of the driving amplifier, a(μm) the average air gap, SS(mV/W) the overall system sensitivity x(nm) the displacement of the moving layers, VTR (V/mV) the ratio of driving to receiving voltages across the series inductor, $R_s(\Omega)$ the series resistance of the inductor to meet the Q criterion, L, the series inductance required to match $-X_1$ at 20 kHz, OLS(mV/Pa) the open load sensitivity ($C_i \neq 0$), 2 HD (%) the second harmonic distortion, and η(%) the radiation efficiency. These figures afford a very clear picture of what is happening in the tape transducer as V_e is increased but the achievable Q is constrained.

2.2.4 Optimum Design

In examining Figures 2-12 thru 2-14 carefully, it is noted that for each value of maximum Q there is some electret voltage for which

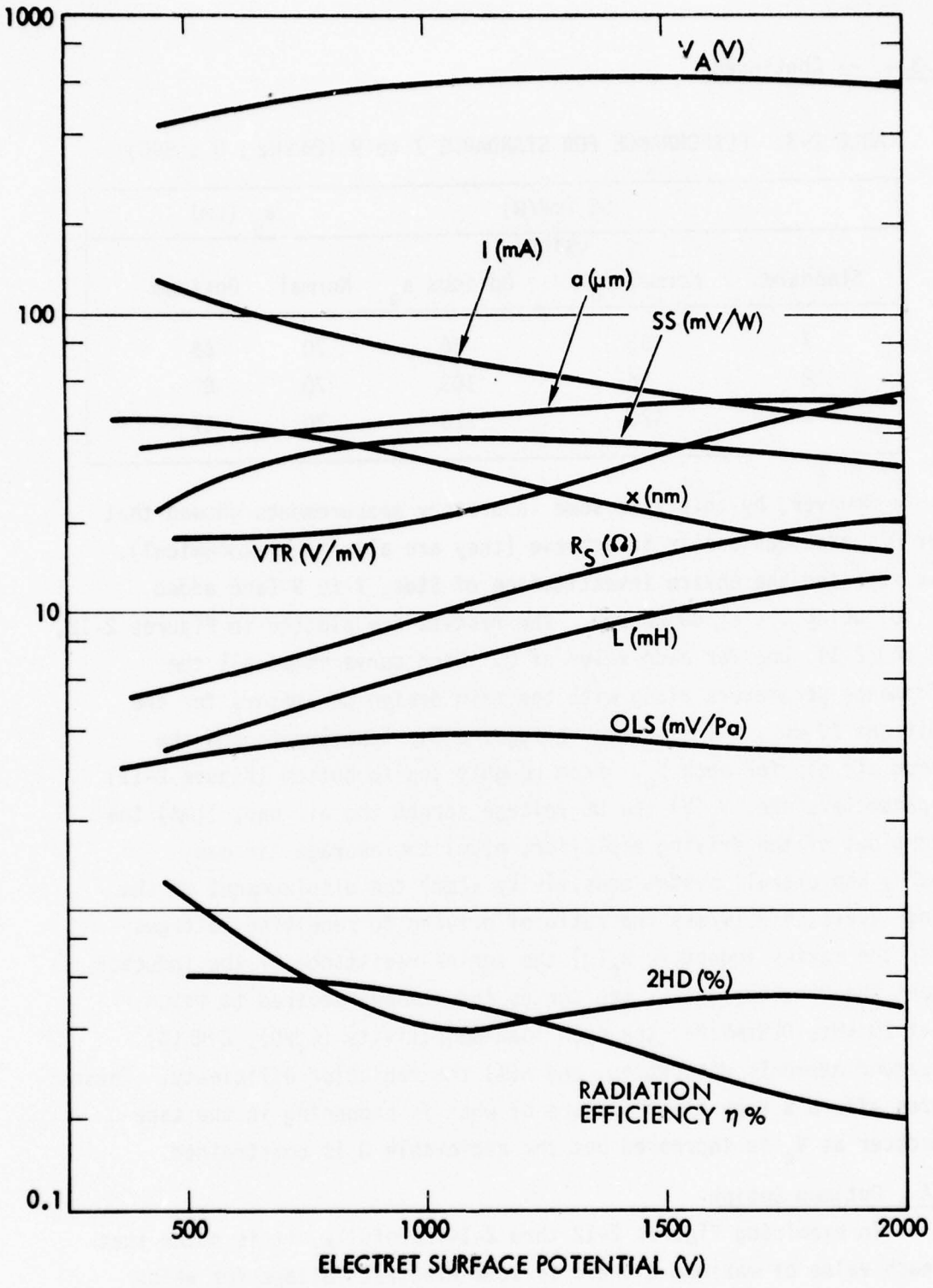

Figure 2-12. Effects of Electret Strength on Transducer Parameters, Q=80

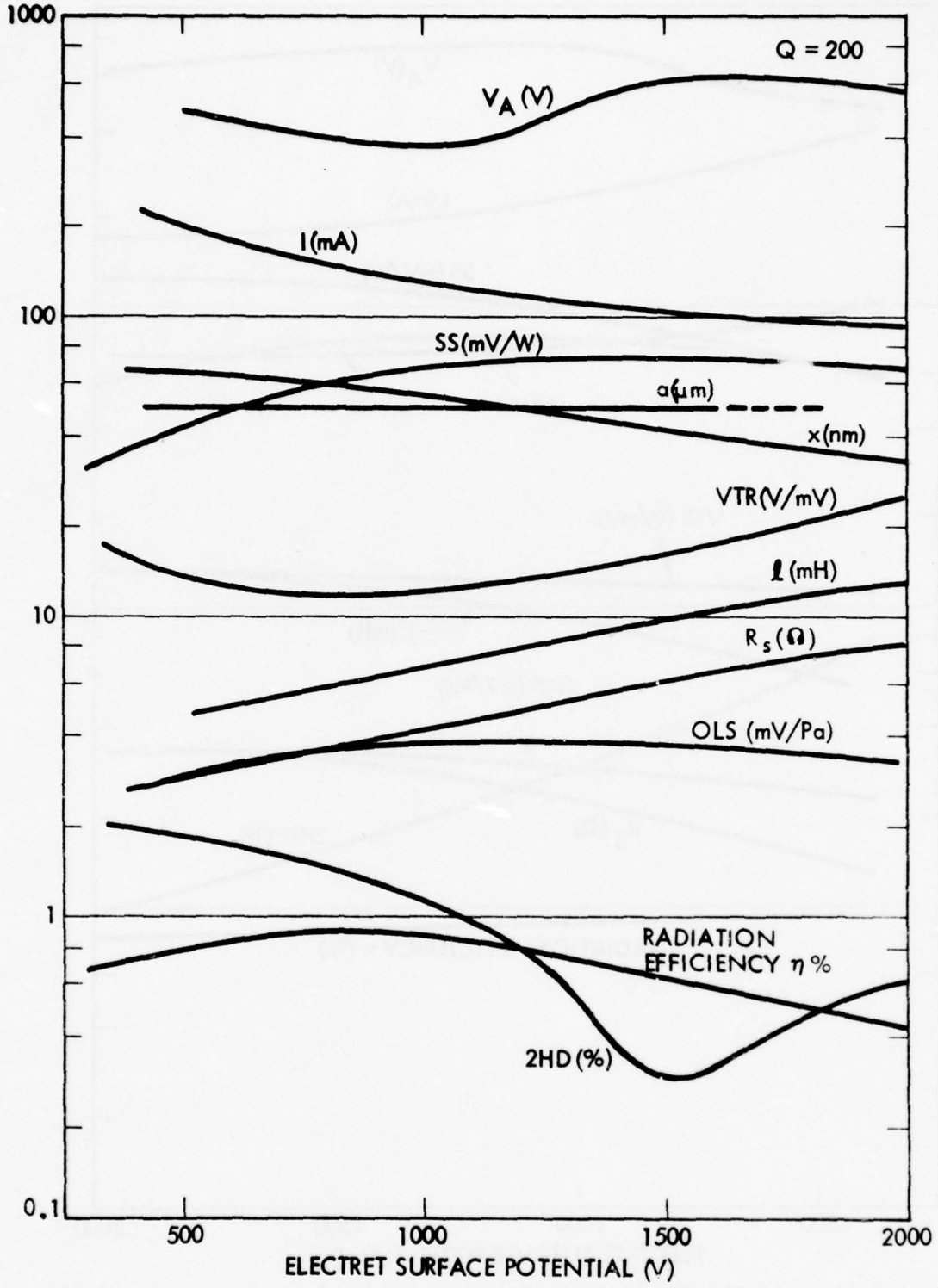

Figure 2-13. Effects of Electret Strength on Transducer Parameters, Q=200

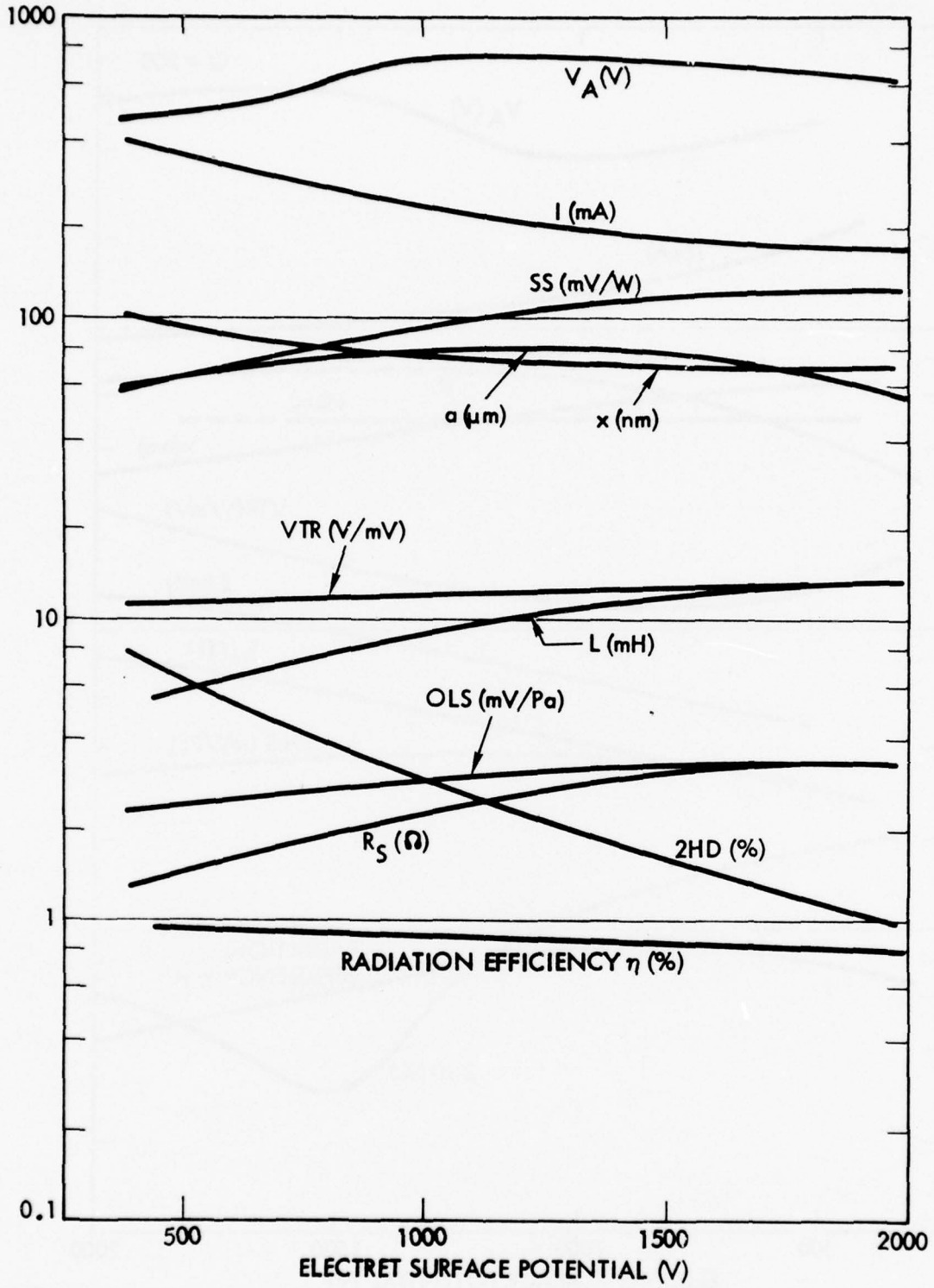

Figure 2-14. Effects of Electret Strength on Transducer Parameters, Q=500

2.2.4 -- Continued

SS is a maximum; and the bigger Q is the bigger the value of SS_{max} is. Since the best values of air gap and no breakdown dielectric thickness are already incorporated into these curves, the conclusion is that once the value of Q of the source circuit is fixed, the design of the optimum transducer can be obtained. Figure 2-15 shows the design parameter values for these optimum designs as functions of the achievable Q, and Figure 2-16 shows the resulting performance parameters as functions of Q (all for 3 m tape with 1 V drive at 20 kHz).

We see that it is advantageous to have as high a Q as possible but that this requires a fairly high value of electret voltage (1150 V for Q of 100) that increases monotonically with Q. It also requires increasing current drive from the power amplifier (but the current at Q = 500 is still only 57 mA/m). The required matching inductance also increases with Q while the source resistance, of course, decreases with Q. Still, under these optimum conditions, the series resistance R_s can be as big as 5 Ω at Q = 250 and even 10 Ω at Q = 90.

Curiously, the open load sensitivity and optimum air gap thickness are nearly independent of Q being 3 to 4 mV/Pa and 40 to 54 μm , respectively. It appears highly desirable to achieve a Q of about 200 or more since the performance drops off more rapidly below that value.

One of the more important parameters for purposes of designing the associated signal extraction electronics is the ratio of driving to receiving voltages across the inductor. The smaller this quantity, the easier it will be to extract the target reflected signal from the composite that includes the driving signal. It is noted that for a Q of 100 or more, this ratio is 20,000 or less ($\leq$ 86 dB). This means that the hybrid and multiplier must be able to achieve about 98 dB rejection of the fundamental in order to successfully extract the doppler-shifted received signal.

2.2.5 Effect of Tape Length

The optimum design in the previous section was developed for a tape length of 3 m . We were quite interested in finding out how

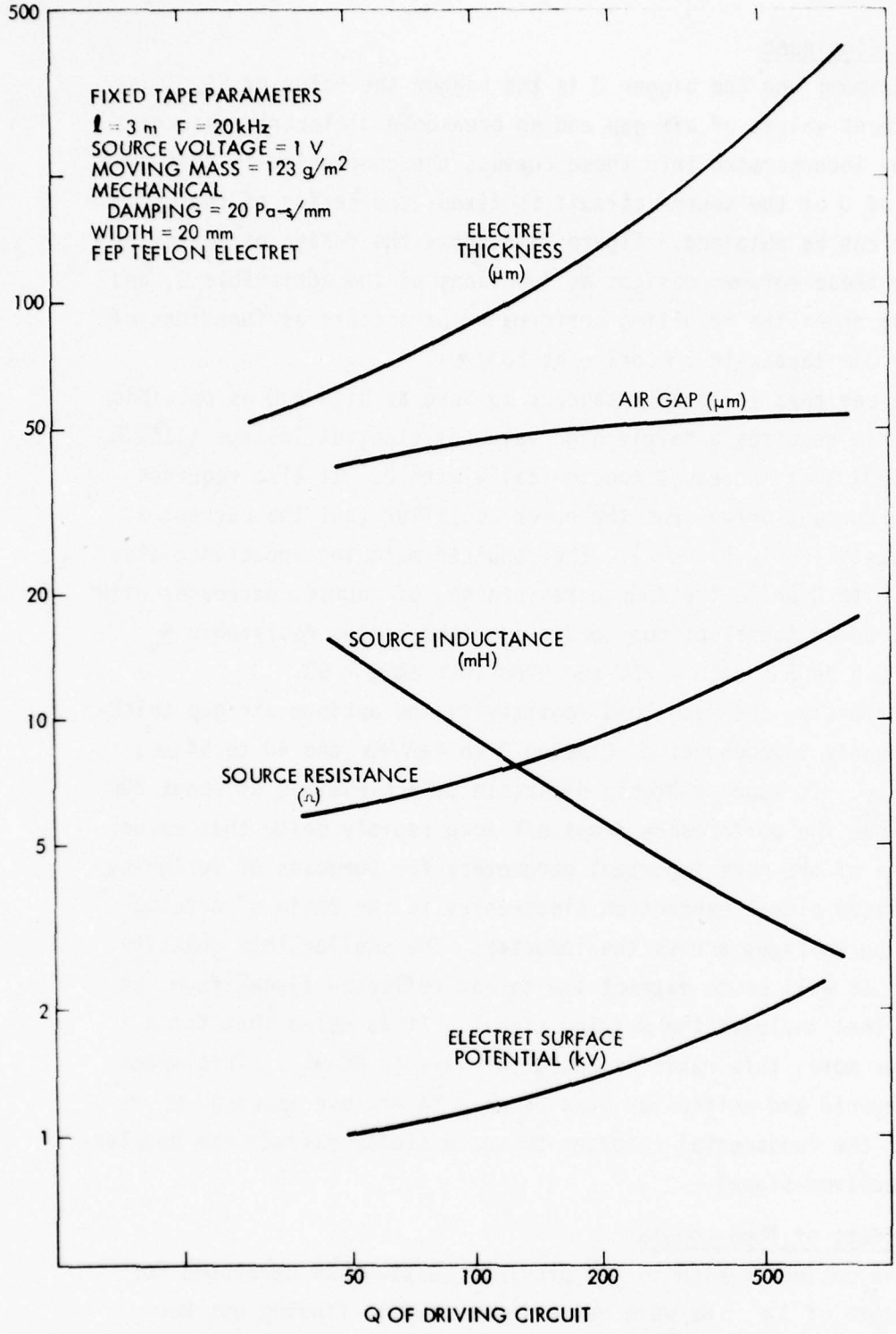

Figure 2-15. Effect of Source Q on Optimum Transducer Design Parameters

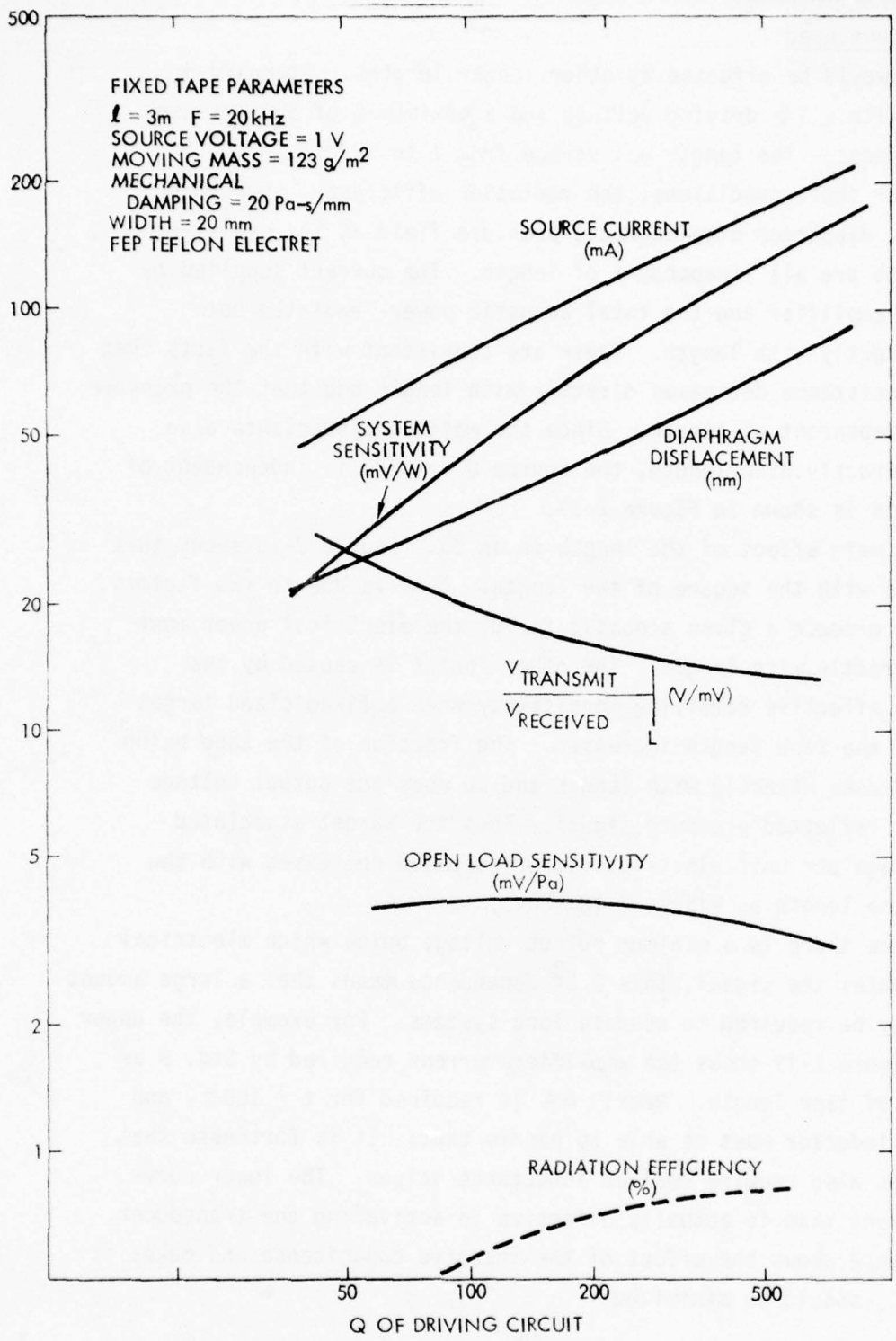

Figure 2-16. Effect of Source Q on Performance Using Optimum Design

2.2.5 -- Continued

performance would be affected by other longer lengths. Standard 9 at 20 kHz, with a 1 V driving voltage and a maximum Q of 500 was used for this purpose. The length was varied from 1 to 100 m.

Under these conditions, the radiation efficiency, open load sensitivity, diaphragm displacement, pressure field at any cross section, and beamwidth are all independent of length. The current supplied by the driving amplifier and the total acoustic power radiated both increase directly with length. These are consistent with the facts that the input resistance decreases directly with length and that the pressure field is independent of length. Since the matching inductance also decreases directly with length, the source $Q = \omega L/R_s$ is independent of length. This is shown in Figure 2-17.

The main effect of the length is on SS. Figure 2-18 shows that SS decreases with the square of the length. This is due to two factors. In order to produce a given acoustic field, the electrical power must increase directly with length. The other factor is caused by the decrease in effective receiving sensitivity when a fixed sized target is used and the tape length increases. The fraction of the tape being exited decreases directly with length and so does the output voltage for a given reflected pressure signal. Thus the target associated output voltage per unit electrical power supplied decreases with the square of the length as Figure 2-18 shows.

Since there is a minimum output voltage below which electrical noise dominates the signal, this $1/L^2$ dependence means that a large amount of power may be required to operate long systems. For example, the upper curve of Figure 2-19 shows the amplifier current required by Std. 9 as a function of tape length. Nearly 6 A is required for ℓ = 100 m, and the series inductor must be able to handle that. It is fortunate that longer tapes also require smaller inductance values. The lower curve is the current that is actually effective in activating the transducer. The difference shows the effect of the inactive capacitance and makes it clear why C_i should be minimized.

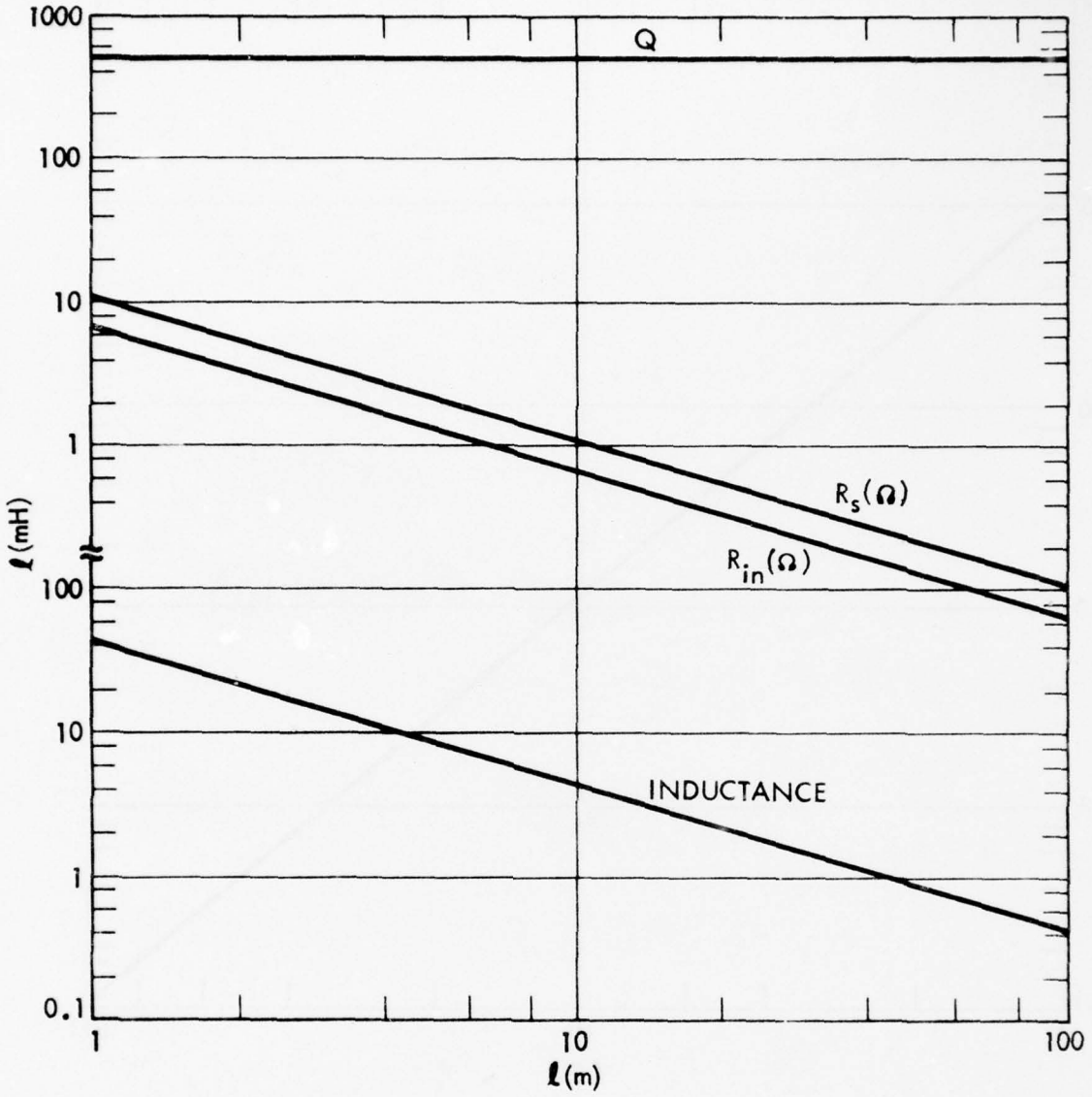

Figure 2-17. Effect of Tape Length on Source Q and Impedance

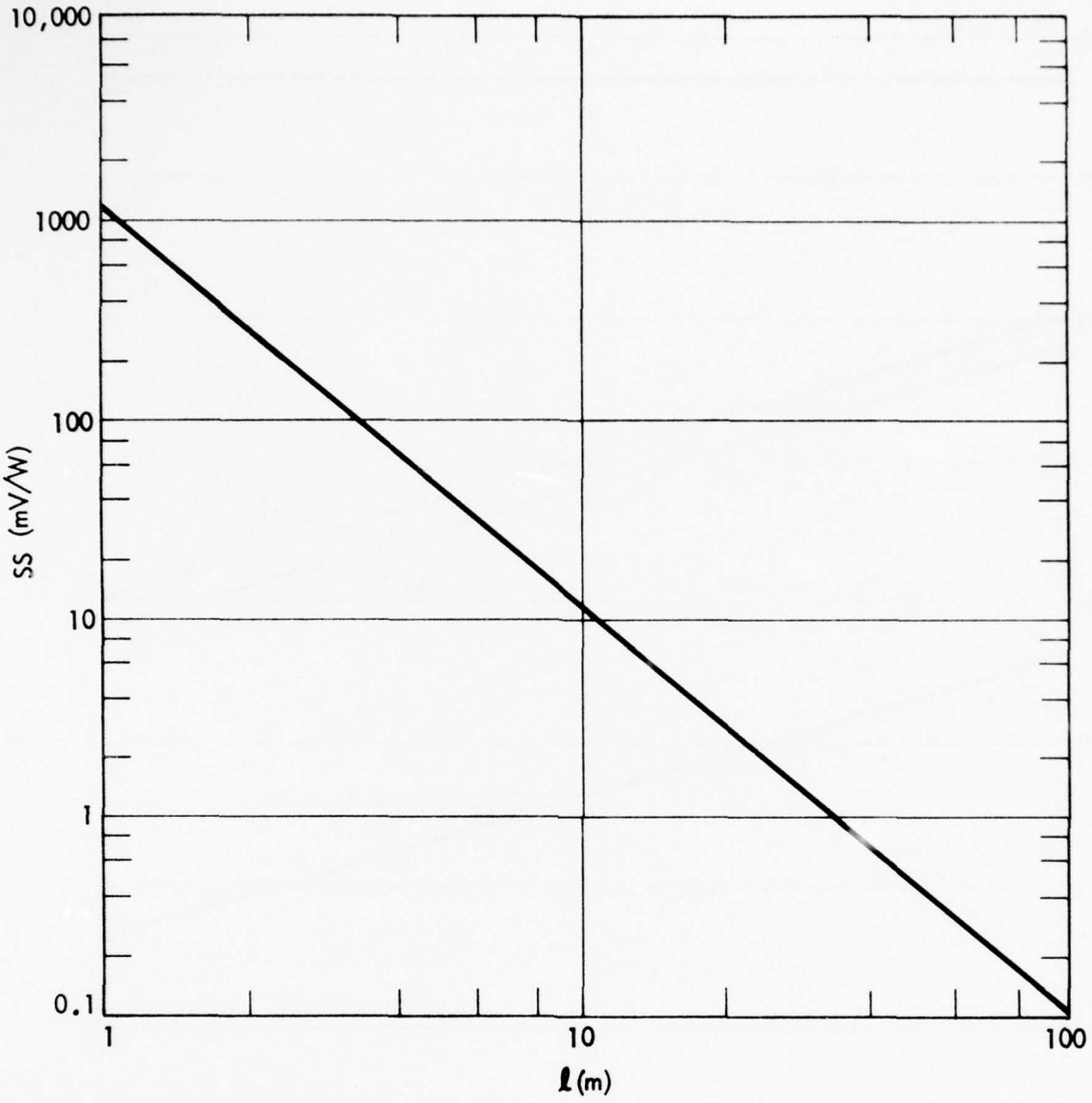

Figure 2-18. Effect of Tape Length on System Sensitivity

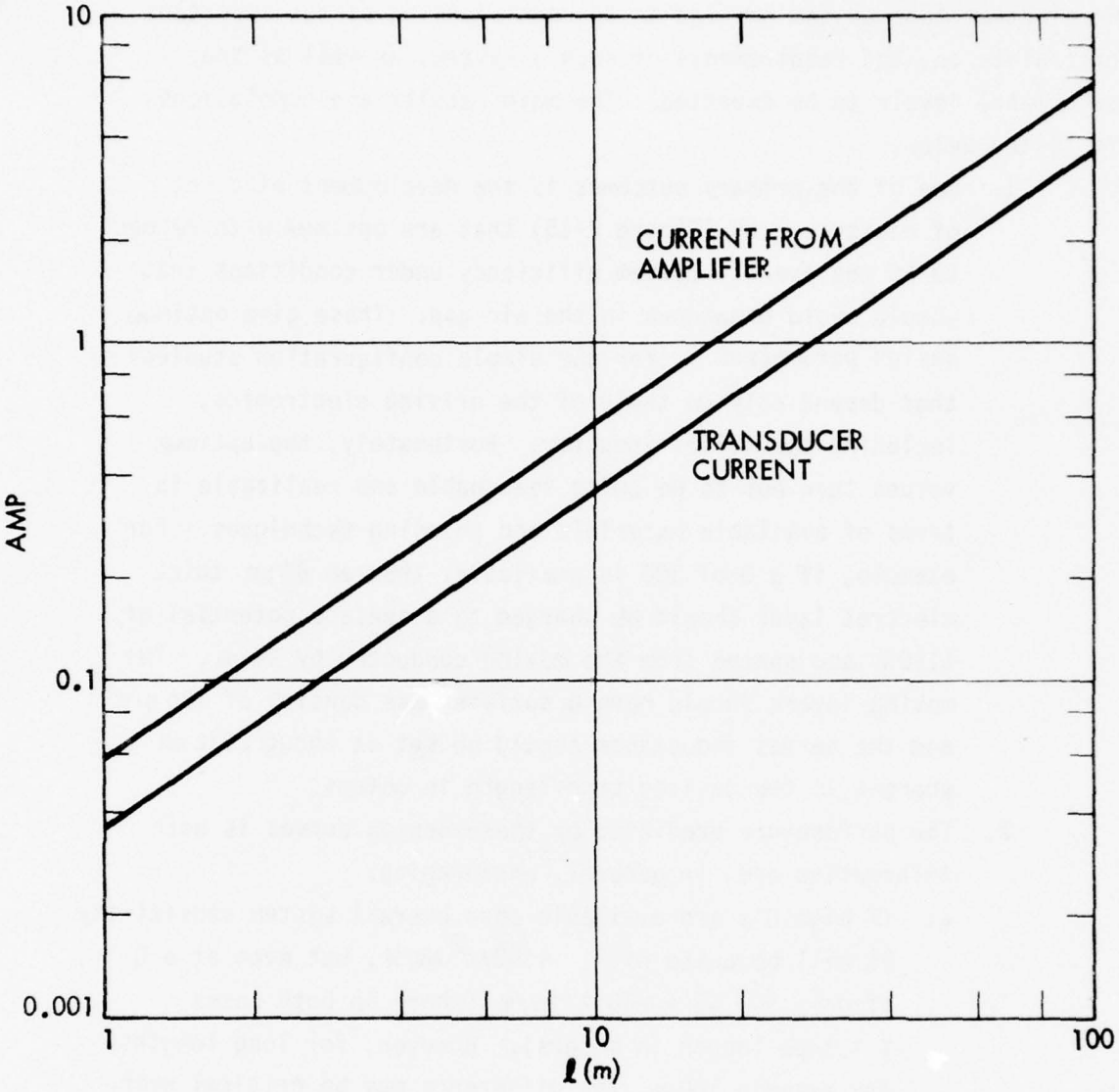

Figure 2-19. Effect of Tape Length on Electrical Current

2.3 CONCLUSIONS FOR MODELING

As described above the use of the improved computer model of the electret tape system has led to an understanding of the important constraints on, and requirements of such a system, as well as the performance levels to be expected. The main results and conclusions are listed below.

1. One of the primary outcomes is the development of a set of design curves (Figure 2-15) that are optimum with respect to SS the overall system efficiency under conditions that should avoid breakdown in the air gap. These give optimum design parameters (for the simple configuration studied) that depend only on the Q of the driving electronics, including the series inductor. Fortunately, the optimum values turn out to be quite reasonable and realizable in terms of available materials and charging techniques. For example, if a Q of 100 is available, then an 88 μm thick electret layer should be charged to a surface potential of 1150 V and spaced from the moving conductor by 46 μm. The moving layers should have a surface mass density of 125 g/m^2 and the series inductance should be set at about $22/\ell$ mH where ℓ is the desired tape length in meters.
2. The performance predicted by these design curves is both informative and, in general, encouraging.
   a. If high Q's are available then overall system sensitivity SS will be quite high, $\sim 1150/\ell^2$ mV/W, but even at a Q of only 50, SS $\approx 240/\ell^2$ mV/W (where in both cases ℓ = tape length in meters). However, for long lengths, for example 100 m, the difference may be critical with respect to the extraction of the reflected signal without requiring an impractical amount of drive power.
   b. The radiation efficiency is from 0.4 to 0.8 % over the range of Q from 70 to 500. These are very good efficiencies for active electrostatic devices.

2.3 -- Continued

c. The open load sensitivity is between 3.5 and 4 mV/Pa . This is only about 10 dB below the sensitivity of the 1/2" B&K condenser microphone.

d. Drive current is on the order of 20 to 60 mA/m for a 1 V source. The higher the Q the more current drawn.

e. The ratio of voltages across the inductor due to the transmitting and receiving operation decreases with Q, but is in the range 4.5 ℓ to 10 ℓ V/mV for Q's from 50 to 500 (where ℓ = tape length in meters). This number represents the difficulty with which the received signal can be extracted, so the smaller the better. If it is assumed that only 100 dB of extraction can be obtained in the hybrid and multiplier stages of the processor, then the maximum usable length is given by $\ell \leq$ 10 to 20 m . Another way of showing the problem is to observe that a 100 m long tape will require a signal extraction capability of 113 to 120 dB (the smaller number applies to the larger Q's and vice versa).

f. If an optimum design is used then the second harmonic distortion will be negligible, and the displacement of the moving layer will never be as large as 100 nm for a 1 V drive at 20 kHz .

Section 3

TAPE FABRICATION CONSIDERATIONS

During and following the modeling tasks just described, a major effort was undertaken to actually design, assemble, and test ultrasonic tape transducers as both radiators and receivers. In particular, the task objectives were to develop an improved long tape with optimized dimensions and materials, with increased and controlled electret strength, with improved uniformity of interlayer spacings and of such configuration that it could be easily adapted to large scale manufacturing techniques. This section documents the progress made in each of these areas (except dimensional optimization which came out of the modeling effort).

3.1 CONTROLLED CONTINUOUS ELECTRET CHARGING TECHNIQUE

Even before the computer analysis showed the necessity for achieving specific charge levels in the electrets in order to obtain best performance from a given configuration, it was considered important to develop a charging method that would be both controllable and adaptable to continuous operation on long lengths. In the previous effort[1] a liquid-contact method was developed using a sponge saturated with ethyl alcohol as the positive electrode. It was adequate for the short samples, but the electret strengths varied considerably among samples using what seemed to be identical treatments.

3.1.1 Mechanical Apparatus

Even if the same charging method were used we knew that an apparatus capable of allowing continuous charging of long samples would be required to make the long tapes anticipated for this program. The design of such an apparatus was one of the first tasks undertaken. It was designed to be adaptable to several charging techniques as well as a charge measurement procedure. Figure 3-1 is a sketch of the basic concept. The central member is a large smooth-surfaced wheel that is held

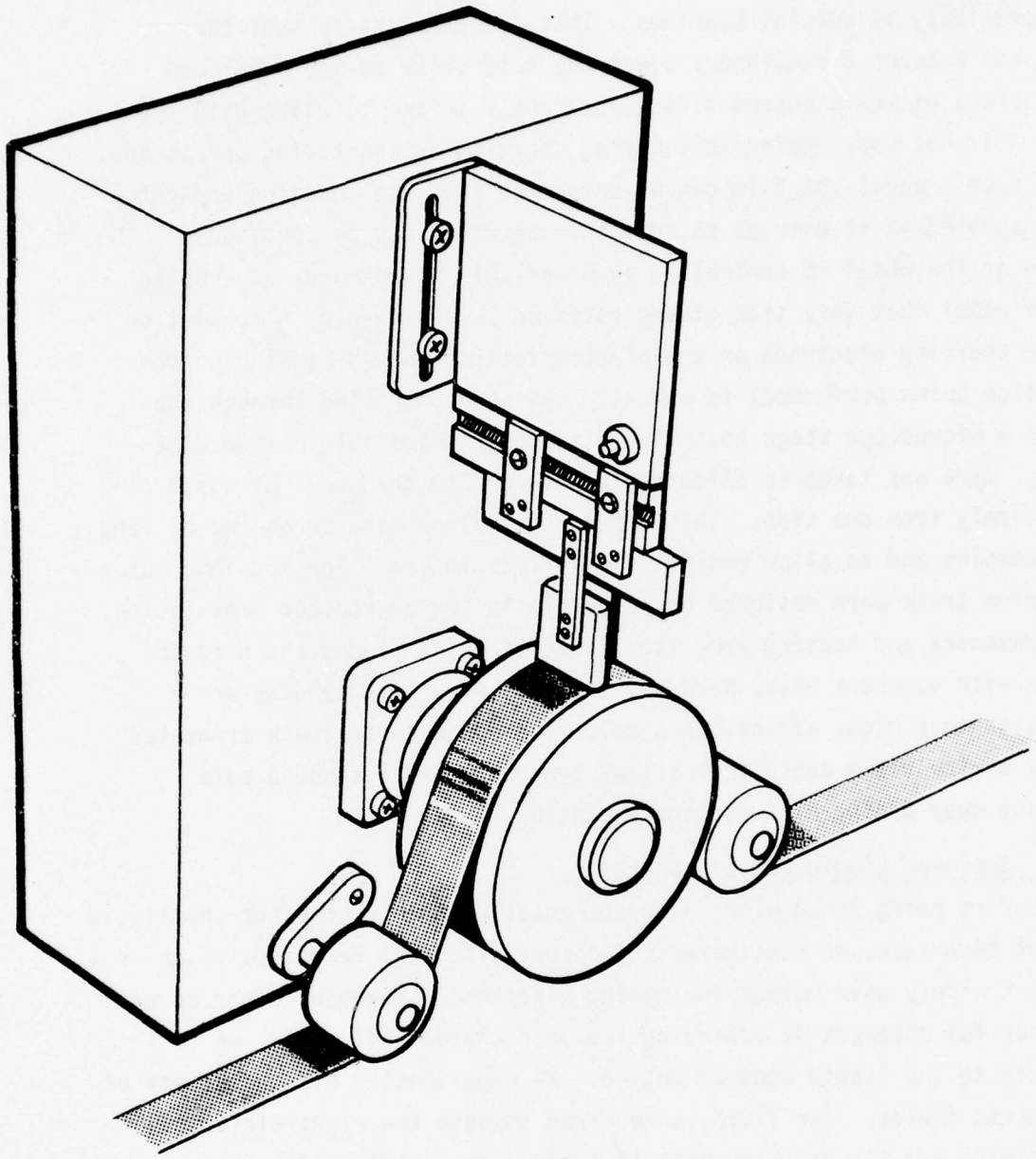

Figure 3-1. Long Electret Tape Charging and Measuring Apparatus

3.1.1 -- Continued

very precisely by special bearings. This is necessary so that the clearance between a stationary electrode held close to the wheel and the surface of the electret film held tightly to and rotating with the wheel will not vary appreciably during charging or monitoring operations. Using such a wheel the film can be unspooled into the charging apparatus and respooled as it emerges so that the operation may be continuous. The motion of the wheel is controlled by a variable speed motor so coupled to the wheel that very slow steady rotation is achievable. The portion of the charging electrode or the electrostatic probe (depending on the operation being performed) is manually set and controlled through the use of a microscope stage that is continuously adjustable in two dimensions. Care was taken to allow maximum access to the wheel by supporting it entirely from one side. This was done to allow easy threading of long tape samples and to allow maximum flexibility in use. The housing, motor, and drive train were designed to be usable in any convenient orientation. The framework and housing were fabricated of thick plates and held together with numerous heavy hardware to avoid excessive bending or vibration that might affect the wheel. The speed control was connected to the device via a cable that allows the operator to stand a safe distance away during high voltage operation.

3.1.2 Improved Liquid Contact Charging

Before going ahead with an experimental program to improve the liquid contact technique, we considered the corona discharge technique which is the most widely used method for making electrets. However, after several unsuccessful attempts at achieving improved charge uniformity, we returned to the liquid contact method. We experimented with a variety of dielectric fluids. The fluid is required to have the right electrical resistivity and the property that it evaporates rapidly under room conditions. It was eventually found that a mixture of clean ethyl alcohol, pure isopropyl alcohol, and acetone was consistently able to charge FEP films to surface potentials approximately equal to applied DC voltage.

3.1.2 -- Continued

In addition, it was found unnecessary to use a sponge that pushes against the film to be charged. Instead, a bead of the dielectric fluid is self-containing under the influence of the applied field. Thus, even as the tape continues to move past the stationary charging field, very little of the fluid leaves the bead at the tip of the sponge where the electric field is most concentrated. This effect is called electrophoresis, and it is found to be much more effective in electret charging than physical sponge contact. It was also discovered that the reason for the variability in previous results using ethyl alcohol is the tendency for this fluid to become contaminated unless great precautions are taken. The contaminants change its resistivity by varying but significant amounts.

Because of the relative simplicity and effectiveness of the improved liquid contact method (using a special fluid mix and electrophoresis to hold the charging bead in place), we were concerned that the resulting charge might not be as permanent as that obtained in other more difficult ways. We tried several kinds of heat treatments to see if the charge decay process could be reduced significantly. Only one seemed to have any beneficial effect. When two charged samples are placed face-to-face (negatively-charged-surface to negatively-charged-surface) and then baked in an oven at 300°F for 1.5 hours, the uniformity of the charge distribution over the surface is significantly enhanced (although the charge level is approximately halved).

We also tried fixing the charge by spraying a dielectric coating over the charged surface. When a TFE spray (Crown) was used, the result was immediate and complete discharge (or neutralization) of the sample charge. A silicone spray (MS-2300) had a negligible effect on the charge level, but also did not seem to effect the charge decay.

Subsequent measurements over a period of time indicate that the improved liquid contact charging method produces permanent electrets with decay rates typically as low as those reported in Ref. 1 (1 dB/time doubling after first ten days). Figure 3-2 is a photograph of the

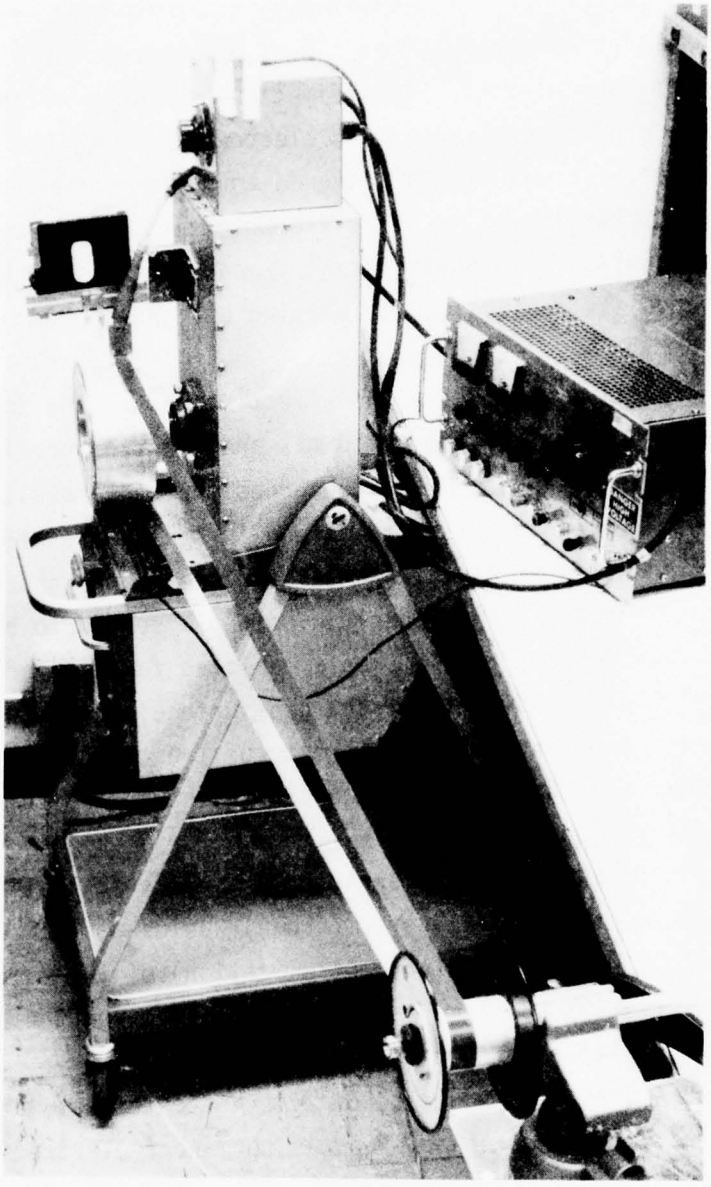

Figure 3-2. Continuous Tape Charging Apparatus

3.1.2 -- Continued

charging apparatus being used to charge a ten-foot long, fuze-bonded, FEP-to-copper strip made into a continuous loop. Figure 3-3 shows a measurement of the surface potential on a foot-long electret produced by this method. It is scanned lengthwise three times in the figure -- near the bottom, center, and top. The applied voltage was -2 kV. The charge level and uniformity over the surface are both excellent. We conclude that the objective of developing a controllable charging technique, suitable for long continuous tape lengths, has been met.

3.2 MATERIALS

Although the desirable layer thicknesses are usually specified for a given design by the computer, the materials to be used are much less constrained. Considerable thought was given and numerous contacts were made to provide a rational basis for choosing materials. Each layer (refer to Figure 2-1) is considered in the following paragraphs.

The moving layers consist of an outer protective insulating jacket and a conducting layer. These layers are usually supplied by a manufacturer as a laminated unit. According to the computer model, the combination should have a surface mass density of about 125 g/m^2. The conductor must be thick enough to conduct the driving current onto the active area (that facing the electret across the air gap). This, however, may be a rather high resistance because the shielding layer may be designed to be the primary ground conductor (since it has no mass constraint to meet as the moving layers do).

The requirement of low mass and low resistivity indicate that a useful figure of merit for moving conductor materials might be the product $F=(\rho \cdot r)^{-1}$ where ρ is the mass density and r the resistivity of the conductor. Table 3-1 compares F for various metals.

TABLE 3-1. FIGURE OF MERIT FOR MOVING CONDUCTOR MATERIALS

Metal	Aℓ	Mg	Be	Cu	Ag	Au	Ni	Steel	Stainless Steel
$F(m^2/g\text{-}\Omega)$	14	13	12	6.5	5.9	2.1	1.6	0.8	0.2

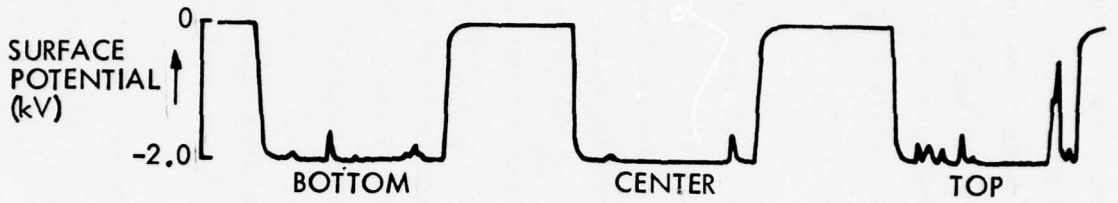

Figure 3-3. Measured Electret Surface Potential

3.2 -- Continued

Aluminum appears a clear winner when availability and cost facts are added to the information supplied by the table. However, at least one maker of electret microphones has abandoned the use of aluminized mylar for the moving layer because of deterioration of these layers with time when exposed to normal environmental temperatures and humidities.

The insulating protective jacket should be of a material that is tough, abrasion resistant and resistant to the effects of sun and moisture. It should also have a very low water vapor transmissivity since moisture that penetrates the moving layers will seriously degrade the transducer.

Mylar is the most plentiful of the jacket candidates that come with conducting layers, but many other strong but light plastics, capable of being fabricated in tape form would do. In particular, Tedlar (PVF) has outstanding weather resistance properties (but is somewhat expensive). We decided to use aluminum-coated Mylar for our laboratory work mainly because of its availability in a wide variety of thicknesses and widths.

In some designs, the air gap is maintained by use of a spacing material. Such a spacer must be quite thin, quite uniformly so, acoustically transparent (high percentage of open area), and must not exhibit electrical polarization under the influence of an adjacent electret layer. These constraints turn out to be difficult to satisfy. We tried nylon stockings (too thick and chargeable), open weave glass fabrics by Clark-Schebel, and a spun-bonded nylon fabric called Serex (Monsanto). The results are inconsistent and appear to indicate that the effective electret strength is degraded by the presence of the spacing layer. (Spacers were not used until the program was well advanced. They were difficult to obtain and were not carefully studied.) We found that using a textured moving layer was at least as good as using one of the spacing materials.

The electret layer is of FEP teflon. Other workers have already determined that this makes one of the best electrets. It's only drawback for this application is it's tendency to defeat the best adhesives.

3.2 -- Continued

In the transducer design it is very important that the FEP be rigidly bonded to a relatively massive center conductor. So far TME Corp., a small company near Boston, Massachusetts, supplies the most successful laminate, an FEP film fuze-bonded to a copper substrate. The copper center conducting layer must be thick enough to substantially outweigh the moving layer (125 g/m^2, remember?). A 7 mil thick layer of copper (giving a density ratio of 12.7 compared to the moving layer) is considered adequate (especially since the FEP also has its own mass to contribute).

The insulating layer beneath the central conductor is chosen to minimize the inactive capacitance. Hence, it should have a minimum dielectric constant and the maximum allowable thickness. A number of foam dielectrics are adequate for this. Silicone rubber foam and vinyl foam were used the most. Both are available in a variety of thicknesses and widths and with adhesives on one or both surfaces for convenience in fabrication.

The shielding conductor is required to provide electrostatic shielding (of the central conductor) and a low resistance path for the driving current. It may be required to handle several amperes of current and should not cause more than a few volts drop in potential out to the end of the transducer (perhaps 100 m). Surprisingly, a 4 mil thick layer of 1¼" wide aluminum has only 1 Ω resistance in 100 m. A similar copper strip would have only 0.6 Ω, so the shield layer need not be especially thick and can be of whatever conductor is more convenient or available.

The protective insulating base jacket should be of a tough material with high abrasion resistance and weather resistance. It should also be flexible so that the transducer may be rolled up without distorting the active layer appreciably. We used mylar for laboratory model purposes since it was readily available.

3.3 FABRICATION TECHNIQUES

Once materials and a design have been chosen, there is still the problem of how to put things together. In the previous effort; we hand-fabricated very short samples that usually turned out to have a rather high degree of non-uniformity. We gave no thought to possible large scale manufacturing methods. In this effort our fabrication objectives were to learn to make long tapes with more uniformity and to seriously consider the techniques and constraints of a future large scale manufacturing operation.

3.3.1 Laboratory Fabrication

3.3.1.1 Juicy-Fruit Configuration

One of the first transducer samples fabricated in this effort is sketched in Figure 3-4. The main feature of this configuration is the wrap-around layer of aluminum foil that serves as both moving layer and shielding layer and therefore requires no separate electrical connection between the two. The first model was only a few inches long and strongly resembled a foil-wrapped stick of gum; hence, the name, juicy-fruit (JF). The JF configuration has no protective insulating jacket, but this is no problem for laboratory work. The wrap-around concept seems a good simplification and the sensitivity of the first sample was about the same as those measured on samples made in the prior effort. One problem encountered with this design is breakdown between the edges of the center conductor and the aluminum wrap-around layer. To prevent this in subsequent samples a narrow strip of FEP adhesive tape was folded over the edges of the center conductor also enclosing the edges of the insulating layers on either side of it.

A 3m long JF sample was constructed using a 1/8" thick (rigid) aluminum strip for the substrate and shielding layer to see what fabrication problems would arise with the longer lengths. In this case, the moving layer (Aℓ foil) was tensioned over the sublayers and then bonded to the underside of the rigid substrate. Aside from the normal

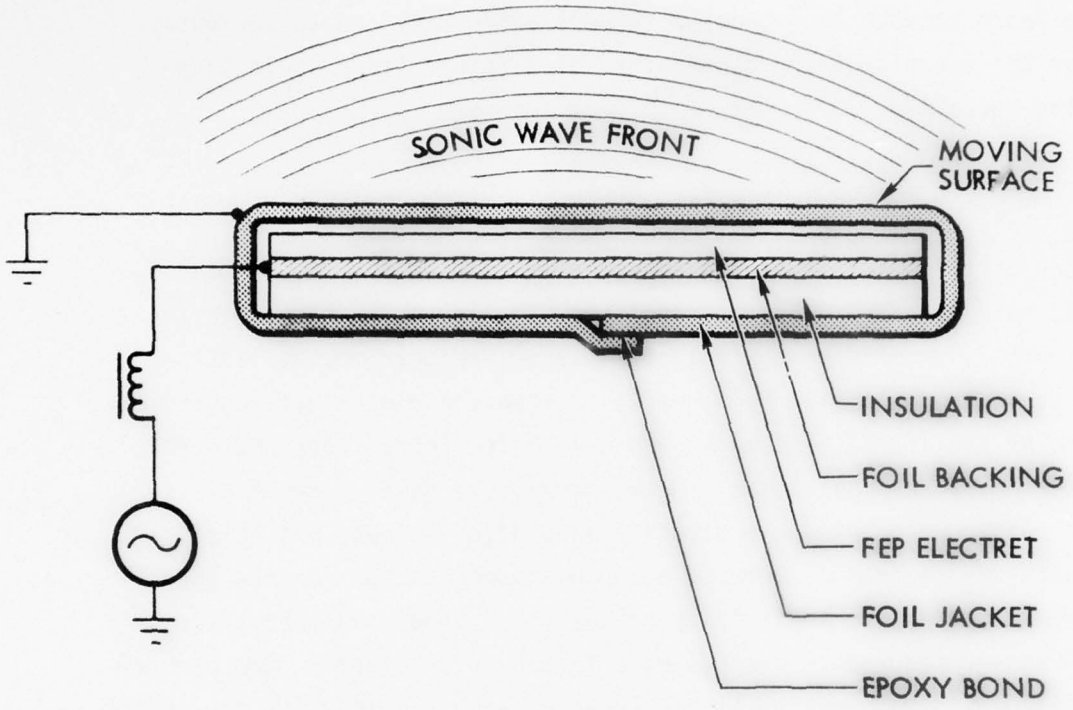

Figure 3-4. "Juicy Fruit" Transducer Configuration

3.3.1.1 -- Continued

problems of working with long strips to be bonded together, the only significant drawback was the problem of achieving uniformity of interlayer spacings, particularly with regard to the air gap layer. Even with the tension applied as uniformly as we could, the moving layer was visibly nonuniform in its spacing above the electret layer. This is perhaps the number one fabrication problem. After bending the sample (as in rolling), the nonuniformity becomes even more evident.

3.3.1.2 Bowed Configuration

The first configuration designed particularly to solve the nonuniform air gap problem is sketched in Figure 3-5. It is evident that now a tension applied to the moving layer develops a force normal to the sublayers thus tending to hold the moving layer against the supporting layers. Using this configuration it now becomes possible to not only maintain uniformity in the air gap but also to control the air gap itself by using a spacing material of the desired thickness. The layers above the substrate conform to its shape under the influence of the tensioned top layer. The bow will spread out the directivity pattern of the radiation somewhat, but this is not expected to be a problem.

When a flat tape is rolled up it tends to crinkle the moving layer surface. If stored rolled up for a long time, this would surely contribute to nonuniformity. However, when a bowed tape is rolled up, the upper surface is detensioned as it flattens. This means that the moving layers would be under tension only when the tape is in use, a fact that is expected to contribute significantly to its life as well as uniformity of performance. The key questions concerning this configuration are:

1. Is the required bowed substrate available or can it be easily manufactured?
2. How can the FEP layer be uniformly applied to the substrate?
3. How should the moving layer be tensioned?

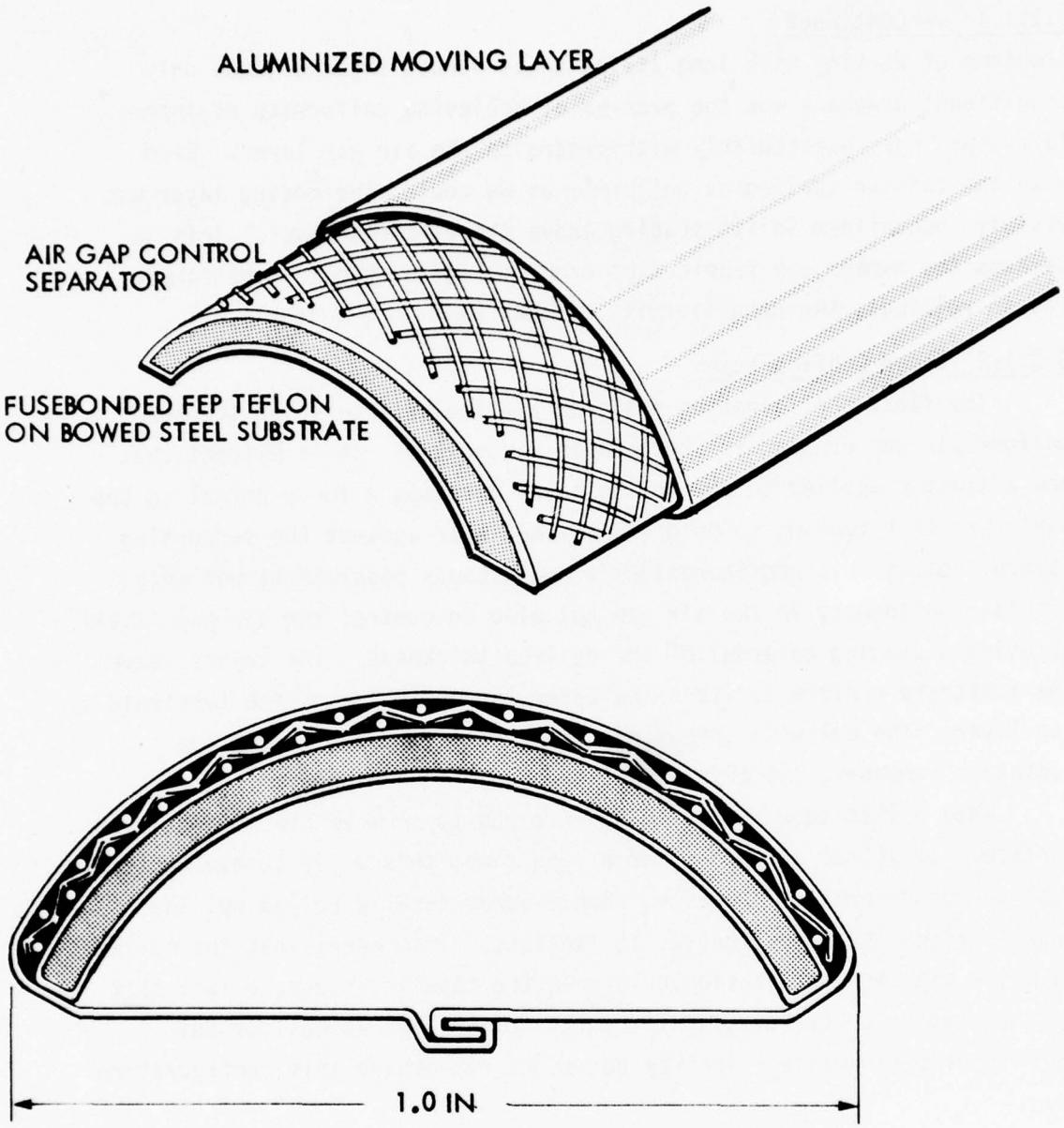

Figure 3-5. Bowed Tape Configuration

3.3.1.2 -- Continued

The key to this concept is the center conductor made of a spring steel or berylium-copper strip that is bowed so that its center is higher than its edges. In an effort to make our own bowed substrate we purchased a steel strip 200 feet long and had part of it bowed by a local company. However, it was not tempered sufficiently to hold its form and was distorted on receipt even though wound on a large 6' diameter form. The rest of the stock was then sent to another company for tempering. The tempering heat treatment, however, caused the bulk-wound steel to warp erratically, so that it was unusable for transducer samples. The short bowed samples we eventually made were on Be-Cu strips that were manually bowed using a bending machine or on undistorted short pieces of the commercially bowed steel stock.

It was thought that it might be difficult to accurately bond an FEP layer onto the bowed substrate in long lengths, so the possibility of spraying on the FEP coating was investigated. A local company, Fluorocarbon Co., is able to spray coat with FEP for lengths up to 18" at temperatures of 675^{o}F. We had them coat a number of foot-long bowed steel samples. The FEP layer turned out to be unsatisfactory because we could not charge it as desired. Either there were too many pinholes, or foreign particles deposited in the FEP during the process allowed localized breakdown under the application of high voltage. The insulation of the edges of the bowed center conductor is also unsatisfactory using the spray technique. The few remaining bowed samples we fabricated were made with adhesive FEP tape applied to the bowed substrate and with insulating edge strips folded around the center conductor's edges to prevent breakdown there.

However, the most difficult problem with the bowed configuration was found to be the tensioning of the moving layer. Figure 3-5 shows the moving layer neatly folded and bonded to itself at the midline on the bottom of the bowed sample. How do you do this in such a way that the tension is uniform all along the tape? We built a special apparatus to

3.3.1.2 -- Continued

spread and control the applied force uniformly along the tape on both sides, but we were unable to satisfactorily bond the loose edges of the moving layer without going to a solid rigid substrate.

Figure 3-6 is a photograph of a two-foot long bowed sample on a rigid base. The base is a 1" square aluminum tube. A short, solid square rod fits into the ends of two tubes to allow their connection. Seven such samples were built. Nylon stocking material was used as the spacing material. The resulting air gap is quite uniform even though this produced a gap larger than desirable. These handmade samples were among the most sensitive we measured, but they were very difficult to make and were rigid in sections. After we visited the potential tape manufacturers, this approach was abandoned.

3.3.1.3 Vacuum Concept

When it became clear that the bowed concept was not going to be practical (at least without extensive development in cooperation with a manufacturer), we developed a vacuum concept as a means for achieving the desired air gap uniformity in a flexible tape configuration. A sample of this configuration is shown in Figure 3-7. The idea is to apply a vacuum to the sealed air gap region to pull the moving layer down against the spacer (against it's own or textured surface) in a fairly uniform manner. To make an air tight seal for the vacuum, the moving layer and a base layer are extended to the sides and heat sealed between pressure rollers. There are machines available that do this kind of thing in packaging processes. The process is amenable to continuous manufacture, and it appears that tapes made in this way could be rollable without degrading subsequent performance.

The final transducer samples made in our lab during this program were of this type. Although we did not get a chance to thoroughly evaluate them, they appear to be good designs. One of the problems we came up against is finding a suitable conducting thermal adhesive for

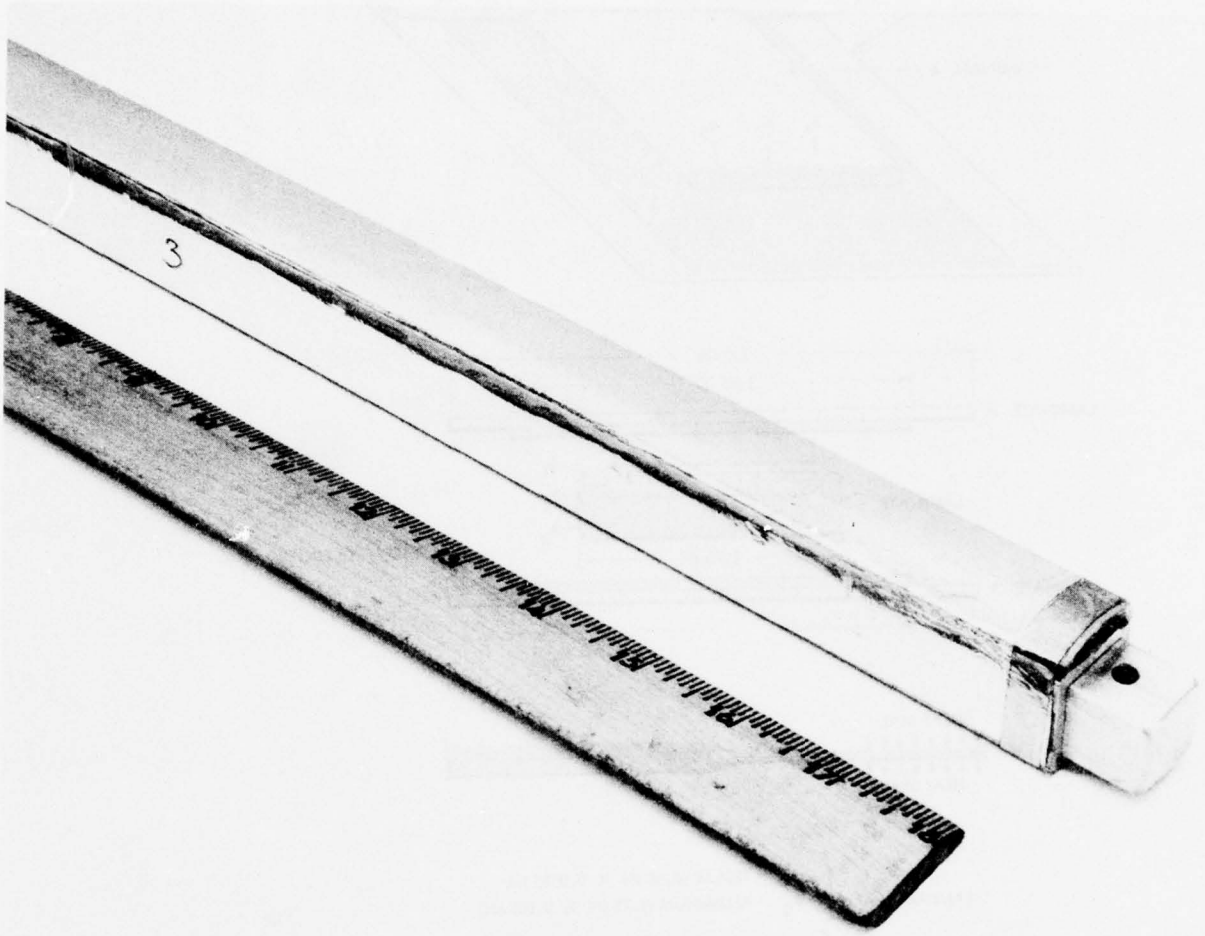

Figure 3-6. Bowed Tape Sample on Rigid Base

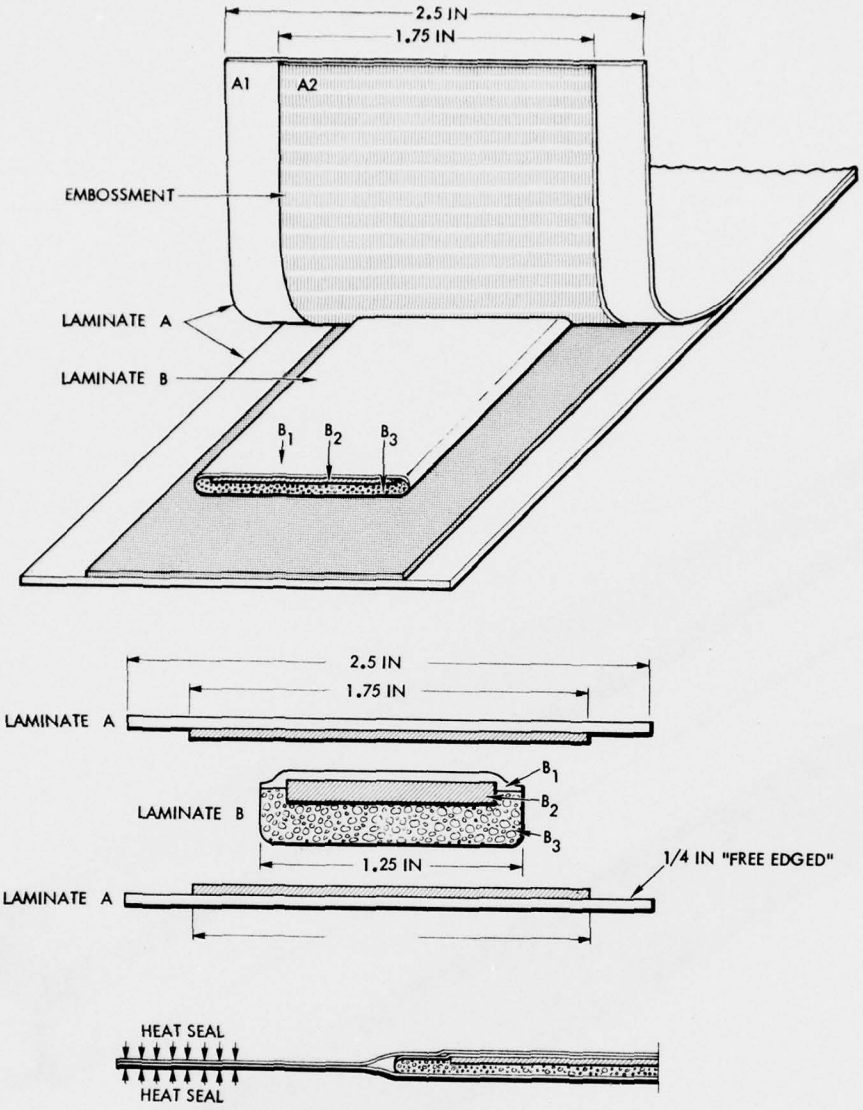

LAMINATE "A"
- A_1 → TEDLAR (2.50 IN X 0.0015 IN)
- A_2 → ALUMINUM (1.75 IN X 0.001 IN)

LAMINATE "B"
- B_1 → FEP TEFLON (1.25 IN X 0.003 IN)
- B_2 → COPPER 1/2 HARD (1.00 IN X 0.010 IN)
- B_3 → PVC FOAM (1.25 IN X 0.032 IN)

EMBOSSMENT
- LIGHTLY EMBOSSED METAL FOIL ZONE WITH DIMPLES ON METAL SIDE

1: LAMINATE A MOVING LAYER MASS 120-135 gm/m^2

2: BONDING LAYER B_1 → B_2 SHOULD BE FUSEBONDED

Figure 3-7. Vacuum Tape Configuration

3.3.1.3 -- Continued

between the top and bottom conducting layers. Good conduction is desired here to keep the resistance seen by the driver down, and good adhesion is required to maintain the internal vacuum. An adhesive made by Acme Chemicals and Insulation of New Haven, Connecticut appears to be adequate, but it was not discovered in time to order for this program. We used conventional conducting adhesives painstakingly applied by hand.

The longest tape samples we fabricated (9 m) were of the vacuum type. To give an idea what is involved, a description of the process is given below.

1. Moving layer preparation: Emboss wire screen imprint on moving layer with wire mesh on mylar side of MF-310 (by Lamart). This is done by rolling the MF 310 between the screen and a silicone rubber tape with all three materials in a pinch roller machine. The moving layer is cut to 2¼" width.
2. Center laminate (Electret) preparation:
   (a) Photo etch 1/8" of the copper from both edges of TME's FEP-copper 1" wide laminate strips. Solder these two foot long strips end-to-end for the desired length.

   (Alternate (a): On one side of a 1¼" wide 10 mil thick copper strip, roll on a layer of FEP adhesive tape 2 mils thick so that the FEP is centered.)

   (b) On the results of (a) roll on a strip of closed cell vinyl foam with adhesive on both sides. (Leave paper on exposed adhesive side.)
3. Tape moving layer mylar side down to a working surface and carefully clean the exposed conducting layer.
4. Charge the electret to -800 V and immediately place the entire center laminate with electret side down on the exposed aluminum surface of the moving layer so that it is well centered.

3.3.1.3 -- Continued

5. Cut a strip of aluminized mylar (MF 310) to 1¼" width, clean metal side carefully, and bond mylar side to the available adhesive side of the vinyl foam layer of the base substrate.
6. Bond the overlapping edges of the moving layer laminate to the exposed aluminum surface on the top of the 1¼" wide exposed aluminum surface using 1/8" wide conducting adhesive tape on both sides.
7. Lay two strips of 1" wide FEP tape to entirely cover the aluminum bottom of the sample as well as the conducting adhesive strips.

The tape is then ready to be turned over and used. This entire process takes about a day after practice.

3.3.2 Commercial Fabrication

One of the objectives of this program was to find out directly from potential electret tape transducer manufacturers just what constraints and capabilities should be considered in the design of a tape to be economically manufactured in quantity. Accordingly, in the last week of April we visited three companies and presented sketches of the bowed and vacuum concepts. The following paragraphs summarize our impressions.

TME Corp., Salem, New Hampshire

This is the company that makes the fuze-bonded FEP-copper laminate used most successfully in current and past samples. According to F. E. Driggers (V.P. Sales) this company has had financial difficulties. It is now operating in a turn-around-or-else mode and cannot do any research type jobs. They can, however, do the standard laminating tasks, and believe they can make the two multilayer strips to be used on each side of the air gap. They did not show us their facilities. The minimum stainless thickness they feel comfortable with is one mil.

Lamart Corp., Clifton, New Jersey

Mr. Willis Gray of Lamart felt that his company could make both the five-layer base laminate and the two-layer moving laminate. However,

3.3.2 -- Continued

they have no equipment for pulling a vacuum, and would prefer to simply supply the laminates rather than try to assemble them into the finished tape transducer. A tour of the facility was quite impressive. Numerous full-width laminating machines and a smaller research machine for multiple layers were in use. The main conducting materials were aluminum and copper while the main plastic was polyester (Mylar). Mr. Gray assured us that they can handle all of the materials we have been using so far and in the thicknesses that appear to be best to us.

He also cautioned us about the delay that we might expect to encounter due to the delay in obtaining materials after ordering them. The worst case mentioned was for FEP Teflon (6 weeks). Lamart also can do slitting if needed. Finally, when asked if they would like to get this kind of business, Mr. Gray responded, "Definitely".

Sheldahl, Northfield, Minnesota

Mr. G. P. Maas (Sales Manager) turned out to be a pleasant host who was technically knowledgeable in the area of mutual interest as well. He feels certain that Sheldahl could make the entire tape, but they would prefer to supply the laminated sections to someone else who specializes in continuous fabrication.

In Mr. Maas' experience, a laminate consisting of 1/2 mil mylar, sandwiching an aluminum layer and including a dacron fabric on one side can maintain a good vacuum for long periods (this was done inside helicopter blades to detect cracks in them). Sheldahl actually manufactures some products that use the laminated materials they produce (e.g., tethered streamlined balloons). We were given an interesting tour through the plant.

In summary, it appears that all three companies feel qualified to make the flat laminates required for the vacuum fabrication technique. None, however, really wants to manufacture the entire device by charging the FEP surface of one laminate, putting the two laminates together, sealing the edges, potting on connectors, and drawing a vacuum to make

3.3.2 -- Continued

a uniform air gap. None felt that the bowed tape concept was as easy to manufacture as the flat vacuum tape concept. Apparently, none has experience laminating onto a bowed surface or was anxious to start now.

Section 4

PERFORMANCE

So far we have discussed the theoretical analysis of the system and the fabrication of the tape transducers. Now we consider the performance as measured in the laboratory. First the transducer by itself, then the processing electronics and finally the combination operating as a system.

4.1 TRANSDUCER PERFORMANCE

In the previous effort[1] where the samples measured were only a few inches long, the open circuit sensitivity was found to be about -69 dBV/Pa after correcting for the inactive capacitance.

During the current study, considerable improvement over this figure was achieved with a variety of sample types. Values in the range -45 to -50 dBV/Pa are typical and this is the open load sensitivity (before correction for inactive capacitance which always degrades the sensitivity). Figure 4-1 shows a plot of measured sensitivity (solid line) along with a plot of the model prediction for a fairly similar sample. The agreement is suspiciously good both in shape and absolute level, yet absolutely no "adjusting" was done to improve the agreement. This gives us confidence that the value used for mechanical damping (20 kPa-s/m) must be reasonably close to what is happening.

Because of the length of many of the samples (up to 24"), it is likely that the actual sensitivity is somewhat higher than measured. This is because the path length from the source to the center of the sample often differs by several wavelengths from that to the ends of the sample. This means that there is appreciable interference included in the output of the sample, and that its output would be greater if the incident wave were in phase all along its length.

Our measurement procedure was improved by fitting a 12" plane-wave tube to the JBL super tweeter. The inner surface of the $3\frac{1}{2}$" diameter

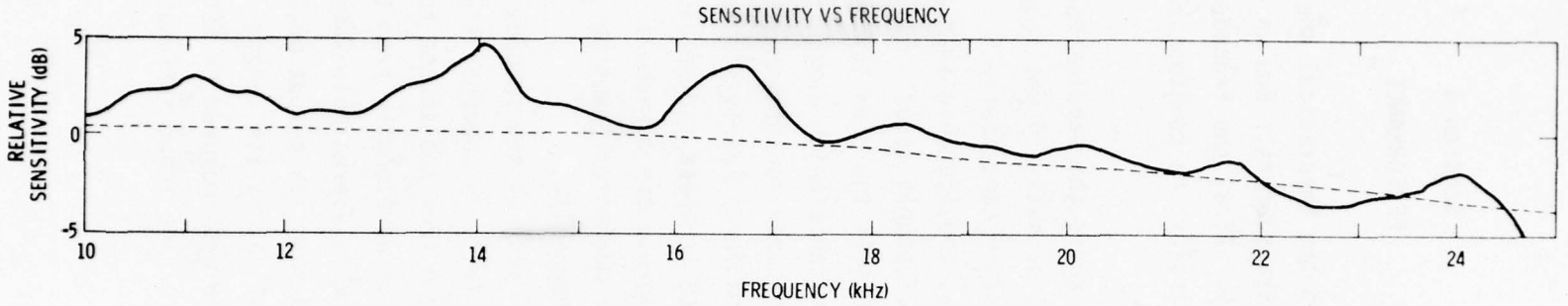

Figure 4-1. Comparison of Measured and Theoretical Receiving Sensitivity

4.1 -- Continued

aluminum tube was fitted with 1/2" thick absorptive acoustic foam. At 20 kHz only sound traveling axially emerges from the open end (see Figure 4-2). This is then used to excite a specific portion of the tape sample from a few inches away. It is simply not possible to get far enough away to get true plane wave incidence over the entire tape surface in any anechoic chamber at Sylvania. The plane wave apparatus was also used to excite selected portions of the longer samples much too long to fit in the anechoic chamber.

The radiation measurements are also complicated by the long tapes and for the same reasons. We only measured radiation efficiency on one 2' JF sample. The value calculated is just under .01% which agrees with the measured efficiency of the previous effort. The fact that the sensitivity of the JF samples is much improved while the radiation efficiency is not, shows that they are not affected in the same ways by the design parameters; i.e., optimizing sensitivity does not necessarily result in optimized radiation efficiency.

The radiated pressure on axis of one sample of the vacuum design ("vactret") was measured as a function of frequency and applied vacuum. This sample was circular with a 2" diameter so that there would be no question about the uniformity of the vacuum applied and so that the entire sensitive surface could be exposed to the same phase of the incident pressure wave. The instrumentation set-up is shown in Figure 4-3. Note that the frequency responses can be recorded automatically for each desired vacuum setting. Figure 4-4 shows the results for 0, 1/2", 1", 4", 9", and 20" of vacuum. In general, the sensitivity is seen to decrease with increased vacuum. The high frequencies are affected first and then successively lower frequencies as the vacuum is increased. This indicates that the vacuum used in the vactret design (if any) should not be greater than about 1" of water.

When driving a transducer we always used a step-up transformer or a series inductor adjusted for series resonance with the tape at the operating frequency. At first, we used the same General Radio decade inductor

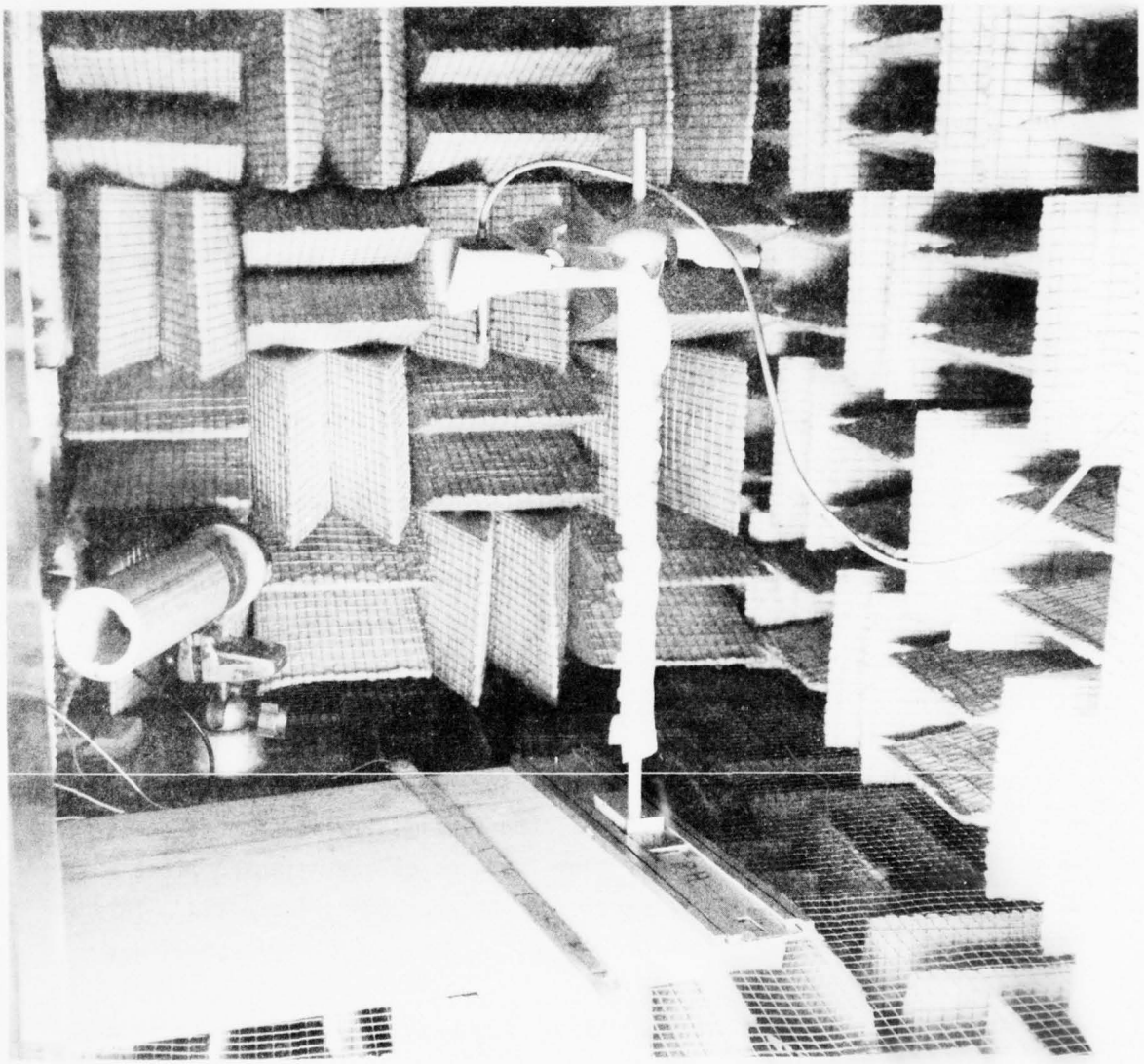

Figure 4-2. Plane Wave Tube and Microphone in Anechoic Chamber

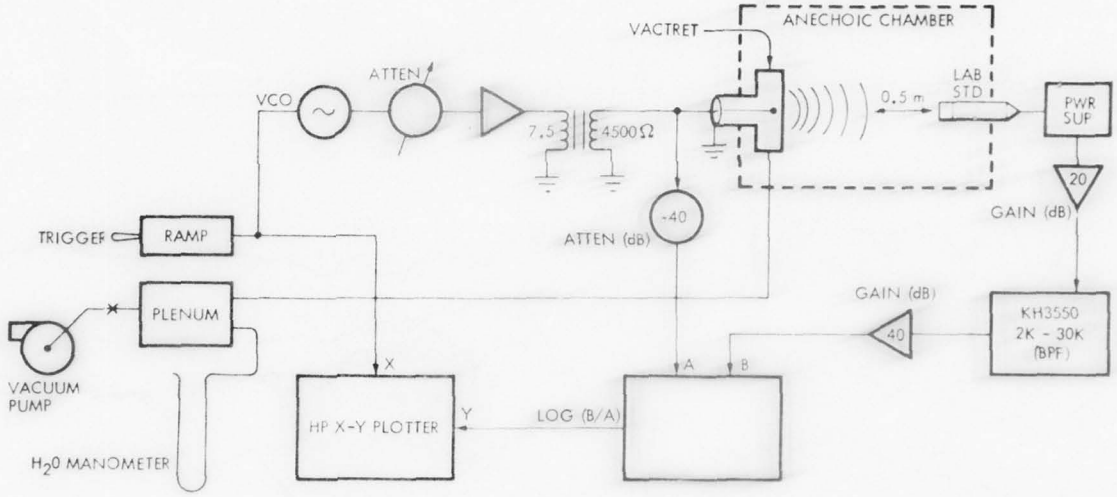

Figure 4-3. Instrumentation for Measuring Radiation of Vactret

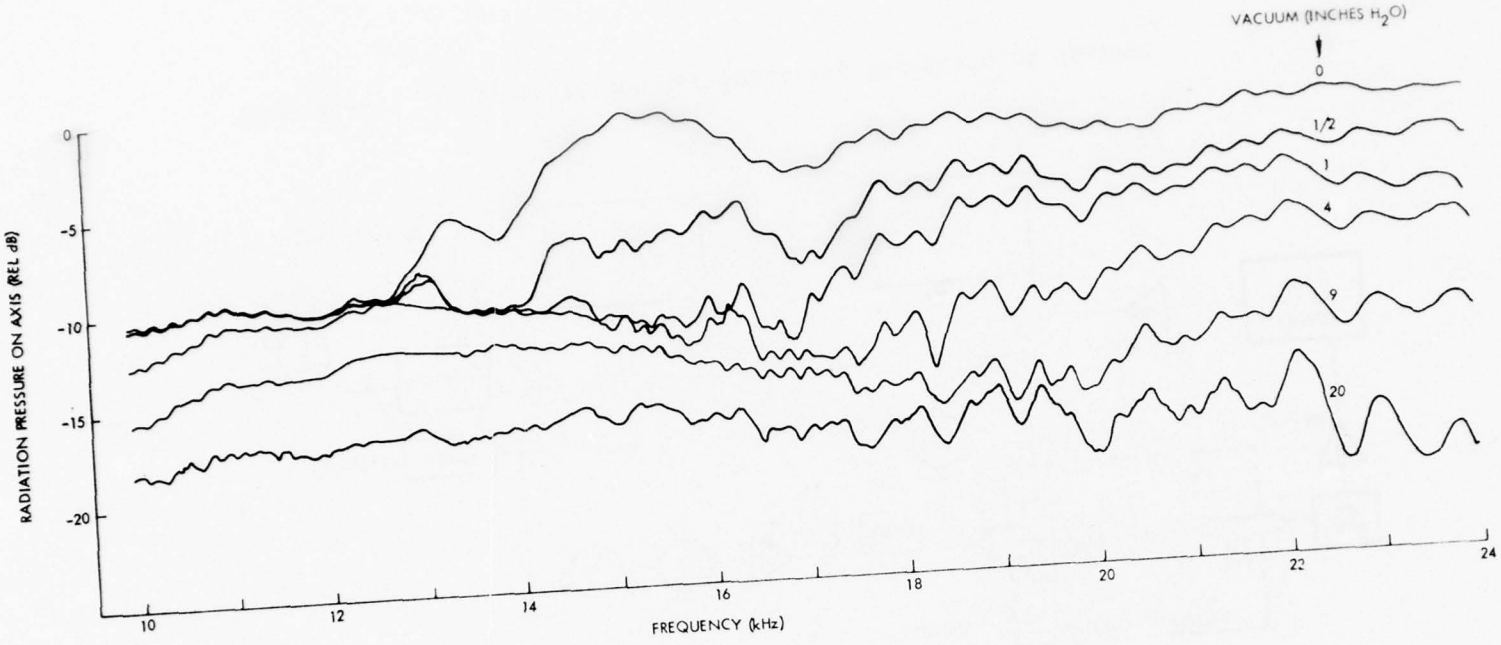

Figure 4-4. Effect of Vacuum Level on Radiated Axial Pressure

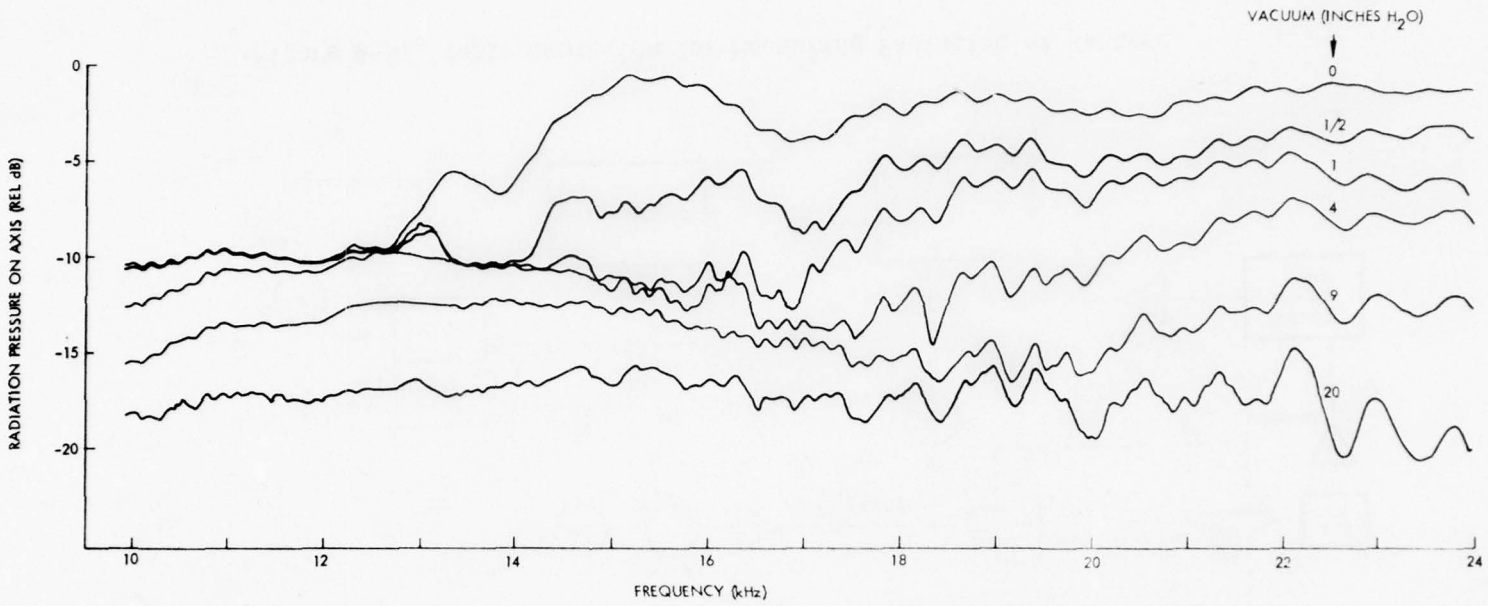

Figure 4-4. Effect of Vacuum Level on Radiated Axial Pressure

4.1 -- Continued

used previously, but when the importance of driving Q became clear, we tried winding our own high-Q toroid inductors. After several attempts, unloaded Q's over 1,000 were achieved for inductances of about 5 mH.

4.2 HYBRID AND ASSOCIATED ELECTRONICS

Whereas in the previous effort[1] we used entirely separate tapes for radiating and receiving to demonstrate the system concept, in this program we designed and built the electronics that enables a single tape to be used as both transmitter and receiver simultaneously. This may seem a little like magic, but such devices have been used for radar systems for many years.

The basic idea is to first null out the driving signal and then to mix the remaining signal with the driving signal and recover the doppler signal by low pass filtering. The output is a voltage that varies as the motion of the reflecting object. Figure 4-5 shows a block diagram of this concept with the addition of a second nulling device, the dual phase shifter-summer.

Though simple in concept, the hybrid and associated circuitry turned out to be difficult to develop satisfactorily. The first model was designed to automatically drive at the frequency of resonance, but it instead drifted to higher and higher frequencies and was abandoned. After going through several other models and learning how to wind balanced toroids, we eventually wound up with the arrangement illustrated in Figure 4-6. The upper diagram shows the hybrid coils with means for balancing their Q's. A separate winding on each provides the desired differential output through a transformer. Because the voltage across the main coils is approximately Q times the driving voltage at series resonance, rather high voltages can exist in the hybrid. We have accidentally broken down several of our hand-wound coils. Note in Figure 4-6 that there are two tape inputs. If two equal tape samples are available, then they can be used for the common mode nulling. If only one tape is to be used, the other input is terminated in the capacitance

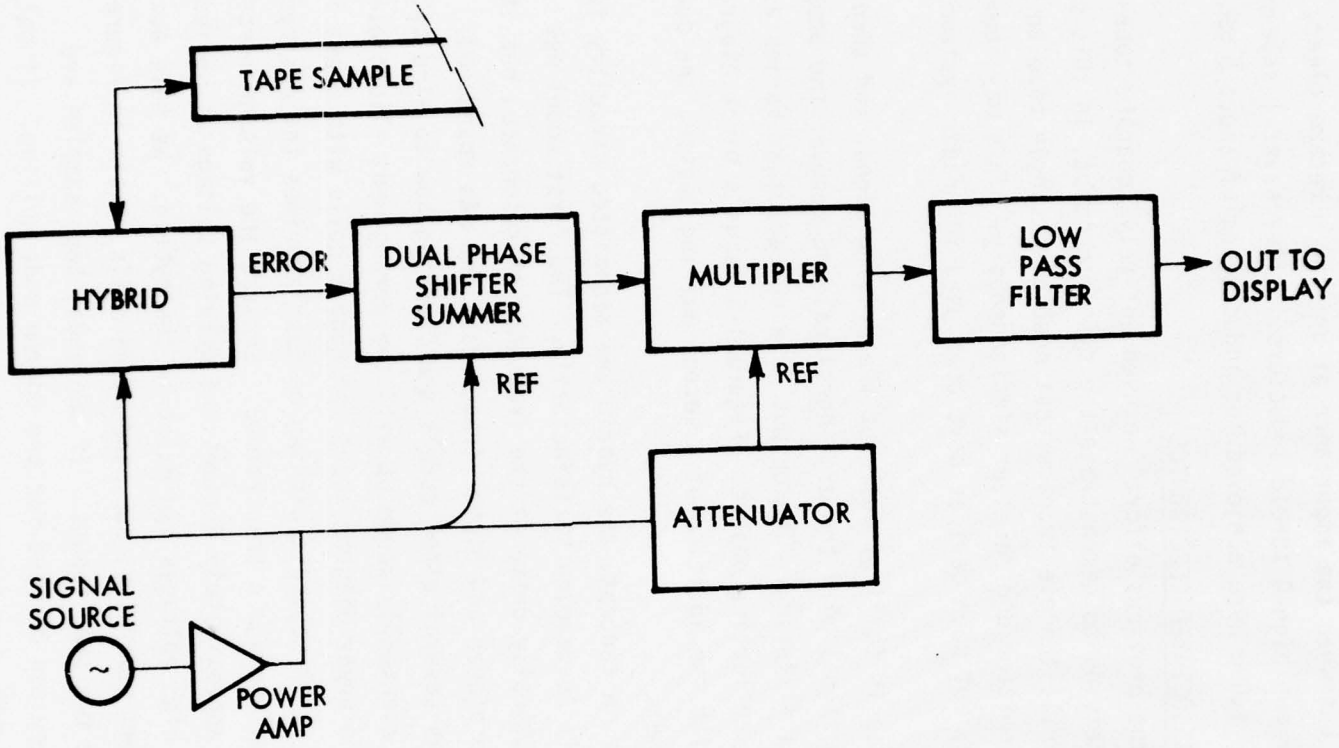

Figure 4-5. Signal Extracting Electronics

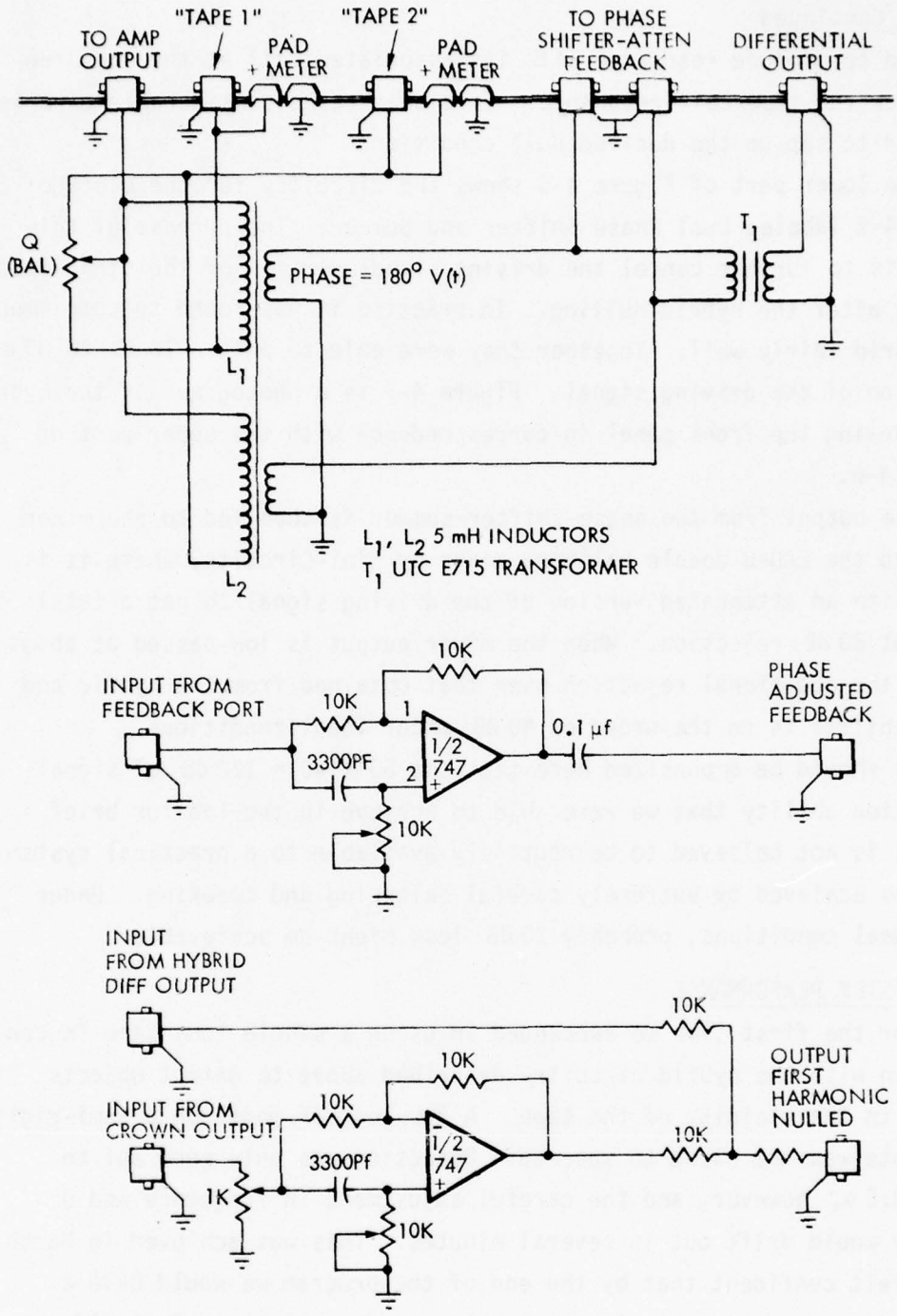

Figure 4-6. Hybrid and Phase Shifter Summer

4.2 -- Continued

required to produce resonance with its associated coil at the same frequency as the tape-coil resonance. In either case, considerable care is required to set up the desired null condition.

The lower part of Figure 4-6 shows the circuitry for the block of Figure 4-5 labeled Dual Phase Shifter and Summer. The purpose of this device is to further cancel the driving signal portion of the signal that remains after the hybrid nulling. In practice it was found to complement the hybrid fairly well. Together they were able to obtain 70 dB to 80 dB rejection of the driving signal. Figure 4-7 is a photograph of the hybrid unit showing the front panel in correspondence with the upper part of Figure 4-6.

The output from the phase-shifter-summer is then fed to the mixer (we used the ZAD-8 double balanced mixer by Mini-Circuits) where it is mixed with an attenuated version of the driving signal to get a total of about 80 dB rejection. When the mixer output is low-passed at about 100 Hz the additional rejection over that obtained from the hybrid and phase-shifter is on the order of 40 dB under ideal conditions.

It should be emphasized here that the 80 + 40 = 120 dB of signal extraction ability that we were able to achieve in the lab for brief periods is not believed to be routinely available to a practical system. This was achieved by extremely careful balancing and tweaking. Under less ideal conditions, probably 20 dB less might be achievable.

4.3 SYSTEM PERFORMANCE

For the first time we succeeded in using a single long tape in conjunction with the hybrid circuitry described above to detect objects moving in the vicinity of the tape. A 3 m long JF model on a semi-rigid substrate was the first to succeed. Detection was only good out to about 0.5 m, however, and the careful adjustment in frequency and Q balance would drift out in several minutes. This was achieved in March so we felt confident that by the end of the program we would have a greatly improved long single-tape system to demonstrate. This did not

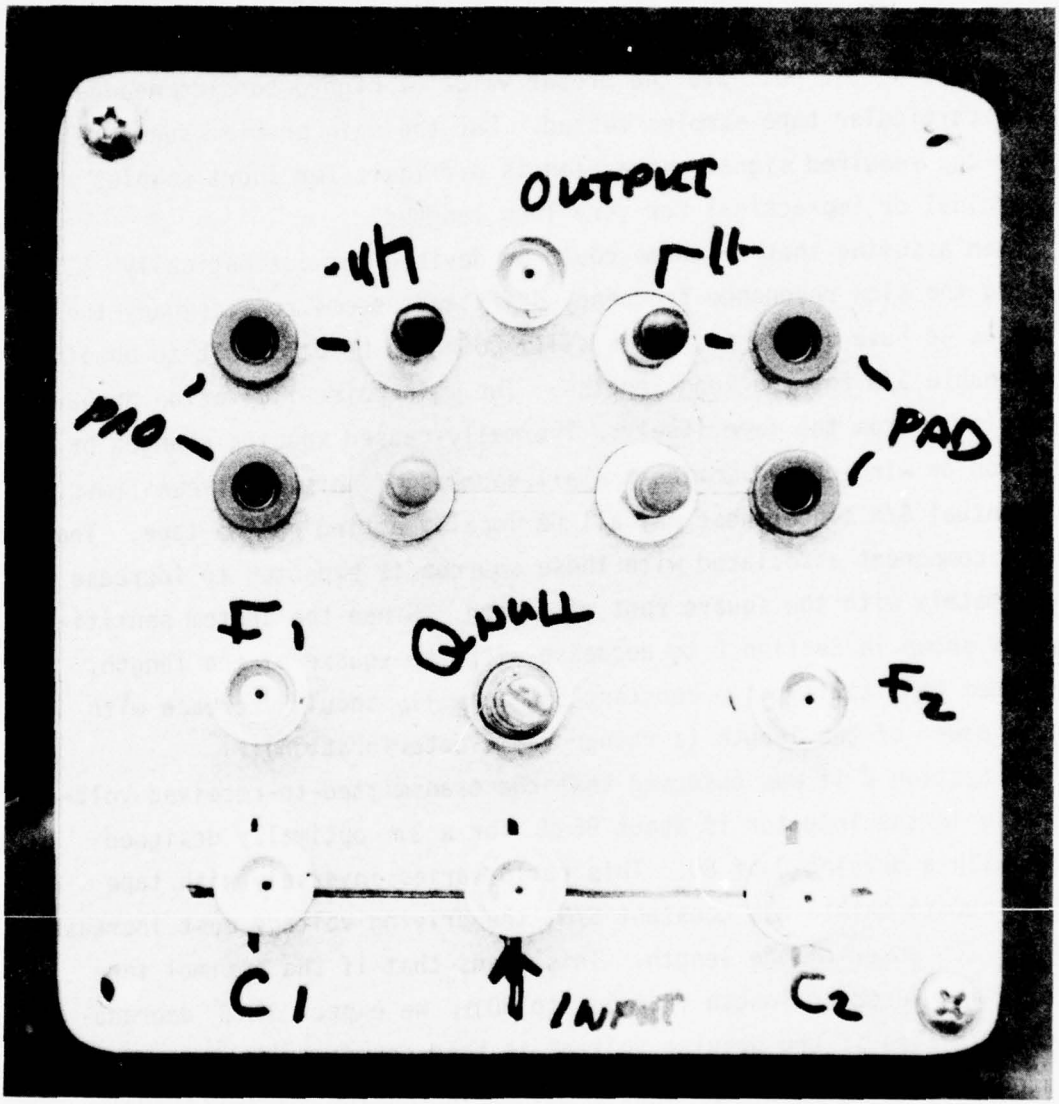

Figure 4-7. Hybrid Electronics Front Panel

4.3 -- Continued

turn out to be the case. We still feel that some improvement can be made even though very little system performance improvement was obtained in the remaining three months of the program using the single tape. There are many reasons for this: we spent considerable effort on the bowed tape concept only to have it nixed by the manufacturers; materials ordered for the vactret design did not arrive until too late to be used in a development series; we did not have the proper value of high-Q toroids needed for the particular tape samples tested. But the main problem seems to be that the required signal extraction is difficult for short samples and marginal or impractical for very long lengths.

Even assuming that a scheme could be devised for automatically tracking the slow resonance frequency drift that seems to accompany the system as we have set it up, it is still going to be difficult to obtain a reasonable S/N for the long lengths. The main noise limitation appears to originate from the tape itself. Thermally-caused spacing changes or vibration or wind-caused motion are all sources of noise that can limit the eventual S/N since these may all be locally acting on the tape. The voltage component associated with these sources is expected to increase approximately with the square root of length. Since the system sensitivity was shown in Section 2 to decrease with the square of the length, the system sensitivity at a constant S/N actually should decrease with the 2.5 power of the length (a rather rapid deterioration).

In Section 2 it was observed that the transmitted-to-received voltage ratio in the inductor is about 86 dB for a 3 m optimally designed sample with a driving Q of 80. This ratio varies inversely with tape length, but to maintain a constant S/N, the driving voltage must increase with the 1.5 power of the length. This means that if the optimal tape above is increased in length from 3 m to 30 m, we expect 30 dB degradation in S/N even if the driving voltage is held constant (i.e., the radiated pressure field is held constant by increasing the electrical current by a factor of 10). Where at 3 m we needed perhaps 98 dB of

4.3 -- Continued

signal extraction capability for an adequate S/N, at 30 m we require 128 dB which is believed to be beyond practical limits.

Thus, a conclusion coming out of both the experimental and theoretical work is that a single electret tape system is not likely to be practical in long lengths. We do not know at just what length the scheme becomes impractical, but it is probably between 3 and 30 m.

4.4 DUAL TAPE SYSTEM

Toward the end of the program, when it became clear that a single tape system was going to be difficult for long lengths, we began to look more carefully at a dual tape concept. What we mean by "dual tape" is a single substrate on which are layered two electrically independent transducers. One transducer is used for radiating exclusively and the other exclusively for receiving, but both are mounted side-by-side in parallel strips on a flexible substrate perhaps 8 cm in total width with each active transducer area taking up perhaps 2 cm of the total. This leaves 4 cm for physical separation and edge sealing.

Two 9 m samples were used to demonstrate the potential of this concept. The electronics for this system, Figure 4-8, is much simpler than that required for the single tape system. No hybrid for nulling out the driving signal is required since the only signal received is the desired reflected signal. (This assumes that the radiator tape width and frequency are properly designed to achieve a radiation null at 90^{o} off axis and that the separation between the transducers is great enough that the receiver is out of the near field.) The narrow band pass filter is required to eliminate normal background noise, and the balanced mixer output is filtered as before to yield the signal proportional to the motion of the reflector. The Q of the series inductor is no longer a critical or expensive consideration and in fact a step-up transformer was used instead of the series inductor to achieve the high driving voltage for the demonstration.

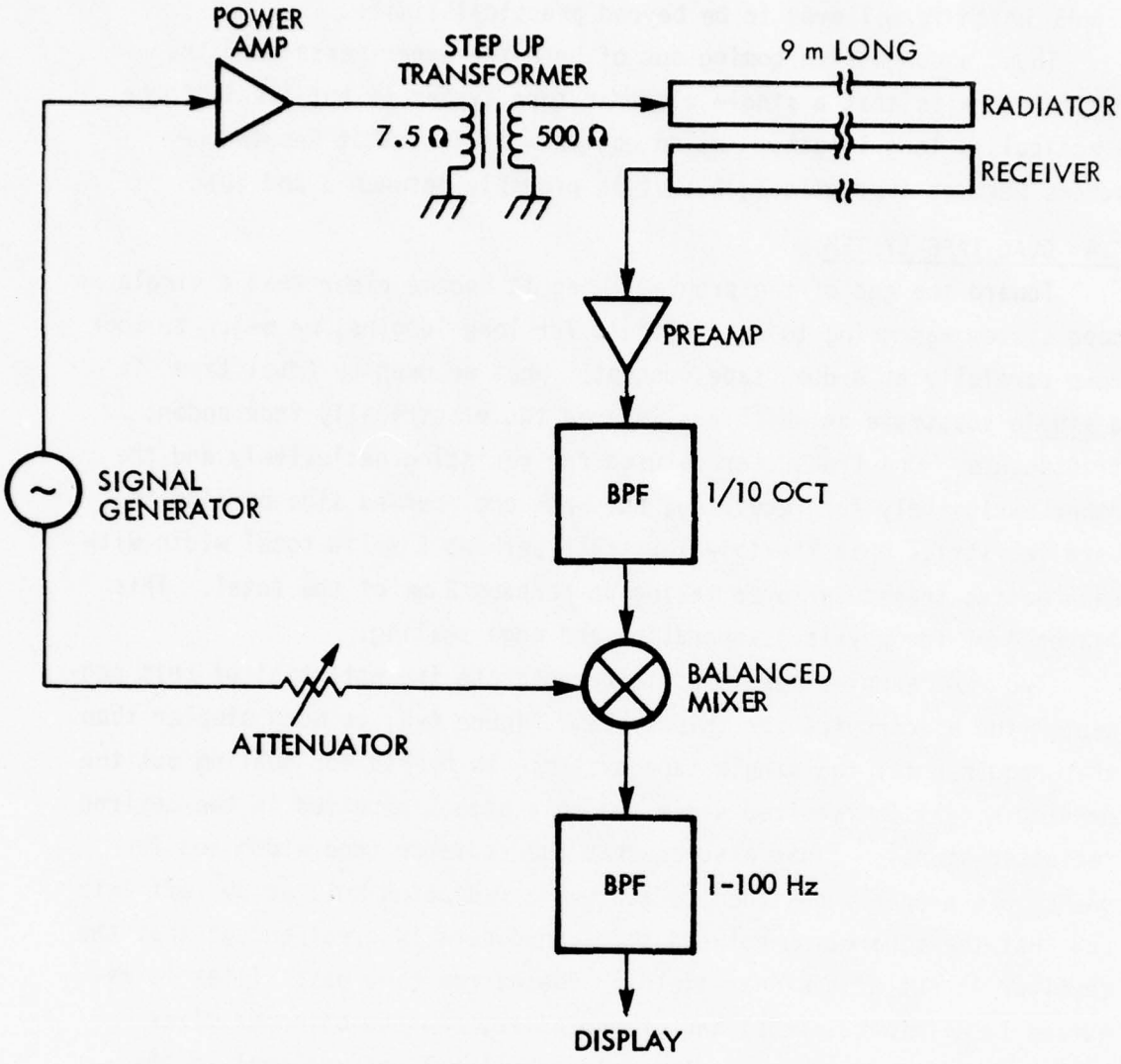

Figure 4-8. Dual Transducer System

4.4 -- Continued

Using the two 9 m samples (see Section 3.3.1.3 for construction details) as shown in Figure 4-9 we were able to observe a high S/N for reflector motions all along the tape out to ranges of about 1 m. Considering that neither of these tapes has been optimized with respect to either radiation or receiving and that the 9 m length is a factor of 25 greater than the longest demonstration sample from the previous study, these results are quite gratifying.

Figure 4-9. Demonstration of Two Tape System

Figure 4-2. Plane Wave Tube and Microphone in Anechoic Chamber

Section 5

ACCOMPLISHMENTS, CONCLUSIONS AND RECOMMENDATIONS

This program has included a very broad range of activities: A theoretical analysis and computer simulation of the transducer and detection system; a study of electret charging techniques; conception, design, fabrication and evaluation of three different tape transducer configurations; design and fabrication of special electronics for doppler signal extraction; visits and discussions with potential manufacturers concerning the likely manufacturing processes for the tape transducer; and integration of the handmade tape transducers with the electronics into demonstrable detection systems for evaluation. In the following paragraphs we attempt to single out the most important accomplishments and conclusions resulting from this effort and go on to recommend the logical sequel.

5.1 ACCOMPLISHMENTS AND CONCLUSIONS

1. The use of a computer model believed to simulate all the important aspects of the electrical drive, acoustic radiation, target reflection, and receiving transduction processes in the single transducer detection concept, has resulted in an optimum transducer design whose parameters depend only on the Q of the driving elements. The optimum design parameters turn out to be reasonable and obtainable (see Section 2.2.4).

2. A simple method for reliably charging electrets uniformly and to a desired level has been developed and adapted for use on a continuous tape basis (see Section 3.1).

3. Potential tape manufacturers feel that the vactret tape design would not be difficult for them to make and that the dimensions and materials all fall well within the commercial state-of-the-art (see Section 3.3.2).

5.1 -- Continued

4. The ultrasonic doppler detection concept, based on electret tape transducers, has been demonstrated to be viable in two different ways. For the first time ever, a single transducer electret tape was successfully used as radiator and receiver simultaneously to achieve a short range detection capability. So far the longest sample used in this way is 3 m in length. The concept was also successfully demonstrated for a 9 m length using two side-by-side single transducer tapes (thus simulating a dual transducer tape), (see Section 4.3).

5. It appears that unless significant improvements in the transducer or in the driving and processing circuitry are made, single transducer tapes may only be practical for relatively short lengths (somewhere between 3 and 30 m) (see Section 4.3).

6. Dual transducer tapes, however, are expected to be practical for considerably greater lengths. In addition to several other distinct advantages (see following recommendations), they are expected to retain nearly all of the desirable attributes (see Section 1.1.1) of the single tape transducer.

5.2 RECOMMENDATIONS

1. In view of the results of this study we recommend that for long perimeter applications, the dual transducer tape be developed. This tape containing two transducers on a single substrate:

   a. Eliminates the need for a critically balanced hybrid and has much simpler driving and receiving electronics.
   b. Is no more difficult to make than a single transducer tape according to the potential manufacturers (since they would fabricate in multiple parallel rows at any rate).
   c. The expected cost is thus increased only by the cost of the increased material since the labor and handling costs will be about the same as for the single transducer tape.
   d. Is only about twice as wide as a single transducer tape, but has at least an order of magnitude improvement in performance and is still rather narrow (8 cm estimated).

5.2 -- Continued

e. Allows radiator and receiver transducers to each be optimally designed for it's specific function since each is mechanically and electrically independent.

f. Retains all the other attributes listed in Section 1.1.1 for the single transducer tape; i.e., flexibility, adhesive surface, rapid deployment, no critical alignment, etc.

2. An analysis should be performed to derive a good design. For this purpose the current computer model need only be modified slightly to help come up with the designs for each transducer. Rather than trying to optimize a total system with a single transducer, each of the two transducers can be designed to do its task optimally within the constraints of breakdown, material availability, and manufacturability all of which are pretty well understood at this point.

3. A manufacturer should be subcontracted to make experimental quantities of the dual transducer tape design based on the above modeling analysis.

4. These experimental tapes should be evaluated with regard to the effects of lengths, ambient noise, wind, temperature and precipitation using laboratory equipment to provide the necessary electrical drive and signal conditioning.

5. If these tests are encouraging then an electronic breadboard package of the electronics should be designed and fabricated.

6. The breadboard electronics and the experimental tapes comprise a demonstration system that can be further evaluated.

7. The single transducer tape should be further developed for short indoor intrusion detection applications by:

a. Subcontracting to have an optimum design fabricated in experimental quantities.

b. Developing an improved hybrid and associated signal extraction electronics package

c. Evaluating the resulting detection system with respect to ambient noise, air currents and temperatures.

REFERENCES

1. "Electret Tape Transducer," G. K. Miller, GTE Sylvania, Mountain View, California, RADC-TR-76-22, February 1976. (A021736)

APPENDIX A
TAPE TRANSDUCER ANALYSIS

In this appendix we derive the basic equations for the electret tape transducer including inactive capacitance, second harmonic distortion, and external DC bias voltage.

A.1 BASIC ANALYSIS

A.1.1 Coupled Non-Linear Differential Equations

Consider the diagram of the tape and driving electronics of Figure A1. Here a voltage source e_s (which may contain a DC bias) with its source impedance Z_s, is shown driving an electret tape transducer with active input impedance, Z_{in}, in parallel with a capacitor C_i. C_i represents all the parallel inactive capacitance including the cable and connecting capacitance. The input impedance, Z_{in}, corresponds to the same expression used in the analysis of the prior effort[1], and does not include the inactive portion of the transducer's total capacitance.

In the prior analysis (Appendix A of Reference 1) the voltage, e, across the transducer is shown to be

$$e = \frac{\sigma}{C_e} + \frac{\sigma a}{\varepsilon_o} + V_e \qquad \text{(A1}$$

where $C_e = \frac{\varepsilon_e}{d}$ is the capacitance per unit area of the electret layer. Using Kirchoff's voltage law around the source loop and A1 results in

$$e_s = iZ_s + \frac{\sigma}{C_e} + \frac{\sigma a}{\varepsilon_o} + V_e \qquad \text{(A2}$$

Now using Kirchoff's current law at the upper node and using $i_i = C_i\dot{e}$ we find

$$i = i_i + \dot{\sigma} S = C_i\left(\frac{\dot{\sigma}}{C_e} + \frac{\dot{\sigma}a}{\varepsilon_o} + \frac{\sigma\dot{a}}{\varepsilon_o}\right) + S\dot{\sigma} \qquad \text{(A3}$$

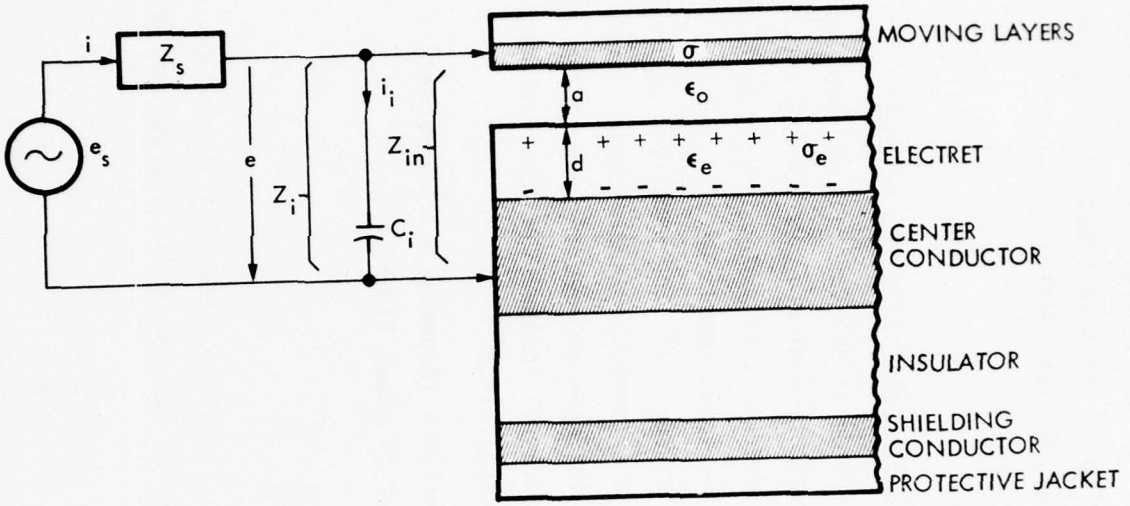

Figure A-1. Basic Tape Transducer and Driver Configuration

A.1.1 Continued

where S is the area of the layers of the transducer. Putting A2) into A3) results in the first-order non-linear differential equation in σ and a:

$$\dot{\sigma} Z_s \left(S + \frac{C_i}{C_e} \right) + \dot{\sigma} a \frac{Z_s C_i}{\varepsilon_o} + \frac{\sigma}{C_e} + \frac{\sigma a}{\varepsilon_o} + \frac{Z_s C_i}{\varepsilon_o} \sigma \dot{a} = e_s - V_e \qquad \text{(A4}$$

This corresponds to Eq. A-7 of Reference 1. All the terms containing C_i are new. The mechanical coupling part of this electrical equation is through the air gap thickness, a. The mechanical equation is unchanged from the prior derivation and is repeated here for completeness only:

$$M\ddot{x} + (D + Z_A)\,\dot{x} + Kx + \frac{\sigma^2}{2\varepsilon_o} = -p_i \qquad \text{(A5}$$

where M = Moving mass per unit area (kg/m^2)

D = Mechanical damping per unit area (Pa-s/m)

Z_A = Acoustical radiation impedance of tape (Pa-s/m)

x = Displacement of moving layer

K = Effective stiffness per unit area of the air layer

p_i = Incident pressure signal

A.1.2 Zeroth Order Equations

As before, we now linearize the basic equations by expanding e_s, σ, a, and p_i in Fourier series and collecting like ordered terms. However, we include a DC bias term for e_s and we collect not only zeroth- and first-order terms but also second-order terms.

Using:

$$\left.\begin{aligned} e_s &= E_o + \frac{E}{2} e^{j\omega t} \\ \sigma &= \sigma_o + \frac{\sigma_1}{2} e^{j\omega t} + \frac{\sigma_2}{2} e^{2j\omega t} \\ p_i &= \frac{P}{2} e^{j\omega t} \end{aligned}\right\} \qquad \text{(A6}$$

and $$x = x_o + \frac{x_1}{2} e^{j\omega t} + \frac{x_2}{2} e^{2j\omega t}$$

A.1.2. Continued

we obtain the following linear equation sets:

For the zeroth order set:

$$\sigma_o \left(\frac{1}{C_e} + \frac{a_o + x_o}{\varepsilon_o} \right) = E_o - V_e$$

$$\frac{P_o a_o x_o}{(a_o + x_o)^2} + \frac{\sigma_o^2}{2\varepsilon_o} = 0 \qquad \text{(A7}$$

These equations govern the DC voltages and steady charges as well as the static displacement, x_o, caused by the presence of the electret. The bias voltage only appears here. These equations can be solved as described in Reference 1, Appendix A.

A.1.2.1 Static and Dynamic Stiffness

A short diversion is necessary at this point to explain how the application of A6 to A5 leads to the second of A7. We consider the stiffness reaction pressure, Kx, in Equation A5. The stiffness of the air trapped in the air gap is dependent on the speed with which the compression takes place. At ultrasonic frequencies the process is adiabatic (constant heat) and the stiffness is $K = \gamma P_a / a$ where $\gamma = 1.4$, P_a is the absolute pressure and a the air gap thickness. However, for very slow pressure changes as in the case of barametric pressure, the process is isotropic (constant temperature) and the stiffness is simply $K = P_a / a$. Now, since the pressure-volume product for air is a constant,

$$P_a a = P_o a_o$$

where a_o is the air gap thickness when the pressure of the air is the same as the ambient pressure P_o and no electrical fields or other external pressures are present.

A.1.2.1 Continued

Using this in the equation for the stiffness reaction force (static case), we have

$$Kx = \frac{P_a x}{a} = \frac{P_o a_o x}{a^2}$$

Since $a = a_o + x$ this becomes

$$Kx = \frac{P_o a_o x}{(a_o + x)^2} = \frac{P_o x/a_o}{(1+x/a_o)^2} \qquad \text{(A8}$$

Since x/a_o is less than 1 we may expand the fraction in the form

$$\frac{Kx}{P_o} = \sum_{m=1}^{\infty} m(-1)^{m-1} \alpha^m \qquad \text{(A9}$$

where $\alpha \equiv x/a_o$ is defined for convenience.
But the last equation of A6 can be written in terms of α as

$$\alpha = \alpha_o + \frac{\alpha_1}{2} e^{j\omega t} + \frac{\alpha_2}{2} e^{2j\omega t}$$

and more generally, the n-th power of α can be written as

$$\alpha^n = \alpha_o^n + \left(n\alpha_o^{n-1} \frac{\alpha_1}{2}\right) e^{j\omega t} + \left[\binom{n-1}{\sum_{\ell=1}^{\ell}} \alpha_o^{n-2} \frac{\alpha_1^2}{4} + n\alpha_o^{n-1} \frac{\alpha_2}{2}\right] e^{j2\omega t} \qquad \text{(A10}$$

Substituting A10 into A9 and collecting terms in zeroth, first and second order we arrive at

$$Kx|_o = P_o \sum_{m=1}^{\infty} (-1)^{m-1} m \alpha_o^m = \frac{P_o \alpha_o}{(1 + \alpha_o)^2} = \frac{P_o a_o x_o}{(a_o + x_o)^2} \qquad \text{(A11}$$

This checks the first term of the second equation of A7 (which is the corrected form of Eq. 2-4 in Reference 1).

A.1.2.1 Continued

The first order equation is:

$$Kx|_1 = \gamma P_o \frac{\alpha_1}{2} \sum_{m=1}^{\infty} m^2(-\alpha_o)^{m-1} \qquad \text{(A12}$$

and the second order expression is

$$Kx|_2 = \gamma P_o \left\{ \frac{\alpha_2}{2} \sum_{m=1}^{\infty} m^2(-\alpha_o)^{m-1} - \frac{\alpha_1^2}{4} \sum_{m=1}^{\infty} (m+1)\left(\sum_{\ell=1}^{m} \ell\right)(-\alpha_o)^{m-1} \right\} \qquad \text{(A13}$$

A.1.3 First and Second Order Equation Sets

After applying A6 to A4 and A5 and collecting the driving frequency terms, we get the equation set:

$$\left.\begin{aligned} &\sigma_1 \left[j\omega Z_s S\left(1 + \frac{C_i}{SC_o}\right) + \frac{1}{C_o} \right] + x_1 \frac{\sigma_o}{\varepsilon_o}(1 + j\omega Z_s C_i) = E \\ &\sigma_1 \frac{\sigma_o}{\varepsilon_a} + x_1 \left[-\omega^2 M - \omega X_A + j\omega(D + R_A) + \frac{\gamma P_o}{a_o}\left(1 - \frac{4x_o}{a_o} + \frac{9x_o^2}{a_o^2} \ldots\right) \right] = -P \end{aligned}\right\} \qquad \text{(A14}$$

where $C_o^{-1} = C_e^{-1} + \left(\frac{\varepsilon_o}{a_o + x_o}\right)^{-1}$ is the total static capacitance per unit area between the active conducting layers.

If we define

$$Z_{ei}(\omega) = j\omega Z_s S\left(1 + \frac{C_i}{SC_o}\right) + \frac{1}{C_o}$$

$$T_i(\omega) = T(1 + j\omega Z_s C_i)$$

where $T = \frac{\sigma_o}{\varepsilon_o}$

and $Z_m = -\omega^2 M - \omega X_A + j\omega(D + R_A) + \frac{\gamma P_o}{a_o}\left(1 - 4\frac{x_o}{a_o} \ldots\right)$

A.1.3 Continued

these equations take on the simple form:

$$\begin{aligned} \sigma_1 Z_{ei}(\omega) + x_1 T_i(\omega) &= E \\ \sigma_1 T + x_1 Z_m(\omega) &= -P \end{aligned} \qquad \text{(A15}$$

Note that these are quite similar to the first order equations derived before that excluded the inactive capacitance. The only differences are contained in the expression Z_{ei} and T_i and these reduce to their former values, Z_e and T if $C_i = 0$.

These equations have the solutions:

$$\sigma_1 = \frac{E Z_m + PT_i}{Z_{ei}Z_m - TT_i} \quad , \quad x_1 = \frac{-ET - PZ_{ei}}{Z_{ei}Z_m - TT_i} \qquad \text{(A16}$$

The second order equation set is derived in the same manner (applying A6 to A4 and A5 and collecting terms at the double frequency, 2ω). These are:

$$\left.\begin{aligned} \sigma_2 Z_{ei}(2\omega) + x_2 T_i(2\omega) &= G \\ \sigma_2 T + x_2 Z_m(2\omega) &= H \end{aligned}\right\} \qquad \text{(A17}$$

where $$G = -\frac{\sigma_1 x_1}{2\varepsilon_o}(1 + j2\omega Z_s C_i)$$

and $$H = \frac{\gamma P_o}{a_o^2}\left(1 - \frac{9}{2}\frac{x_o}{a_o} + \ldots\right) x_1^2 - \frac{\sigma_1^2}{4\varepsilon_o}$$

Note that the terms on the LHS of this equation are the same as in Eq. (A15) but with 2ω substituted for ω. The RHS terms are the driving terms and depend on the first order solutions x_1 and σ_1. The second order solutions are:

A.1.3 Continued

$$\left.\begin{aligned} \sigma_2 &= \frac{GZ_m(2\omega) - HT_i(2\omega)}{Z_{ei}(2\omega)\, Z_m(2\omega) - TT_i(2\omega)}, \\ x_2 &= \frac{HZ_{ei}(2\omega) - GT}{Z_{ei}(2\omega)\, Z_m(2\omega) - TT_i(2\omega)} \end{aligned}\right\} \qquad \text{(A18}$$

The second harmonic distortion is defined as the magnitude of the ratio of the diaphragm velocities, $|\omega x_1 / 2\ \omega x_2|$.

A.2 QUANTITIES OF INTEREST

A.2.1 Input Impedance

The presence of inactive capacitance changes the impedance seen by the driving amplifier looking into the tape (and connecting cable). The complex active input impedance of the tape was derived in Appendix A of Ref. 1 as:

$$Z_{in} = \frac{T^2(D + R_A)}{S\left[r_m^2 + \omega^2(D+R_A)^2\right]} + \frac{j}{\omega S}\left(\frac{T^2 r_m}{|Z_m|^2} - \frac{1}{C_o}\right) \qquad \text{(A19}$$

where $r_m = \mathrm{Re}(Z_m)$

and $C_o^{-1} \equiv C_e^{-1} + \frac{a}{\varepsilon_o}$

Putting a capacitance C_i in parallel with Z_{in} results in the actual input impedance, $Z_i = (Z_{in}^{-1} + j\omega C_i)^{-1}$ or

$$Z_i = \frac{R_{in}X_c^2 + jX_c\left[R_{in}^2 + X_{in}\,(X_{in} + X_c)\right]}{R_{in}^2 + (X_{in}+X_i)^2} \qquad \text{(A20}$$

where $X_c \equiv \frac{-1}{\omega C_i}$

A.2.2 Input Power

The electrical power drawn from the amplifier is dependent on the real part R_i of the actual input impedance Z_i. Putting (A19) into (A20) and solving for the real part we find

$$R_i = \frac{D + R_A}{\frac{S Z_m^2}{T^2}(1 + \frac{C_i}{SC_o})^2 + \frac{T^2 C_i^2}{S} - 2r_m C_i(1 + \frac{C_i}{SC_o})} \qquad \text{(A21}$$

Note that if $C_i = 0$ only the first term in the denominator remains and the expression reduces to R_{in}. The power drawn from the amplifier is simply

$$P_{in} = \frac{E^2}{R_s + R_i}$$

where R_s is the real part of the driving impedance including any series inductor. Clearly the greater R_i/R_s the greater the fraction of power delivered to the tape. Equation A21 shows that, in general, the effect of C_i is to lower the resistive load R_i presented by the transducer.

A.2.3 Voltage Across the Tape Conductors

In general, the ratio of voltage across the tape to voltage supplied by the ideal source (Figure A1) is given by

$$\frac{e}{e_s} = \frac{Z_i}{Z_s + Z_i} \qquad \text{(A22}$$

Now for conditions of conjugate impedance matching where $Z_s = Z_i^*$

$$\frac{e}{e_s} = 1/2\left(1 + \frac{X_i^2}{R_i^2}\right)^{1/2} = 1/2(1 + Q_i^2)^{1/2} \qquad \text{(A23}$$

A.2.3 -- Continued

where the above equation defines Q_i the effective Q of the tape. If $R_s << R_i$ then the 1/2 factor becomes unity. In terms of the input impedance of the active portion of the tape, Z_{in},

$$\left|\frac{e}{e_s}\right| = \left[1 + \left(\frac{X_{in}}{R_{in}} - C_i\frac{|Z_{in}|^2}{R_{in}}\right)^2\right]^{1/2} \qquad \text{(A24}$$

Here the presence of C_i clearly shows a modification of the tapes input Q ($Q_{in} = X_{in}/R_{in}$) that would otherwise control the voltage ratio. For $C_i \rightarrow 0$ and $Q_{in} >> 1$ we would have a tape voltage about Q_{in} times as great as the driving voltage when the series inductance is properly tuned to the tape ($X_s = \omega L = -X_{in}$) and $R_s << R_{in}$. Using A19 and A20, A24 can be expressed in the more elemental form

$$\left|\frac{e}{e_s}\right| = \left[1 + \left(\frac{r_m}{X_m} - \frac{|Z_m|^2}{C_o T^2} - \frac{\omega C_i |Z_{in}|^2}{R_{in}}\right)^2\right]^{1/2} \qquad \text{(A25}$$

where $\frac{r_m}{X_m} = \frac{r_m}{\omega(D+R_D)}$ is like a mechanical Q.

A.2.4 Receiving Voltage

When a pressure wave P, impinges on the tape, a charge $s\sigma$ flows into the external electrical circuit consisting of inactive capacitance in parallel with the source impedance which is the load impedance in receiving mode. The voltage this causes to appear across the parallel combination is

$$e = \frac{j\omega S Z_s \sigma}{1+j\omega C_i Z_s} \qquad \text{(A26}$$

Using A16 for $\sigma(=\sigma_1)$ and putting E = 0 (to find the received voltage component across Z_s) we have

$$e = \frac{j\omega S Z_s TP}{Z_{ei} Z_m - TT_i} \qquad \text{(A27}$$

AD-A047 316 GTE SYLVANIA INC MOUNTAIN VIEW CALIF ELECTRONIC SYST--ETC F/G 17/1
ELECTRET TAPE DETECTION SYSTEM.(U)
SEP 77 G K MILLER F30602-76-C-0375

UNCLASSIFIED RADC-TR-77-298 NL

2 OF 2
AD A047316

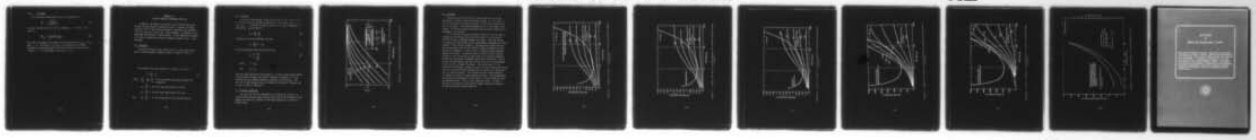

END
DATE FILMED
1 -78
DDC

A.2.4 -- Continued

The effective voltage sensitivity of the transducer is

$$\left|\frac{e}{P}\right| = \frac{ST|Z_s|}{|Z_{ei}Z_m - TT_i|} \qquad \text{(A28}$$

The open load sensitivity is found by letting $Z_s \to \infty$ in (A28). The result is:

$$\left|\frac{e}{P}\right|_{OL} = \frac{T}{|Z_m|(1 + C_i/SC_o)} \qquad \text{(A29}$$

Note that this reduces to the open circuit sensitivity ($e/P|_{oc} = T/|Z_m|$) when $C_i = 0$. The factor $(1 + C_i/SC_o)$ in the denominator of (A29) represents the decreased sensitivity resulting from the inactive capacitance C_i. It is negligible as long as $C_i << SC_o$.

APPENDIX B
ELECTRET GENERATED BREAKDOWN CONDITION

In general, the higher the electret surface charge density the greater the electrostatic transduction action. However, the upper practical limit to the electret strength is imposed by the breakdown limits of the air in the air gap. Such breakdown, if allowed to occur, discharges the electret in that vicinity. In this appendix we examine the relations between the relevant transducer parameters and air gap breakdown.

B.1 DERIVATION

Consider an electret layer covered by an air layer with the two layers contained between conducting layers as shown in Figure B-1.

The voltage across the conductors is from Eq. A-5 of Ref. 1.

$$e = \frac{\sigma}{C_o} + V_e \qquad \text{(B1}$$

where $\frac{1}{C_o} \equiv \frac{1}{C_e} + \frac{1}{C_a}$ is the reciprocal capacitance between the conductors

$C_e = \frac{\varepsilon_e}{d}$ = per unit area capacitance of electret

$C_a = \frac{\varepsilon_a}{a}$ = per unit area capacitance of air gap

and $V_e = \frac{\sigma_e}{C_e}$ is the voltage across the isolated electret.

B.1 Continued

Assuming no free charges in the air gap, the electric field intensity is uniform in the air gap and perpendicular to the charge layer, σ, such that $\varepsilon_a E_a = \sigma$. Since the voltage V_a across the air gap of thickness a is given by $V_a = E_a a$ we see that

$$V_a = \frac{\sigma a}{\varepsilon_a} = \frac{\sigma}{C_a} \qquad \text{(B2}$$

Putting B1 into B2 to eliminate σ we find

$$V_a = \frac{C_o}{C_a}(e - V_e). \qquad \text{(B3}$$

B3 can be reduced to the more explicit form:

$$V_a = \frac{e - V_e}{1 + \frac{d}{ak}} \qquad \text{(B4}$$

where $k = \varepsilon_e/\varepsilon_o$

and $\varepsilon_a = \varepsilon_o$

Thus even when both plates are shorted (e = o) the air gap voltage depends on the electret voltage, the ratio of dielectric thickness to air gap thickness and the relative dielectric constant of the electret. The ratio of air gap voltage to V_e as a function of dielectric thickness and air gap is shown in Figure B-1.

B.2 Breakdown Conditions

The conditions for the breakdown of air between two parallel conducting plates are well known, and the curve showing the breakdown voltage across the plates as a function of the plate separation is called the Paschen curve.

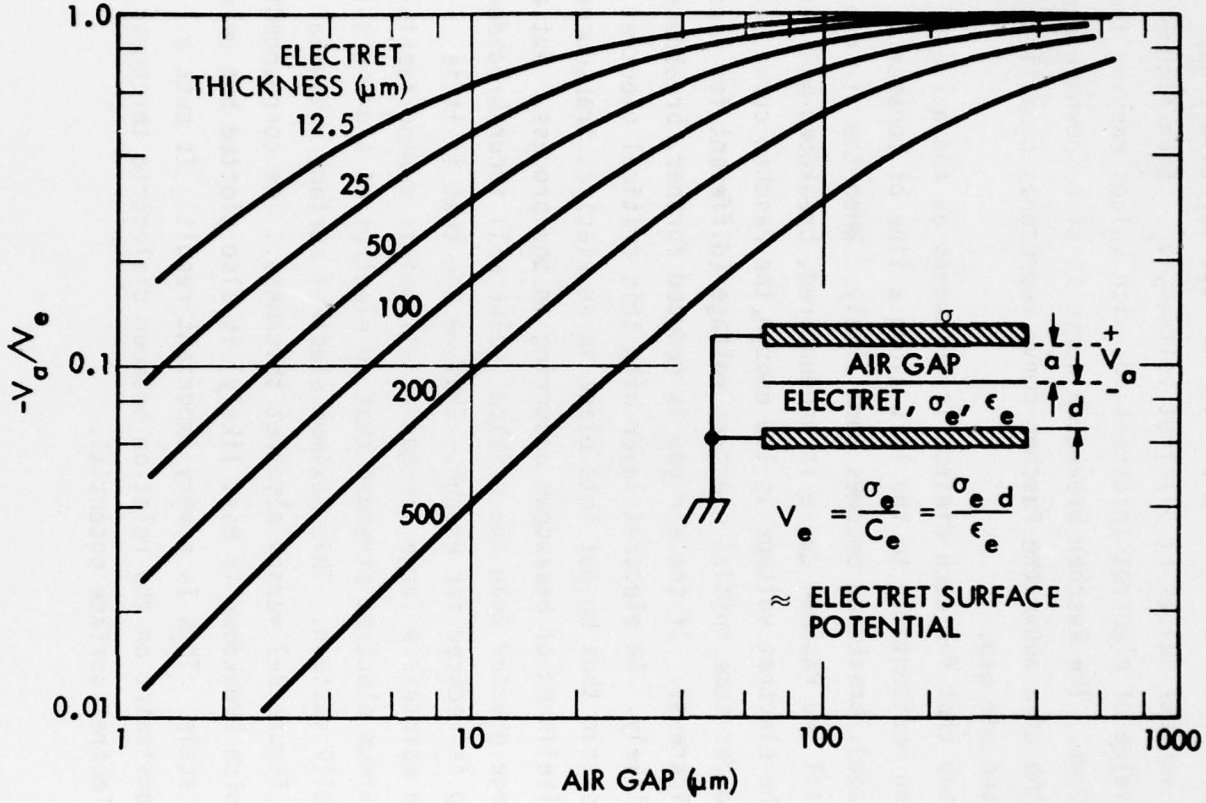

Figure B-1. Voltage Distribution Between Electret and Air Gap

B.2 Continued

Figures B-2 thru B-6 show the air gap voltage versus air gap thickness for various values of electret voltage, V_e. Each figure is for a single value of electret thickness, d, with values ranging from 12.5 μm to 250 μm. The Paschen breakdown curve is also shown in each figure. All the area above the Paschen curve represents conditions of breakdown in the air gap.

It is noted that for each dielectric thickness as the air gap is reduced (moving horizontally to the left along a line of constant electret voltage), breakdown becomes more likely. When the air gap is reduced until the Paschen curve is encountered, breakdown will occur. However, if the electret voltage is low enough, the Paschen curve can just be missed for some initial electret voltage (different for each dielectric thickness). If the air gap is reduced further, breakdown becomes less likely. An electret layer with this critical electret voltage or less can thus be put into place in an electret transducer without the likelihood of breakdown occurring in the process. But an electret voltage greater than the critical value will incur breakdown if the air gap is reduced far enough. Thus we see that if it is impractical to maintain a large air gap at all points during fabrication, there is a maximum electret strength that an electret of a given thickness can usefully sustain. This maximum electret surface potential is plotted in Figure B-7 versus electret thickness. The corresponding air gap (at which breakdown is most likely) is also plotted but using the righthand scale. This is a very important result. It puts a fabrication constraint on the relation between dielectric thickness, air gap and electret surface potential.

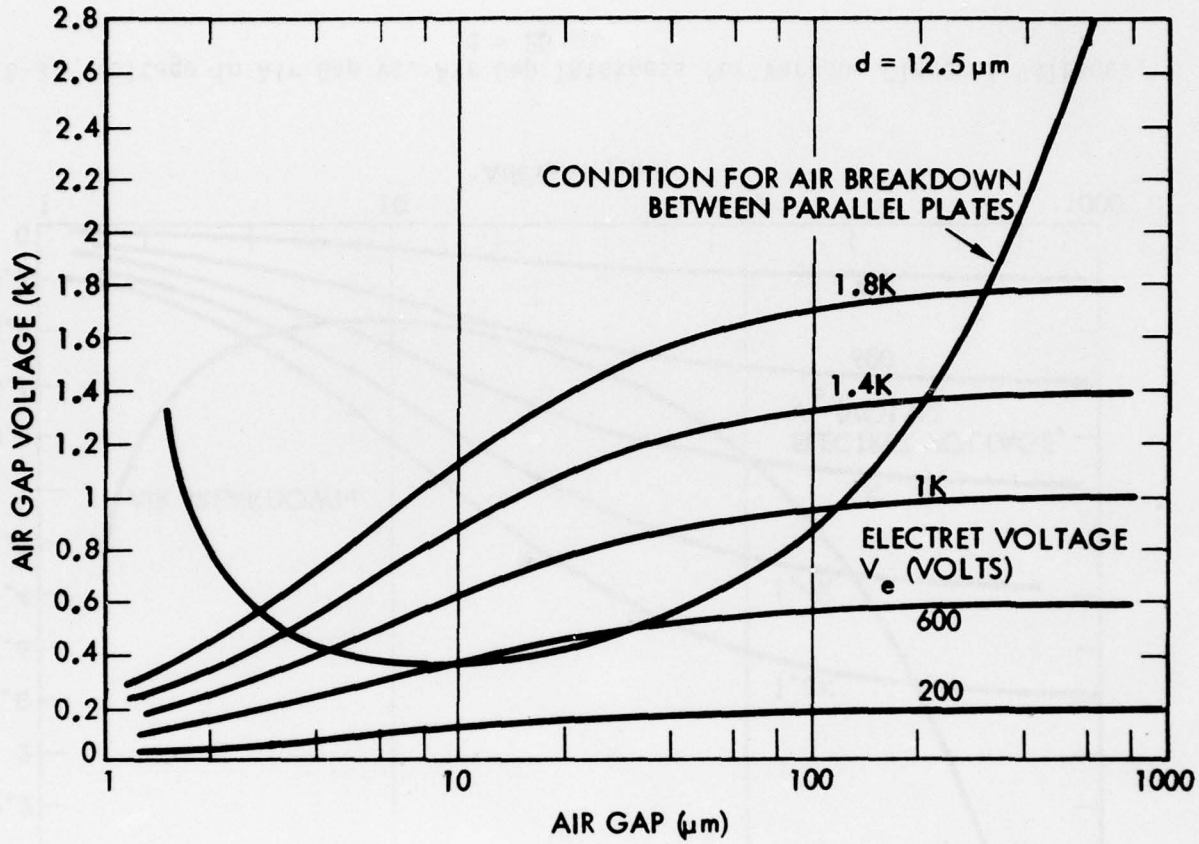

Figure B-2. Voltage in Air Gap vs. Air Gap Thickness for Various Electret Voltages, d = 12.5 μm

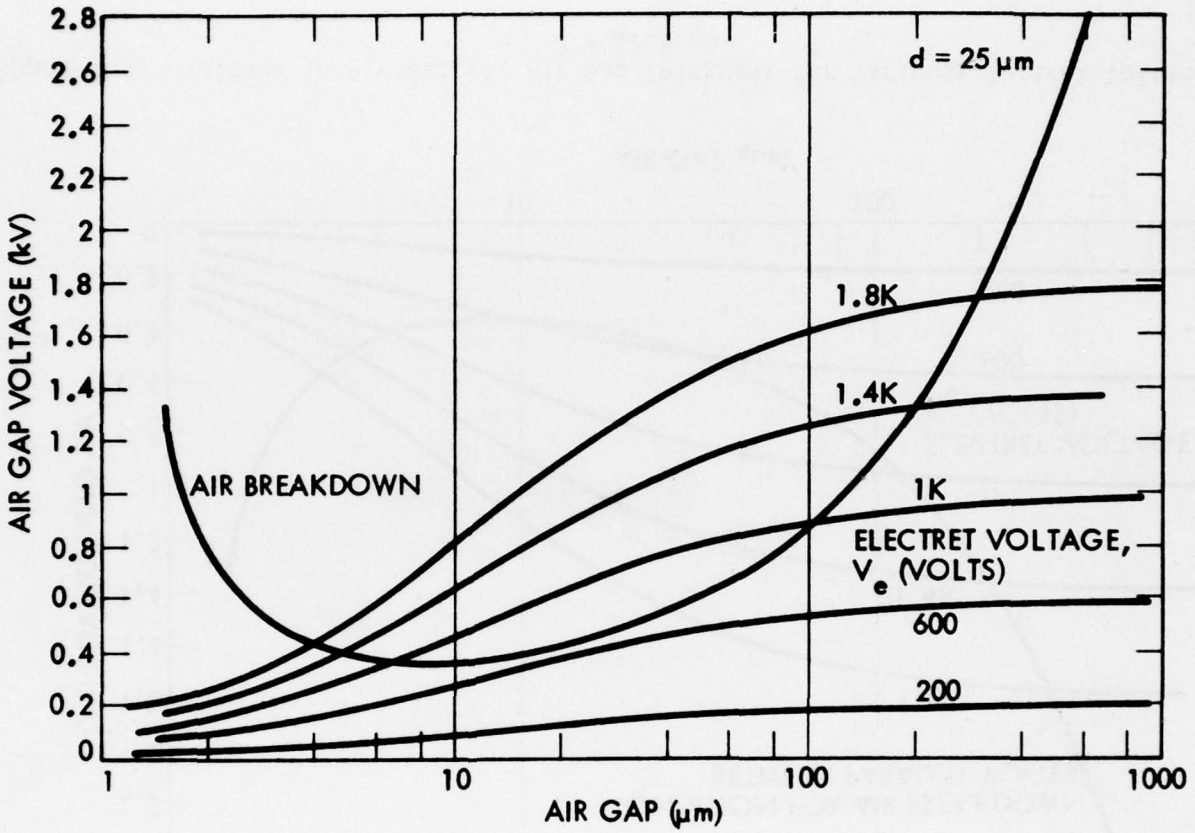

Figure B-3. Voltage in Air Gap vs. Air Gap Thickness for Various Electret Voltages, d = 25 μm

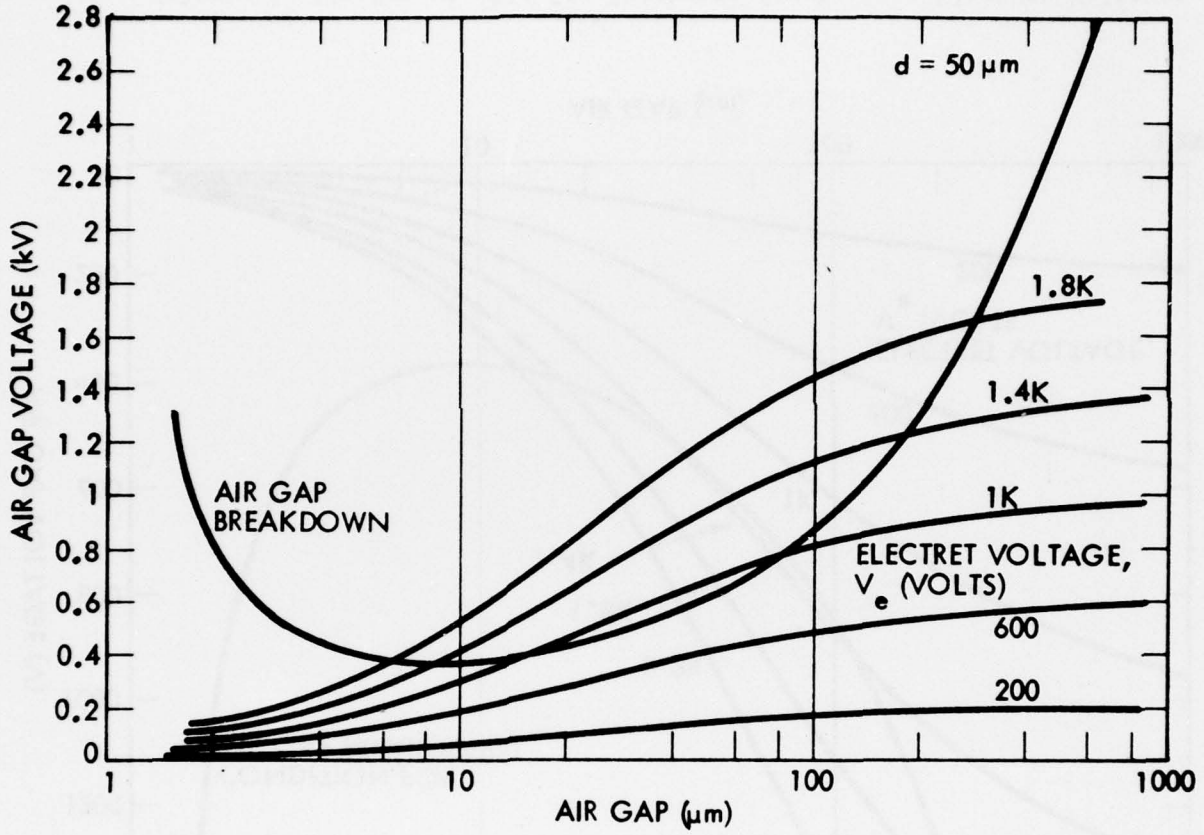

Figure B-4. Voltage in Air Gap vs. Air Gap Thickness for Various Electret Voltages
d = 50 μm

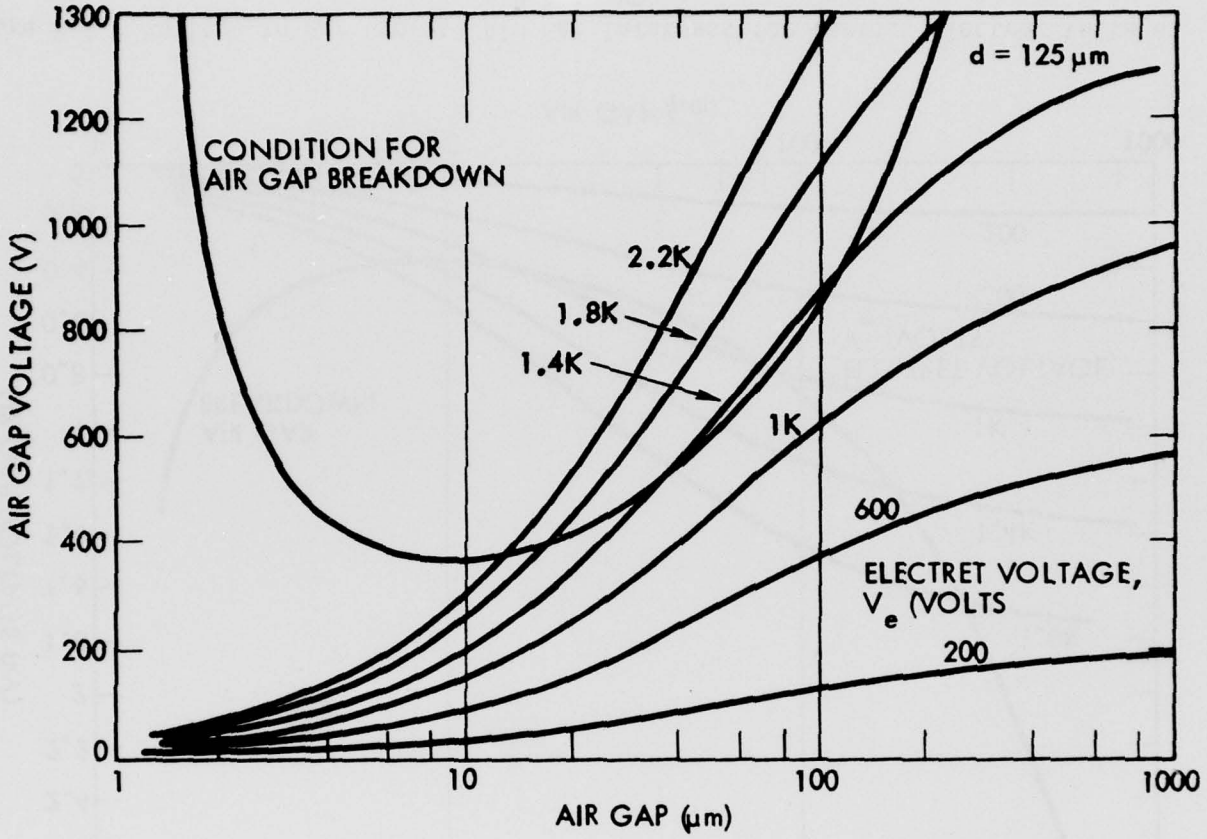

Figure B-5. Voltage in Air Gap vs. Air Gap Thickness for Various Electret Voltages, d = 125 μm

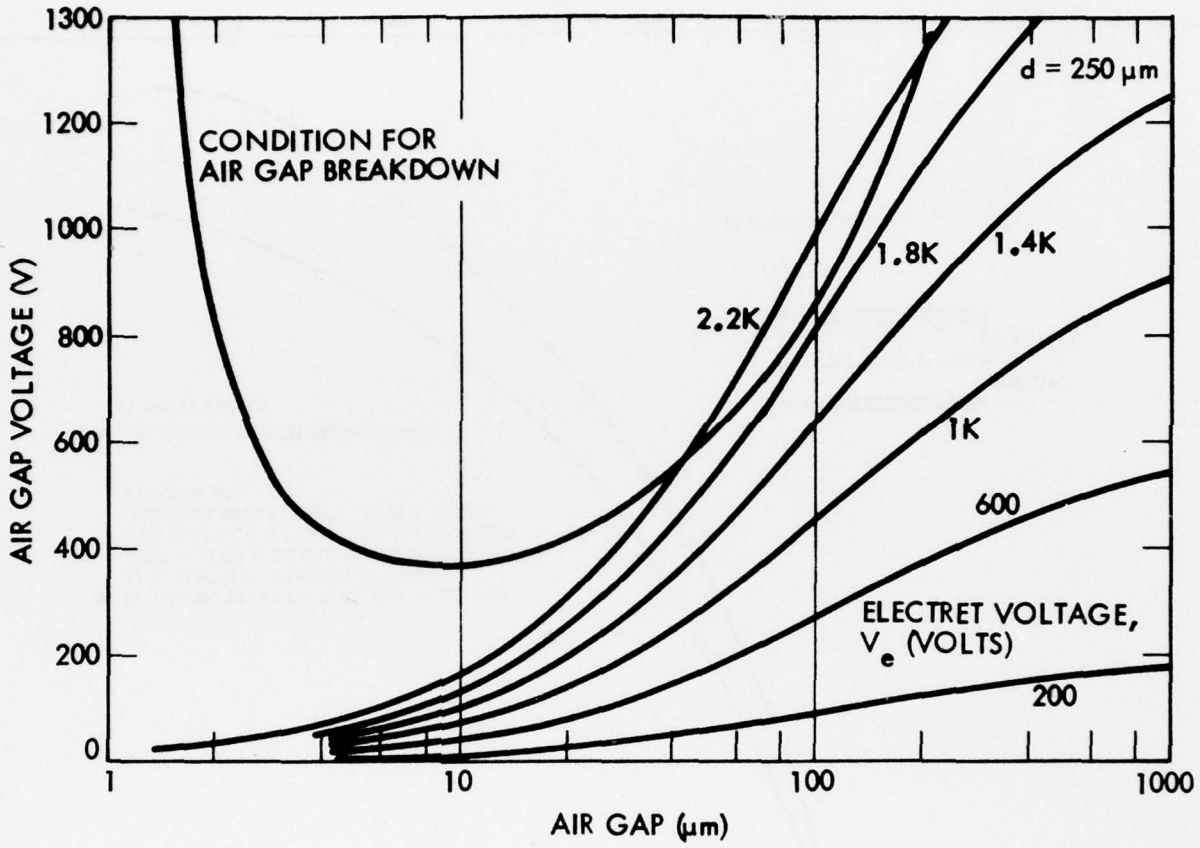

Figure B-6. Voltage in Air Gap vs. Air Gap Thickness for Various Electret Voltages, d = 250 μm

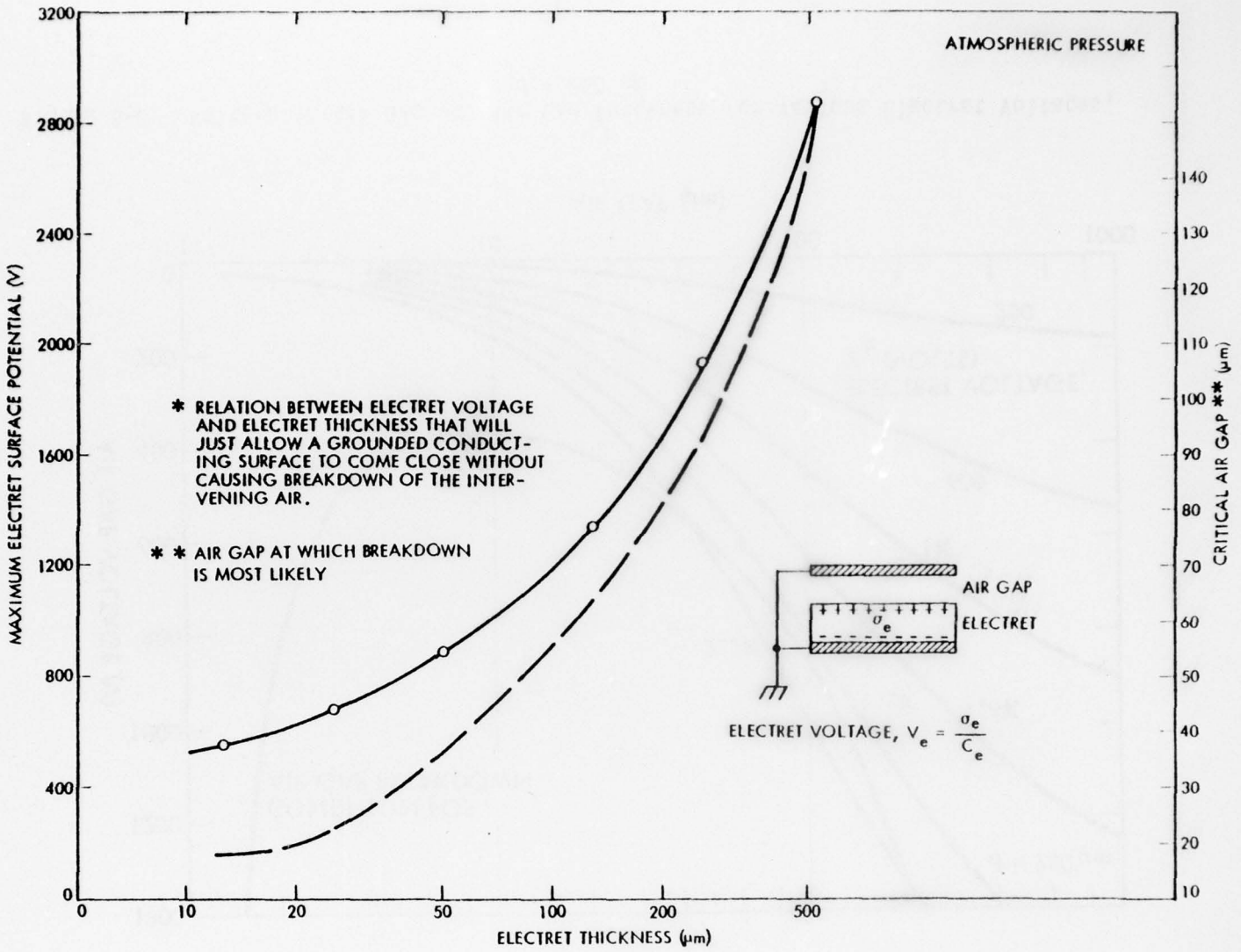

Figure B-7. Critical Electret Voltage vs. Electret Thickness for FEP

MISSION
of
Rome Air Development Center

RADC plans and conducts research, exploratory and advanced development programs in command, control, and communications (C^3) activities, and in the C^3 areas of information sciences and intelligence. The principal technical mission areas are communications, electromagnetic guidance and control, surveillance of ground and aerospace objects, intelligence data collection and handling, information system technology, ionospheric propagation, solid state sciences, microwave physics and electronic reliability, maintainability and compatibility.